



THE UNIVERSITY OF  
**WAIKATO**  
*Te Whare Wānanga o Waikato*

Research Commons

<http://researchcommons.waikato.ac.nz/>

## Research Commons at the University of Waikato

### Copyright Statement:

The digital copy of this thesis is protected by the Copyright Act 1994 (New Zealand).

The thesis may be consulted by you, provided you comply with the provisions of the Act and the following conditions of use:

- Any use you make of these documents or images must be for research or private study purposes only, and you may not make them available to any other person.
- Authors control the copyright of their thesis. You will recognise the author's right to be identified as the author of the thesis, and due acknowledgement will be made to the author where appropriate.
- You will obtain the author's permission before publishing any material from the thesis.

**Determining Canopy Vigour in G3 Kiwifruit  
using  
Remote Sensing  
and  
Geographic Information Systems**

A thesis  
submitted in partial fulfilment  
of the requirements for the degree

of

*Master of Social Science*

at

**The University of Waikato**

by

**Graeme Hull**



THE UNIVERSITY OF  
**WAIKATO**  
*Te Whare Wānanga o Waikato*

2017

## Abstract

Consumers are increasingly demanding that food producers justify their use of water, fertiliser and agrichemicals. Placing the right inputs, in the right place, at the right time, is sometimes called “Precision Agriculture”. However, the adoption of Precision Agriculture by New Zealand kiwifruit growers, has been constrained in part, by the cost and complexity of monitoring seasonal growth. Therefore, any new technology, that can simply and cost effectively measure canopy vigour in a timely way and relate that to fruit quality and production inputs, will ultimately help improve orchard gate returns and keep consumers happy. Using a multispectral camera and UAV (drone), this study monitored two, G3 kiwifruit orchards over three months. Canopy Chlorophyll Content, was found to be the best proxy for canopy vigour. The vegetation index, EVI2 on its own, explained 67% of the variability in canopy vigour. Adding orchard topography measures, extracted from LIDAR data using GIS software, increased the explanatory power of the best model to 85%. In many respects, remote sensing was found to be superior to historical measurement methods. However, uptake by the kiwifruit industry is likely to be conditional on a better understanding of the relationship between canopy vigour, fruit quality and orchard gate returns. The significant correlations observed between orchard topography and canopy vigour, signal a need for closer integration of Geography and Agricultural Science disciplines, in future kiwifruit research.

## Acknowledgements

This research was supported by Zespri International, without which it would not have been possible. A special thank you to Dr Greg Clark for his feedback on the project design.

Thank you also, to Dr Mike Clearwater and Dr Daniel Laughlin (Faculty of Science and Engineering, University of Waikato) for providing essential equipment and laboratory time and for their support from the project's inception.

The friendly cooperation and support of Leighton Oates and his management team at BayGold Orchards was always welcome during my many visits.

Thank you to Dr Lars Brabyn (Faculty of Arts and Social Sciences, University of Waikato) as my supervisor of this Master's thesis. His GIS lectures and tutorials inspired me and made this research possible. His guidance when it came time to putting pen to paper was appreciated.

Finally, I would like to acknowledge the support of my family, especially Jane who was my sounding board at every stage. Thank you for your patience and words of encouragement.

## Table of Contents

Abstract .....	ii
Acknowledgements .....	iii
Table of Contents .....	iv
Table of Figures .....	viii
Table of Tables.....	xiii
1 Introduction.....	1
1.1 Thesis Format .....	1
1.2 Background, Motivation and Scope .....	3
2 Literature Review .....	5
2.1 Precision Agriculture.....	5
2.2 Proximal Sensors .....	7
2.2.1 LI-COR LAI-2200C.....	7
2.2.2 Minolta SPAD 502Plus .....	9
2.3 Remote Sensors .....	11
2.3.1 Multispectral Cameras .....	11
2.3.2 Hyper-spectral Cameras .....	12
2.3.3 LIDAR .....	12
2.3.4 Stereo Photogrammetry.....	13
2.3.5 Thermal Infrared .....	13
2.4 Principles of Multispectral Remote Sensing .....	14

2.5	Image Processing and Analysis .....	16
2.5.1	Pre-processing .....	16
2.5.2	Geographic Information Systems (GIS).....	18
2.5.3	Vegetation Indices.....	20
2.6	Remotely Piloted Aerial Systems.....	23
3	Methods .....	25
3.1	Design.....	26
3.2	Data Collection.....	29
3.2.1	Multispectral Images.....	29
3.2.2	Chlorophyll Measurement – Field .....	32
3.2.3	Chlorophyll a + b Measurement – Laboratory.....	33
3.2.4	Leaf Area Index Measurement.....	35
3.2.5	Orchard Topography Measurements.....	38
3.3	Data Processing .....	39
3.3.1	Image Post-processing .....	39
3.3.2	Leaf Chlorophyll Measurement .....	42
3.3.3	Leaf Area Index Measurement.....	43
3.4	Statistical Analysis .....	44
4	Results.....	46
4.1	Canopy Vigour Measurements .....	47
4.1.1	Leaf Area Index Measurements .....	47
4.1.2	Chlorophyll Measurements .....	49

4.2	Remote Sensing and GIS Measurements .....	52
4.2.1	Canopy Reflectance Measurements .....	52
4.2.2	Orchard Topography Measurements.....	65
4.3	Correlations .....	66
4.3.1	Correlations between Canopy Vigour and Orchard Topography ...	66
4.3.2	Correlation between Leaf Area Index and Chlorophyll.....	66
4.3.3	Correlations between Vegetation Indices.....	67
4.3.4	Correlations between Canopy Vigour and Canopy Reflectance.....	70
4.4	Multiple Regressions .....	71
4.4.1	Analysis of Errors (Model 2) .....	73
5	Discussion.....	76
5.1	Interpretation of Results .....	77
5.1.1	Orchard Topography .....	77
5.1.2	Canopy Vigour .....	78
5.1.3	Canopy Reflectance .....	81
5.1.4	Determining Canopy Vigour using Canopy Reflectance and GIS..	84
5.2	Research Limitations .....	89
5.2.1	Design Limitations .....	89
5.2.2	Data Capture Limitations .....	89
5.2.3	Processing Limitations .....	90
5.2.4	Analysis Limitations .....	91
6	Conclusions.....	92

6.1	Opportunities for Remote Sensing and GIS .....	92
6.2	Contribution to Knowledge .....	93
6.3	Future Research .....	94
6.3.1	Model Validation .....	94
6.3.2	Advanced Terrain Modelling .....	97
6.3.3	Relationship between Canopy Vigour, Fruit Quality and Yield .....	97
6.3.4	Variable Rate Plant and Equipment .....	98
6.3.5	Summary .....	98
7	References.....	99
8	Appendices.....	105

## Table of Figures

FIGURE 1-1 PROJECT SCOPE AND ITS RELATIONSHIP TO STRESS AND PRIMARY PRODUCTION. ....	4
FIGURE 2-1 VIEW ANGLES SEEN BY THE LAI-2200C OPTICAL SENSOR (IMAGE COURTESY OF LI-COR BIOSCIENCES) .....	7
FIGURE 2-2 PEAK CHLOROPHYLL ABSORBANCE IN THE BLUE (400-450NM) AND RED (600-700NM) REGIONS FROM TWO LEAF SAMPLES (A, B).....	9
FIGURE 2-3 MINOLTA SPAD 502PLUS.....	10
FIGURE 2-4 MICA SENSE RED EDGE MULTISPECTRAL CAMERA.....	11
FIGURE 2-5 IMAGE SHOWING TYPICAL LEAF STRUCTURE AND ITS EFFECT ON THE ABSORPTION AND TRANSMISSION OF LIGHT .....	15
FIGURE 2-6 GRAPH SHOWING SOME KEY UNDERLYING REASONS FOR DIFFERENT ELECTROMAGNETIC REFLECTION AND ABSORPTION IN LEAVES. ....	15
FIGURE 2-7 EXAMPLE OF A “FIXED WING” UAV .....	23
FIGURE 2-8 EXAMPLE OF V4 CONFIGURED “MULTI-ROTOR” .....	23
FIGURE 3-1 PVR MAPS FOR EACH OF THE 3 CANDIDATE ORCHARDS SHOWING A TOTAL OF FIVE AREAS OF INTEREST .....	27
FIGURE 3-2 SEGMENTED AREAS OF INTEREST SHOWING RANDOM GROUND-TRUTH SAMPLE POINTS (5 PER SEGMENT).....	28
FIGURE 3-3 MICA SENSE CAMERA MOUNTED ON A “480-SIZE” QUADCOPTER.....	29
FIGURE 3-4 UAV ASCENDING TO TARGET ALTITUDE OF 120M .....	30
FIGURE 3-5 CAMERA CALIBRATION BOARD.....	30
FIGURE 3-6 BAND 1 BLUE .....	31
FIGURE 3-7 BAND 2 GREEN.....	31
FIGURE 3-8 BAND 3 RED .....	31

FIGURE 3-9 BAND 4 RED EDGE .....	31
FIGURE 3-10 BAND 5 NEAR INFRARED .....	31
FIGURE 3-11 SAMPLING ZONES FOR LEAF CHLOROPHYLL MEASUREMENTS.....	32
FIGURE 3-12 LEAF SAMPLES WITH 1CM <sup>2</sup> CORK-BORER AND MINOLTA SPAD.....	33
FIGURE 3-13 UNIVERSITY OF WAIKATO LABORATORY.....	33
FIGURE 3-14 CENTRIFUGE.....	34
FIGURE 3-15 SHIMADZU UV-1280 SPECTROPHOTOMETER.....	34
FIGURE 3-16 LI-COR 2200C INSTRUMENT.....	35
FIGURE 3-17 BASE SENSOR MOUNTED ON TRIPOD WITH ROVING SENSOR IN FOREGROUND .....	36
FIGURE 3-18 SAMPLE PLANTS MARKED WITH RED/WHITE TAPE. ....	36
FIGURE 3-19 LOCATIONS 1-6 INDICATE WHERE LICOR READINGS WERE TAKEN.....	37
FIGURE 3-20 DIGITAL ELEVATION MODEL (BG1) .....	38
FIGURE 3-21 DIGITAL ELEVATION MODEL (BG2) .....	38
FIGURE 3-22 EXAMPLES OF BINARY CANOPY MAPS AFTER EXCLUSION OF NON- CANOPY BACKGROUND.....	40
FIGURE 3-23 EXAMPLES OF VEGETATION INDICES (EVI2) CREATED FOR T1-T4 ON BG1 ORCHARD .....	41
FIGURE 3-24 FV2200 SCREEN SHOT SHOWING EXAMPLES OF “SPLIT” AND SINGLE OBSERVATIONS FOR EACH SAMPLE PLANT. ....	44
FIGURE 4-1 BOX & WHISKER PLOT ILLUSTRATES SIGNIFICANT INCREASE IN LAI ACROSS THE FOUR SAMPLING PERIODS. ....	47
FIGURE 4-2 HISTOGRAM, SCATTERPLOT AND BOX & WHISKER GRAPHS ILLUSTRATE SUMMARY STATISTICS FOR MEAN LEAF AREA INDEX (T1-T4) .....	48

FIGURE 4-3 BOX & WHISKER PLOT ILLUSTRATES SIGNIFICANT INCREASE IN LEAF CHLOROPHYLL ACROSS THE FOUR SAMPLING PERIODS.....	49
FIGURE 4-4 HISTOGRAM, SCATTERPLOT AND BOX & WHISKER GRAPHS ILLUSTRATE SUMMARY STATISTICS FOR MEAN LEAF CHLOROPHYLL (T1-T4).....	50
FIGURE 4-5 SCATTER PLOT ILLUSTRATES CORRELATION BETWEEN LABORATORY & FIELD CHLOROPHYLL MEASUREMENTS* .....	51
FIGURE 4-6 SCATTER PLOT ILLUSTRATES CORRELATION BETWEEN LABORATORY & FIELD CHLOROPHYLL MEASUREMENTS* .....	51
FIGURE 4-7 BOX & WHISKER PLOT ILLUSTRATES SIGNIFICANT INCREASE IN NDVI ACROSS THE FOUR SAMPLING PERIODS .....	52
FIGURE 4-8 HISTOGRAM, SCATTERPLOT AND BOX & WHISKER GRAPHS ILLUSTRATE SUMMARY STATISTICS FOR MEAN NDVI (T1-T4).....	53
FIGURE 4-9 BOX & WHISKER PLOT ILLUSTRATES SIGNIFICANT INCREASE IN EVI2 ACROSS THE FOUR SAMPLING PERIODS. ....	54
FIGURE 4-10 HISTOGRAM, SCATTERPLOT AND BOX & WHISKER GRAPHS ILLUSTRATE SUMMARY STATISTICS FOR MEAN EVI2 (T1-T4) .....	55
FIGURE 4-11 BOX & WHISKER PLOT ILLUSTRATES MINIMAL INCREASE IN MEAN PVR ACROSS THE FIRST THREE SAMPLING PERIODS. ....	56
FIGURE 4-12 HISTOGRAM, SCATTERPLOT AND BOX & WHISKER GRAPHS ILLUSTRATE SUMMARY STATISTICS FOR MEAN PVR (T1-T4).....	57
FIGURE 4-13 BOX & WHISKER PLOT ILLUSTRATES SIGNIFICANT INCREASE IN NDRE ACROSS THE FOUR SAMPLING PERIODS. ....	58
FIGURE 4-14 HISTOGRAM, SCATTERPLOT AND BOX & WHISKER GRAPHS ILLUSTRATE SUMMARY STATISTICS FOR MEAN NDRE (T1-T4).....	59

FIGURE 4-15 BOX & WHISKER PLOT ILLUSTRATES SIGNIFICANT INCREASE IN GCI ACROSS THE FOUR SAMPLING PERIODS. ....	60
FIGURE 4-16 HISTOGRAM, SCATTERPLOT AND BOX & WHISKER GRAPHS ILLUSTRATE SUMMARY STATISTICS FOR MEAN GCI (T1-T4).....	61
FIGURE 4-17 BOX & WHISKER PLOT ILLUSTRATES SIGNIFICANT INCREASE IN RECI ACROSS THE FOUR SAMPLING PERIODS .....	62
FIGURE 4-18 HISTOGRAM, SCATTERPLOT AND BOX & WHISKER GRAPHS ILLUSTRATE SUMMARY STATISTICS FOR MEAN RECI (T1-T4).....	63
FIGURE 4-19 BOX & WHISKER PLOT ILLUSTRATES DIFFERENCES IN OVERALL MEAN VEGETATION INDEX VALUES.....	64
FIGURE 4-20 SCATTERPLOT ILLUSTRATES CORRELATION BETWEEN LEAF CHLOROPHYLL AND LAI (MEAN T1-T4) .....	66
FIGURE 4-21 SCATTERPLOT ILLUSTRATES CORRELATION BETWEEN NDVI AND EVI2 (MEAN T1-T4).....	67
FIGURE 4-22 SCATTERPLOT ILLUSTRATES CORRELATION BETWEEN NDVI AND PVR (MEAN T1-T4).....	67
FIGURE 4-23 SCATTERPLOT ILLUSTRATES CORRELATION BETWEEN NDRE AND GCI (MEAN T1-T4).....	68
FIGURE 4-24 SCATTERPLOT ILLUSTRATES CORRELATION BETWEEN NDRE AND RECI (MEAN T1-T4) .....	68
FIGURE 4-25 SCATTERPLOT ILLUSTRATES CORRELATION BETWEEN RECI AND GCI (MEAN T1-T4).....	69
FIGURE 4-26 SCATTERPLOT ILLUSTRATES CORRELATION BETWEEN EVI2 AND PVR (MEAN T1-T4).....	69

FIGURE 4-27 SCATTERPLOT ILLUSTRATES CORRELATION BETWEEN LEAF CHLOROPHYLL AND EVI2 (MEAN T1-T4) .....	70
FIGURE 4-28 SCATTERPLOT ILLUSTRATES CORRELATION BETWEEN LEAF AREA INDEX AND EVI2 (MEAN T1-T4) .....	70
FIGURE 4-29 HISTOGRAM ILLUSTRATES DISTRIBUTION OF RESIDUALS COMPARED TO A NORMAL DISTRIBUTION .....	73
FIGURE 4-30 SCATTER PLOT ILLUSTRATES RESIDUAL VALUES AGAINST EXPECTED VALUES .....	73
FIGURE 4-31 SCATTER PLOT ILLUSTRATES OBSERVED VALUES COMPARED TO RESIDUAL VALUES .....	74
FIGURE 4-32 SCATTER PLOT ILLUSTRATES PREDICTED VALUES COMPARED TO OBSERVED VALUES .....	74
FIGURE 4-33 SCATTER PLOT ILLUSTRATES RESIDUAL VALUES COMPARED TO DELETED RESIDUALS. ....	75
FIGURE 4-34 SCATTER PLOT ILLUSTRATES PREDICTED VALUES COMPARED TO RESIDUAL VALUES .....	75
FIGURE 5-1 IMAGE SHOWING TYPICAL EFFECT OF PLANT VIGOUR ON REFLECTANCE. .....	81
FIGURE 6-1 EXAMPLES OF CANOPY VIGOUR MAPS BASED ON MULTIPLE REGRESSION MODEL 2 FOR ORCHARD BG1 AND TIME PERIODS T1- T4.....	95
FIGURE 6-2 EXAMPLES OF CANOPY VIGOUR MAPS BASED ON MULTIPLE REGRESSION MODEL 2 FOR ORCHARD BG2 AND TIME PERIODS T1- T4.....	96

## Table of Tables

TABLE 4-1 ANALYSIS OF VARIANCE TABLE - LEAF AREA INDEX .....	47
TABLE 4-2 ANALYSIS OF VARIANCE TABLE - LEAF CHLOROPHYLL.....	49
TABLE 4-3 ANALYSIS OF VARIANCE TABLE - NDVI.....	52
TABLE 4-4 ANALYSIS OF VARIANCE TABLE - EVI2 .....	54
TABLE 4-5 ANALYSIS OF VARIANCE TABLE - PVR.....	56
TABLE 4-6 ANALYSIS OF VARIANCE TABLE - NDRE.....	58
TABLE 4-7 ANALYSIS OF VARIANCE TABLE - GCI.....	60
TABLE 4-8 ANALYSIS OF VARIANCE TABLE - RECI.....	62
TABLE 4-9 TABLE OF ORCHARD TOPOGRAPHY FOR EACH SAMPLE PLANT. ....	65
TABLE 4-10 TABLE OF CORRELATIONS BETWEEN CANOPY VIGOUR AND ORCHARD TOPOGRAPHY .....	66
TABLE 4-11 MULTIPLE REGRESSION SUMMARY – MODEL 1 (3 VARIABLES) .....	71
TABLE 4-12 MULTIPLE REGRESSION SUMMARY – MODEL 2 (2 VARIABLES) .....	72
TABLE 4-13 MULTIPLE REGRESSION SUMMARY – MODEL 3 (1 VARIABLE) .....	72

# 1 Introduction

---

This chapter outlines the format of this thesis. It explains why plant vigour is important in the New Zealand kiwifruit industry and sets out the primary objective of the study, including the research question being asked. It defines the scope of the research.

---

## 1.1 Thesis Format

This thesis begins with discussion about how this research came about. It looks at why plant vigour is important to all primary production systems. The research question is asked in this context. Finally, Chapter 1 defines the scope of the research and shows how it interfaces with primary production more generally.

Chapter 2 is a literature review, looking firstly at Precision Agriculture (PA); what it is, some of its limitations and possible applications in the context of the New Zealand kiwifruit industry. It explains the importance of sensors in PA and looks specifically at proximal and remote sensors used in this study. For comparison, other sensors not used in this study are also discussed. The principals of multispectral remote sensing are discussed in more detail because they are at the heart of this research. This chapter also includes a review of contemporary image processing and analysis concepts. Finally, Chapter 2 explores the growing use of Remotely Piloted Aerial Systems (RPAS, UAVs or Drones).

Chapter 3, builds on the principals discussed in the previous chapter by detailing the specific methods used in this study. It starts by looking at the orchard selection process and the rationale for how the sample plants were laid out. It then explains each of the data collection steps for each of five (5) different data sets. Some

methods were developed specifically for this study because no prior examples were available in the literature, that could be applied to a kiwifruit canopy. Methods used for processing the raw data are also explained. Finally, Chapter 3 discusses the statistical methods used to understand and explain the observations.

Chapter 4 contains the key results, divided into four (4) sections. The first includes an Analysis of Variance for canopy vigour measurements. Box and Whisker Plots illustrate changes in each variable over time and a summary of the differences between the sample plants is provided. Finally, there is a comparison of laboratory-based chlorophyll measurements with field-based measurements. The second section analyses canopy reflectance, in the same way that the first section looks at canopy vigour. This section, tables orchard topography data extracted using Geographic Information System (GIS) tools. Important correlations are illustrated with Scatter Plots in the third section and the last section uses multiple regression models to explain canopy vigour using only remotely-sensed measurements.

Chapter 5 discusses the results. It deals primarily with interpretation from a production system perspective. While this study is strictly observational and does not explain causality, this chapter does include some discussion of possible causes in the interests of promoting further inquiry. As well as answering the primary research question, this chapter also discusses the limitations of the study.

Chapters 6 considers the motivation for the research and what this study means for Precision Agriculture in the kiwifruit industry. Conclusions are drawn by reflecting what new knowledge has been developed. Finally, there is a detailed look at what further research is required, before the learnings from this research can be applied in a commercial orchard context.

Chapters 7 and 8, are the References and Appendices respectively.

## 1.2 Background, Motivation and Scope

Plant stress in kiwifruit can lead to loss of production and a reduction in fruit quality including storage life. Plant stress is often associated with disease, excess soil water, drought, wind, nutrient deficiencies, temperature and many other factors including management practices. There can also be interactions between stresses and there is anecdotal evidence that stressed kiwifruit plants are more susceptible to other stressors. Plant vigour can affect fruit quality in other ways too. An overly vigorous canopy or a plant carrying too much fruit can adversely affect kiwifruit dry matter and taste (Buxton, 2005; Famiani et al., 2012). Therefore, monitoring and managing plant vigour is an important part of orchard management.

The principals of “Precision Agriculture” are at the heart of the “Zespri System” (Jager, 2013). Growing consumer pressure world-wide means that kiwifruit growers are increasingly required to justify their use of production inputs such as water, fertiliser and chemicals. Precision Agriculture is the discipline of placing the right inputs, in the right place at the right time (Mulla, 2013). It requires constant monitoring throughout the growing season.

Traditional techniques for monitoring and quantifying plant vigour are very labour intensive and often technically challenging. This study investigates alternative solutions. Multi-spectrum images were captured with a UAV and processed using Geographic Information Systems (GIS) software. The results were evaluated against traditional methods.

This study did not attempt to determine the causes of any plant variability nor did it try to explain the relationship between plant vigour and fruit quality or yield. Figure 1-1 shows the scope of the study, but more importantly how measuring plant

vigour is an important link between orchard management practices and fruit quality.

The research question that this study seeks to answer is:

**To what extent, can canopy reflectance and orchard topography explain G3 kiwifruit canopy vigour?**

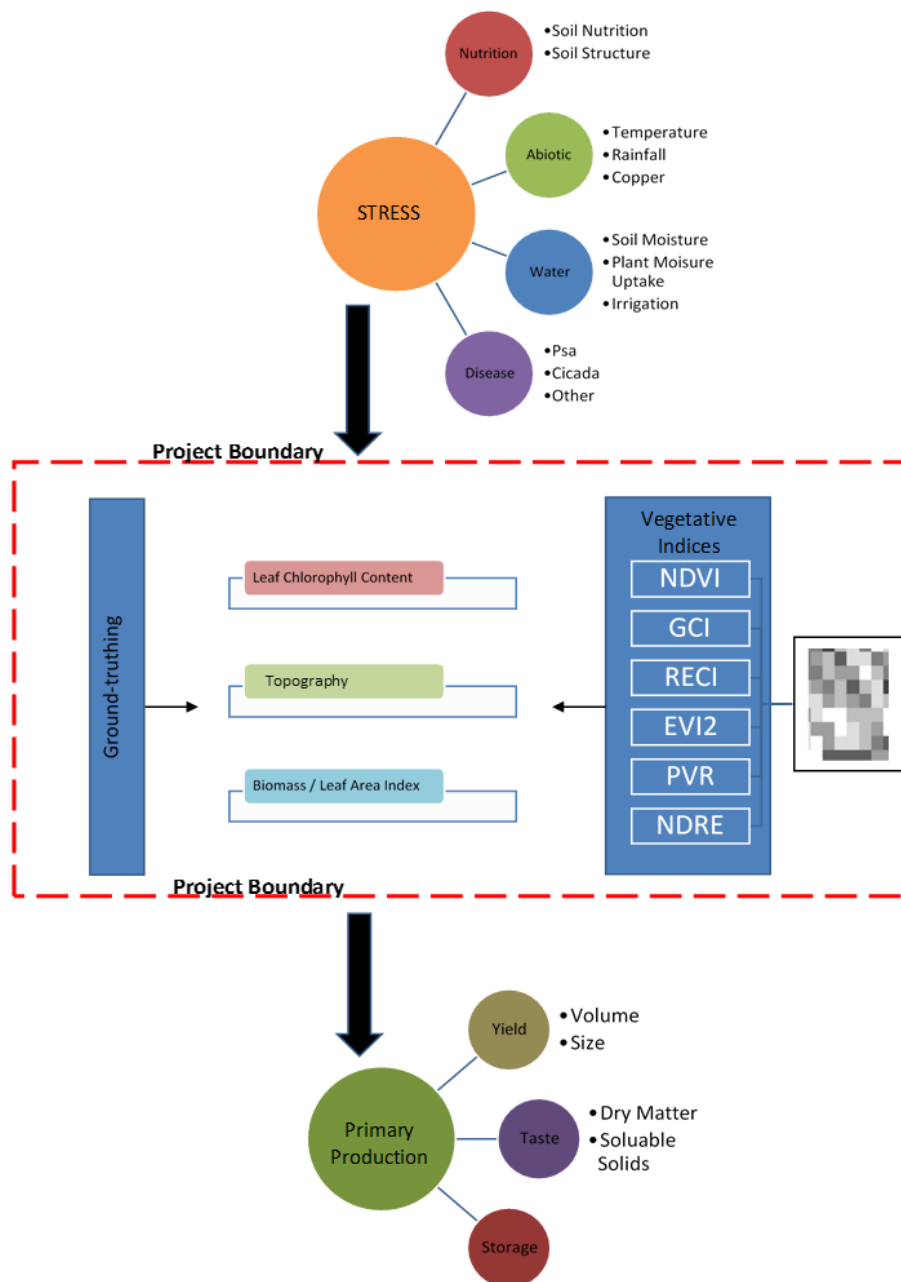


Figure 1-1 Project scope and its relationship to stress and primary production.

## 2 Literature Review

---

This chapter begins by looking at the history of “Precision Agriculture” and explores why it is potentially important to the New Zealand kiwifruit industry. Traditional methods for monitoring plant vigour and their limitations are discussed. Contemporary techniques such as photogrammetry, multi-spectrum remote sensing and GIS are investigated. An overview of the principles behind multispectral remote sensing and post-processing techniques used in this study are also discussed. Finally, this chapter looks at the increasing use of Unmanned Aerial Vehicles (UAVs) as a platform for mounting remote sensors.

---

### 2.1 Precision Agriculture

The underlying principle of Precision Agriculture is to “measure, monitor and then manage” (Hedley, 2015). The concept has been around since the mid-1980s when the organics movement used sensors to monitor soil organic matter (Mulla, 2013). Since then, measuring and monitoring production systems has spread to include soil moisture, soil fertility, disease pressure (Bastiaanssen, Molden, & Makin, 2000; Yuan, Pu, Zhang, Wang, & Yang, 2016) and even to monitoring phenotype expression in plant breeding programs (Deery, Jimenez-Berni, Jones, Sirault, & Furbank, 2014). Weed identification and mapping in crops has also shown promise (Smith, Jackson, Misselbrook, Pain, & Johnson, 2000).

Most commercial examples of Precision Agriculture are being applied to broad-acre crops. Monitoring horticultural crops is much less common (Trout, Johnson, & Gartung, 2008). In New Zealand, it is used most notably in the aerial topdressing industry with considerable cost savings through mechanical variable rate fertiliser

application on pastures. Other New Zealand examples include using sensors to measure pasture quality and manage dairy effluent fertigation systems (Hedley, 2015). There are very few examples in the literature where Precision Agriculture has been adopted by commercial perennial tree crop producers. There are examples of research into soil water variability in vineyards (Bellvert, Zarco-Tejada, Girona, & Fereres, 2014) and yield prediction in apples (Zhou, Damerow, Sun, & Blanke, 2012). Even so, much of the information that is available to producers, has been under-utilised for the past decade (Bastiaanssen et al., 2000; Lindblom, Lundström, Ljung, & Jonsson, 2016).

While the economic and environmental benefits of Precision Agriculture are sometimes questioned (Yost et al., 2016), there is a growing international awareness about sustainable food consumption (Annunziata & Scarpatò, 2014). This awareness, often translates into consumer buying preferences, which ultimately put pressure on producers to justify their production practices. Exporters such as Zespri, place significant importance on building and maintaining a sustainable kiwifruit production system (Jager, 2013), to meet consumer demands.

Precision Agriculture systems typically use sensors to monitor and measure spatial and or temporal variability. This information is often used to control variable-rate equipment such as irrigation systems and fertiliser spreading equipment. Alternatively, data from sensors are used to create zonal management maps to inform management decisions. Sensors can be proximal or remote (Hedley, 2015) and increasingly sensors are networked together (Aqeel-Ur-Rehman, Abbasi, Islam, & Shaikh, 2014). An example of a proximal sensor is the Minolta SPAD, used to measure leaf chlorophyll in this study. In contrast, remote sensors are

usually highly mobile and can be located at significant distances from the area of interest. Satellite multispectral cameras for example are remote sensors.

## 2.2 Proximal Sensors

Proximal sensors can be located in a fixed position or mounted to roving vehicles (Deery et al., 2014). Many proximal sensors are small enough to carry by hand. Delineation between proximal and remote sensors is not always clear and some instruments such as the LI-COR LAI-2200C, which was used in this study, use both types. Generally, proximal sensors are close to or in contact with the area of interest.

### 2.2.1 LI-COR LAI-2200C

Leaf Area Index (LAI) is the ratio of foliage area to ground area. It is one of the recognised measures plant vigour. LAI is an indicator of the amount of energy that a plant can capture from sunlight and therefore its production potential.

The LI-COR LAI-2200C consists of two separate sensors; one used under the canopy (proximal) and the other mounted on a fixed tripod outside the canopy (remote) looking at the clear sky. Each sensor is synchronised to the same time. Both sensors consist of a fisheye lens which “sees” a hemispherical image. An optical system then focuses this image onto an optical sensor which is made up of five concentric rings. Each ring views a different portion of the canopy or sky centred on one of five view angles (Figure 2-1).

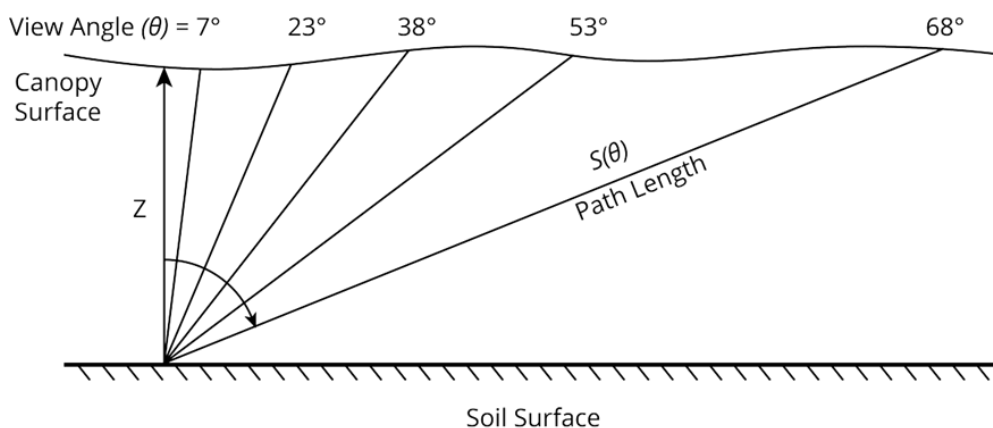


Figure 2-1 View Angles seen by the LAI-2200C optical sensor (Image courtesy of LI-COR Biosciences)

The LAI-2200C computes LAI from measurements made simultaneously above and below the canopy. These measurements are then used to determine canopy light interception at the five angles shown in Figure 2-1. In broad terms, measuring Leaf Area Index is done by calculating the “Gap Fraction” of the canopy. The Gap Fraction is “the fraction of view in some direction from beneath a canopy that is not blocked by foliage (Welles & Cohen, 1996). Calculating the gap fraction makes assumptions about the plant canopy. However, these assumptions are rarely if ever true and therefore a series of corrections are made during the calculation process.

The first assumption is that the leaves and branches (foliage) absorb all light that strikes them. It is assumed that the below-canopy readings do not include radiation that has been reflected or transmitted by foliage. This assumption is removed by applying a scattering correction which accounts for the actual foliage reflectance and transmittance. The next two assumptions are that the foliage is randomly distributed and that it is randomly oriented, i.e., that the leaves are randomly facing all compass directions. The final assumption is that individual foliage elements (e.g. leaves) are small compared to the area being viewed. To fulfil this last assumption, the distance from the optical sensor to the nearest foliage should be at least four times the leaf width. Despite these assumptions, it has been shown that the model still works well even if all the assumptions are not met exactly (Brandenburg, 2012). The LAI-2200C is a precision instrument which is both expensive and technically challenging to use. Post-processing data is also complex. For this reason, it is rarely if ever used by commercial kiwifruit growers. A detailed list of literature references is available on the LI-COR website (“LI-COR References,” 2016). Alternatively, detailed instructions on using the LAI 2200C can be found in a comprehensive user guide (Li-Cor, 2014).

### 2.2.2 Minolta SPAD 502Plus

Leaf chlorophyll concentration is another recognised measure of plant vigour. Chlorophyll is responsible for capturing the sun's energy during photosynthesis. Higher concentrations of chlorophyll are associated with higher levels of gross primary production (A. A. Gitelson, Peng, Arkebauer, & Schepers, 2014).

The Minolta SPAD-502Plus used in this study, determines the relative amount of chlorophyll present by measuring the absorbance of the leaf in two wavelength regions.

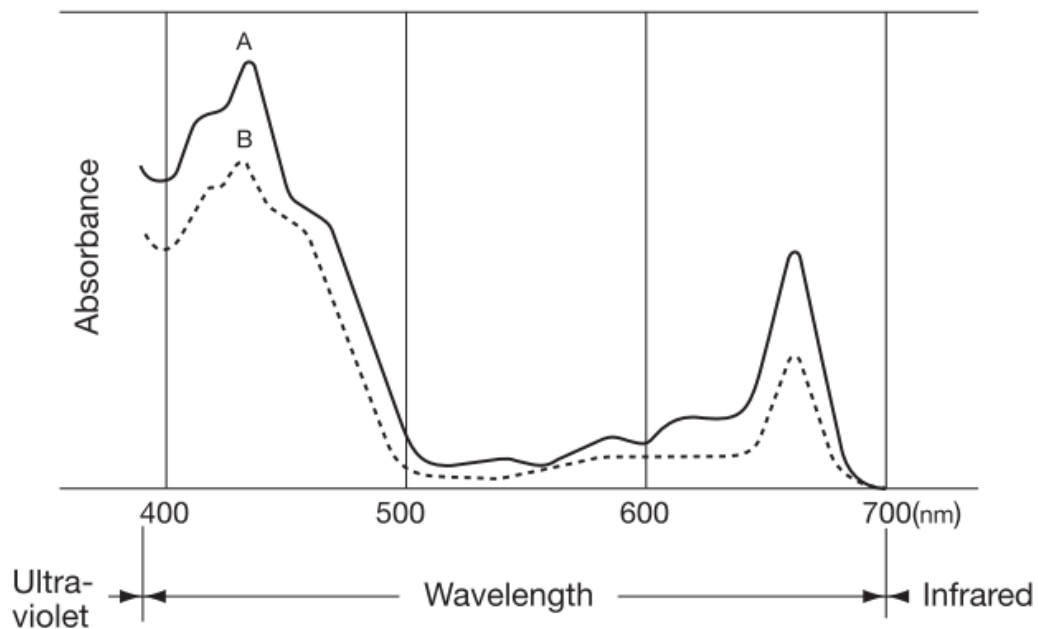


Figure 2-2 Peak chlorophyll absorbance in the blue (400-450nm) and red (600-700nm) regions from two leaf samples (A, B).

(Image courtesy of Konica Minolta)

Figure 2-2 shows the spectral absorbance of chlorophyll extracted from two leaf samples using 80% acetone (Konica Minolta, 2016). It shows that chlorophyll has absorbance peaks in the blue (400-500 nm) and red (600-700 nm) regions, with little or no absorbance in the near-infrared region. To take advantage of this characteristic of chlorophyll, the SPAD- 502Plus measures the absorbance of the leaf in the red and near-infrared regions. Using these two absorbance values, the

meter then calculates a numerical SPAD value which is proportional to the amount of chlorophyll present in the leaf. Studies have shown strong correlations between non-destructive chlorophyll measurement using a Minolta SPAD and destructive laboratory based measurements (Ling, Huang, & Jarvis, 2011).



*Figure 2-3 Minolta SPAD 502Plus*

*(Image courtesy of Konica Minolta)*

The chlorophyll present in the plant leaves is closely related to the nutritional condition of the plant. The chlorophyll content (represented by the measured SPAD value) will increase in proportion to the amount of nitrogen (an important plant nutrient) present in the leaf. For many plant species, a higher Minolta SPAD value indicates a healthier plant (Konica Minolta, 2016).

The Minolta SPAD (Figure 2-3) is a simple instrument to use and requires little operator training. However, obtaining a representative sample within kiwifruit vines, blocks and orchard is very labour intensive. Consequently, few kiwifruit growers if any routinely measure leaf chlorophyll levels. The cost of purchasing a Minolta SPAD is also a likely barrier for most kiwifruit growers in New Zealand.

## 2.3 Remote Sensors

Remote sensors are broadly grouped by their underpinning technology. These broad groups include, multispectral and hyperspectral cameras, microwave radiometers, laser meters, and magnetic sensors. All collect electromagnetic information which is used to measure the Earth's surface and atmosphere (Usha & Singh, 2013).

### 2.3.1 Multispectral Cameras

The MicaSense RedEdge<sup>®</sup> camera used in this study (Figure 2-4), is one of several, purpose-built remote sensors designed for mounting on Unmanned Aerial Vehicles (UAV). Multispectral cameras usually have less than ten (10) discrete spectral bands. Many only have three to five (3-5) overlapping spectral bands, one of which is usually Near InfraRed (NIR). The MicaSense RedEdge has five (5) discrete bands including Blue, Green, Red, Red Edge and NIR.

Typically, this category of sensor comes equipped with on-board GPS to automatically geo-reference images. The MicaSense RedEdge is capable of multiple triggering modes including manual triggering, time interval triggering down to one (1) second and triggering based on distance travelled. Triggering can also be controlled by the UAV on-board flight controller. It also comes with in-built WIFI and is configured using a Smartphone interface application. (“MicaSense RedEdge Multispectral Camera User Manual,” 2015)



*Note five separate lenses for each discrete wavelength band  
(Image courtesy of MicaSense Inc.)*

*Figure 2-4 MicaSense RedEdge Multispectral Camera*

### 2.3.2 Hyper-spectral Cameras

Typically, hyperspectral sensors measure hundreds of spectral bands ranging from 0.4 – 2.5 nm wide across the visible, Near Infrared (NIR) and short wave infrared electromagnetic spectrum (Adam, Mutanga, & Rugege, 2010). Because hyperspectral sensors have a very high spectral resolution compared to multispectral sensors, they can often be used to discriminate between very small differences. For example, hyperspectral sensors have been used to differentiate between off-target spray damage in crops, caused by two different herbicides (Huang, Lee, Thomson, & Reddy, 2016). Hyperspectral cameras have also been used to measure leaf chlorophyll content in grapevine canopies, in Spain (Zarco-Tejada et al., 2005) and kiwifruit, in New Zealand in 2016. This type of sensor was not used in this study.

### 2.3.3 LIDAR

Light detection and ranging (LIDAR) sensors operate in the visible to NIR electromagnetic spectrum. LIDAR is an “active sensor” system (Turner et al., 2003) that send out pulses of light at the target and measures the return time. RADAR uses the same principal but with radio waves instead of light.

While passive sensors like multispectral cameras capture spatial information in two (x, y) dimensions, LIDAR is also able to capture information in the z axis. Capturing data in three dimensions enable point clouds to be created. These are useful for modelling the physical form of a subject and for calculating volumes.

Ground-based LIDAR has proved useful in visualising grapevine canopy structure and airborne LIDAR has also been used to calculate the Leaf Area Index (LAI) of tree vegetation (Mathews & Jensen, 2013).

LIDAR sensors are typically very expensive and are rarely used on UAVs due to the risk of damage. However, this is expected to change as new technologies usually become more affordable over time.

#### 2.3.4 Stereo Photogrammetry

Stereo photogrammetry uses two or more synchronized camera images to measure three-dimensional positions (Romps & Öktem, 2015). While not strictly a remote sensor per se, stereo photogrammetry is an important remote sensing “*technique*” that utilises regular RGB cameras or multispectral sensors. It is a technique regularly used when surveying with UAVs and is therefore included separately in this review.

An RGB camera or multispectral sensor captures hundreds of spatially overlapping and georeferenced images. Software then “stitches” the images together to create an orthomosaic image. Like LIDAR, stereo photogrammetry can be used to generate point clouds and 3-dimensional (3D) models. Volume and slope calculations can also be made. Stereo photogrammetry point clouds typically have many fewer data points than LIDAR point clouds.

Hybrid models can be created using both LIDAR and stereo photogrammetry together. While LIDAR typically measures the solid ground beneath vegetation (within limits) to create a Digital Terrain Model (DTM), stereo photogrammetry measures the surface to create a Digital Surface Model (DSM). By subtracting the DTM from the DSM, volume calculations can theoretically be made (St-Onge, Vega, Fournier, & Hu, 2008)

#### 2.3.5 Thermal Infrared

Thermal infrared sensors are carried on-board some satellites to monitor the temperature of the earth’s surface. The two-band sensor carried by the Landsat-8

satellite for example, measures electromagnetic bands centred at approximately 10.9 and 12  $\mu\text{m}$ . The Landsat-8 sensor has a 100m spatial resolution on the ground. (Barsi et al., 2014). Smaller thermal infrared sensors are used in other ground-based applications, including high resolution aerial mapping in geothermal regions of New Zealand (Harvey, Rowland, & Luketina, 2016).

## 2.4 Principles of Multispectral Remote Sensing

Remote sensing is the science of measuring the world around us from a distance. The ability of a sensor or camera to detect objects from a distance is quantified in terms of its spatial, radiometric, spectral and temporal resolution (Hall, Lamb, Holzappel, & Louis, 2002).

Remote sensing itself is not new. It has been used for many years for non-destructive measurement of the internal properties of kiwifruit (McGlone & Kawano, 1998; Schaare & Fraser, 2000; Slaughter & Crisosto, 1998) and other organic products such as meat (Kamruzzaman, Elmasry, Sun, & Allen, 2012). However, much of the focus in remote sensing has been aimed at identifying, measuring and characterising vegetation (Jackson & Heute, 1991). Determining yield and monitoring diseases in broad-acre crops is an example of where remote sensing is regularly being used in agriculture today.

Healthy plant leaves (Figure 2-5) are high performance photosynthetic structures. Leaves trap and utilise visible light particularly in the Red and Blue wavelengths and reflect light in the green and invisible spectra. Epidermal cells, mesophyll cells, air and cell walls together with internal bodies such as chloroplasts all create optical barriers (A. A. Gitelson & Merzlyak, 1994). These barriers affect the absorption, distribution and reflection of light which can then be measured using multispectral and hyperspectral sensors (Figure 2-6).

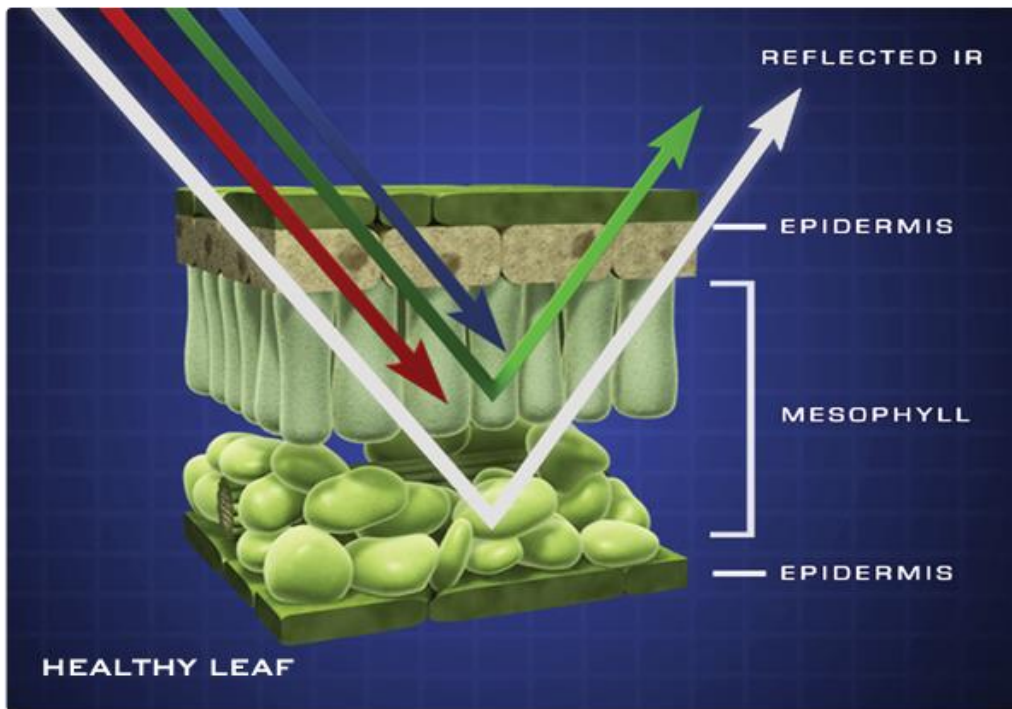


Figure 2-5 Image showing typical leaf structure and its effect on the absorption and transmission of light

Image Credit: NASA Jeff Carns

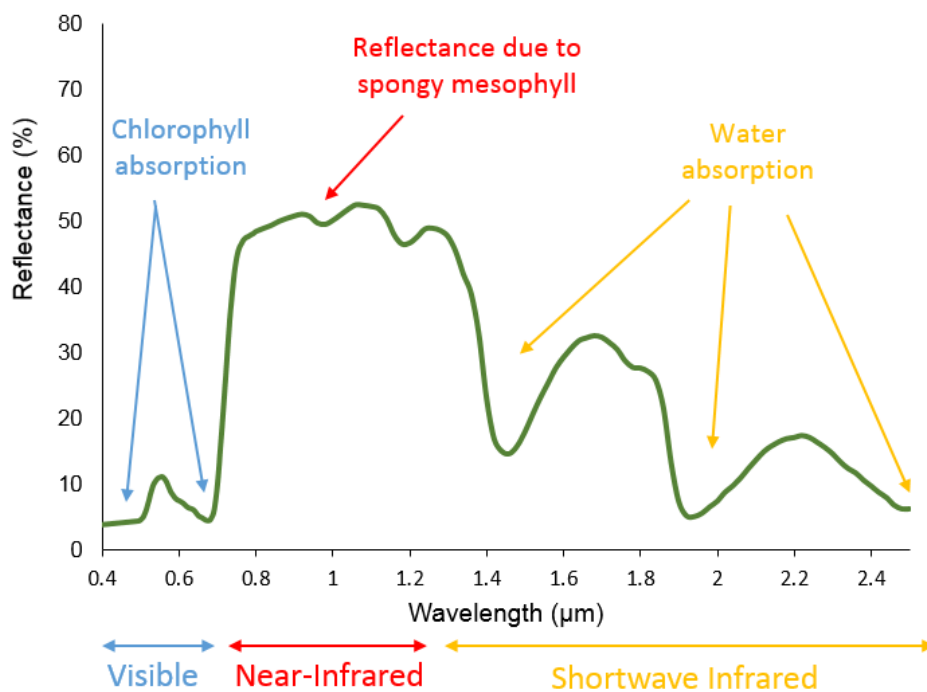


Figure 2-6 Graph showing some key underlying reasons for different electromagnetic reflection and absorption in leaves.

Image Credit: NASA Jeff Carns

## 2.5 Image Processing and Analysis

### 2.5.1 Pre-processing

Multispectral remote sensing usually begins by collecting hundreds of overlapping, multispectral (raw) images. These must first be “stitched” into one or more larger orthomosaic images before further processing. The stitching process involves software identifying common points within adjacent images. Ideally, raw images are geo-referenced which assists the software determine each images order and orientation. However, some software can estimate the relative location without geotags (Boike, Grüber, Langer, Piel, & Scheritz, 2012). Another technique involves placing ground control points (GCP) around the survey area (Berg-Jürgens, 2015). The software uses the GCP common to each raw image, to orientate and stitch the individual images.

Accuracy can be relative or absolute. Relatively accuracy, is where points viewed within an image are accurate relative to each other. This type of accuracy is usually adequate for making grid measurements and extracting information for a single dataset, at a single point in time. In contrast, absolute accuracy is where points within an image are accurate relative to a specific geodetic datum on the earth’s surface. Absolute accuracy is important where multiple measurements are made over time, or comparisons are made between different datasets.

The accuracy of an orthomosaic image is dependent on the technique used to capture the raw images. Where GCPs are used, studies have shown that the absolute accuracy of the orthomosaic can be within 0.132 m while the absolute accuracy without GCP was 1.417 m (Berg-Jürgens, 2015).

Several reputable companies, offer cloud-based processing of raw images to create orthomosaic images. This usually takes twelve to twenty-four hours to

complete. Once completed, orthomosaic images and DSM files can be download onto a personal computer (PC) for further processing. An alternative approach, is to use PC-based software to create orthomosaic images. There are numerous software options available depending on the specific subject matter. Two of the most well-known options are Pix4D (“Pix4D,” 2017) and Agisoft PhotoScan (“Agisoft PhotoScan,” 2017). The disadvantages of using PC-based options are that the software can be expensive to purchase, and usually requires a high-performance computer. It can be time consuming to process large orthomosaic images and usually involves a steep learning curve for an inexperienced operator. The quality of the results can be dependent on the proficiency of the operator. The main advantage of using PC-based software, is that it offers more control over the accuracy of the outputs, in the hands of an experienced operator. However, studies have shown that the accuracy can also vary depending on the software used (Gross, 2015). Another advantage is that many software products available can also create point clouds and 3D models, which many cloud-based services do not offer.

Orthomosaic images contain a large amount of spectral and spatial information; some of which is not wanted. Sometimes this “contamination” must first be removed from an image before any meaningful analysis can begin. Usually unwanted or irrelevant information in an image is removed by classifying it with Geographic Information System (GIS) software and then removing it with a masking tool. Alternatively, some of the more complex Vegetation Indices are designed to automatically compensate for background soil reflectance (Qi, Chehbouni, Huete, Kerr, & Sorooshian, 1994). Removing background reflectance due to grass and weeds that could be seen through holes in the kiwifruit canopy was necessary in this study.

Vegetation classification is an important first step to removing unwanted data from an image. When creating a mask, the accuracy of the classification is important. An inaccurate mask can lead to residual contamination if it is too conservative. Alternatively, relevant information may be lost if the mask is too aggressive. Most commonly, vegetation classifications are done at a pixel level with each pixel being analysed independently of surrounding pixels. In pixel-based classification, the context of each pixel is sometimes lost. Object-based classification is an alternative approach that first segments an image into objects where all the pixels within an object have some pre-defined characteristics in common (Blaschke et al., 2014). Once objects have been created, classification is then performed on each object in a similar way to pixel-based classifications. Studies have shown that object-based classifications can be more accurate than pixel-based classifications in some situations but it can also involve more time and complexity (Duro, Franklin, & Dube, 2012). In this study, unsupervised pixel-based classification was used to create a canopy mask. This is discussed in more detail in the Methods section.

### 2.5.2 Geographic Information Systems (GIS)

Geographic Information Systems (GIS) is a “catch-all” term that has long meant different things to different people (Christian, 2002). In the context of this study, we are specifically interested in the software and workflows, that enable geo-spatial information to be captured (remotely and proximally), analysed, created, managed, and presented as visual maps. Numerous software products are available depending on the focus of the application. Two of the leading products, are ESRI’s proprietary ArcMap (“ESRI ArcMap,” 2017) and the Open Source, QGIS (QGIS Project, 2014). The former was used in this study.

One of the early uses for GIS was to create maps of the earth's surface and to classify vegetation types (Panda, Hoogenboom, & Paz, 2009). To do this, either unsupervised or supervised classification techniques are typically used. Supervised classification requires an operator to "train" the software by defining training areas within an image and then assigning each polygon to a vegetation class. The software then analyses the entire image assigning each pixel to a class. Various methods are then available to measure the accuracy of the final classification. Alternatively, GIS software can perform an unsupervised classification, where one of many algorithms can be used to assign a class to each pixel based on its similarity to other pixels.

Another important application for GIS is extracting information about the terrain. A Digital Elevation Model (DEM) is a georeferenced data layer made up of pixels. Each pixel in a DEM, contains a value of the elevation at a given location. From a DEM it is possible to calculate elevation, slope, aspect and curvature of the earth's surface using GIS software (Erskine, Green, Ramirez, & MacDonald, 2007).

Several national space agencies including the French, Centre National D'Etudes Spatiales (CNES), have developed specialised tools for analysing images captured using satellites. These tools are often available under public domain licences but they do not usually perform traditional GIS mapping functions. Many of these tools, can be applied to identifying and characterising objects in an agricultural context. Image segmentation, object recognition, feature extraction and line identification are just some of the extra functionality found in these specialist tools. While they were not used to any great extent in this study, it is worth noting their potential applications.

### 2.5.3 Vegetation Indices

Most vegetation indices are based on discrete Red and Near Infrared bands because plants exhibit unique properties in these bands. Indices are typically ratios (e.g. NDVI) or orthogonal, with hybrid indices emerging in the last two decades (Broge & Leblanc, 2001). This study only considers ratio-type indices but it is worth noting that other types do exist and that they can be useful particularly where soil reflectance is a factor.

Ratio-type indices typically mirror the slope of the line between electromagnetic (EM) reflectance in different parts of the spectrum. Most indices can be grouped broadly into Red / NIR slope or Green / NIR slope. The notable exception which was used in this study, is PVR (section 2.5.3.3) which reflects the Green / Red slope.

#### 2.5.3.1 Normalised Differential Vegetation Index

$$NDVI = (NIR - Red) / (NIR + Red). \text{ (Rouse, Haas, Schell, \& Deering, 1973)}$$

The Normalised Differential Vegetation Index (NDVI) is arguably the most popular and most reported index. However, NDVI does not discriminate adequately between healthy and diseased plants (Rumpf, Mahlein, Dorschlag, & Plumer, 2009) and for this reason many other improved indices have since been developed for specific purposes.

NDVI has a non-linear behaviour with LAI (Nguy-Robertson, 2013) which results in saturation in dense canopies where LAI is greater than 2 (Gitelson, 2004). It has also been found that NDVI is not as highly correlated with leaf chlorophyll compared to indices that use visible bands only (Hunt et al., 2012).

NDVI was used in this study because it is so widely reported and has become almost the de facto index against which others are compared.

### 2.5.3.2 Enhanced Vegetation Index 2

$$EVI2 = (2.5 \times [NIR - Red]) / (NIR + [2.4 \times Red] + 1)$$
 (Jiang, Huete, Didan, & Miura, 2008)

Enhanced Vegetation Index - 2 (EVI2), is a modification of EVI which itself was developed to improve sensitivity to high levels of biomass. EVI2 behaves very similarly to EVI, but without the need for a Blue band. EVI2 has been shown to accurately estimate the amount of green leaf area (Nguy-Robertson, 2013).

### 2.5.3.3 Photosynthetic Vigour Ratio

$$PVR = Green / Red$$
 (Metternicht, 2003)

The Photosynthetic Vigour Ratio (PVR) is an index that incorporates wavelengths specifically used by plants to derive energy for photosynthesis (Red) and those that are most reflected in the visible spectrum (Green). PVR is expected to have higher values in photosynthetically active canopies where there is strong absorbance in the Red bands and greater reflectance in the Green.

PVR is less commonly referred to in the literature than popular indices that use Red-edge and NIR bands. However, not requiring Red-edge or NIR values is what makes PVR useful for analysing images captured with conventional RGB cameras.

A variation of the PVR index (not used in this study) is the Normalised Difference Photosynthetic Vigour Ratio (NDPVR) which has been used to study stress in plants from a number of factors (Huang, Thomson, Brand, & Reddy, 2016)

### 2.5.3.4 Normalised Differential Vegetation Index -Red-edge

$$NDRE = (NIR - RE) / (NIR + RE)$$
 (Gitelson & Merzlyak, 1994)

It has been shown that indices that use the Red-edge range of the spectrum can be more sensitive than those that do not. This is due to the rapid change in reflectance in the Red-edge region. Indices that use the Red-edge range have potential for

estimating vegetation biophysical characteristics (Nguy-Robertson, 2013). Consistent with this, it has been reported that early signs of plant stress can be detected from reflectance measures in the visible and NIR, especially in the green and Red-edge bands (Metternicht, 2003).

#### 2.5.3.5 Green Chlorophyll Index

$$GCI = (NIR / Green) - 1 \text{ (Gitelson, Gritz, \& Merzlyak, 2003)}$$

Green Chlorophyll Index (GCI) was shown in early studies to be a good indicator of Canopy Chlorophyll Content because it is less susceptible to absorption saturation as Chlorophyll levels increase (A. A. Gitelson et al., 2003). An example of how strongly chlorophyll can absorb Red and Blue wavelengths under a range of conditions can be seen in Figure 5-1.

#### 2.5.3.6 Red-edge Chlorophyll Index

$$RECI = (NIR / RE) - 1 \text{ (Gitelson et al., 2003)}$$

RECI also has its origins in the same study that identified the Green Chlorophyll Index (A. A. Gitelson et al., 2003). Like GCI it is an index that is a good indicator of Canopy Chlorophyll Content.

The Simple Ratio Vegetation Index (RVI), is an index similar to RECI, but it was not included in this study. Some sources report  $RVI = Red/NIR$  (Huang, Lee, et al., 2016), while others report  $RVI = NIR/Red$  (“SEOS Introduction to Remote Sensing,” 2017). The Index Database is a web-based repository for hundreds of vegetation indices (“IDB - A database for remote sensing indices,” 2017). It reports both versions of RVI, together with many other so-called “Simple Ratios”. This highlights the importance of knowing the precise equation when quoting vegetation indices. All too often, popular articles will generically refer to an index as NDVI, even when no NIR bands are used.

## 2.6 Remotely Piloted Aerial Systems

Remotely Piloted Aerial Systems (RPAS, UAVs or Drones) come in a variety of configurations for use in agriculture. Broadly, there are two categories of UAV; fixed wings (Figure 2-7) and multi-rotors (Figure 2-8) as used in this study. Multi-rotors are typically configured as X4, V4 or X6 which describes their rotor layout. They are often used for medium to light payloads, typical of multi-spectrum cameras. Heavy lift multi-rotors often have an X8 configuration.

Depending on the flight controller, most UAVs can be setup for autonomous flight using pre-programmed flight plans. Alternatively, they can be configured for manual or semi-manual operation where the pilot flies each survey mission.



*Figure 2-7 Example of a “fixed wing” UAV  
(Image courtesy of senseFly)*



*Figure 2-8 Example of V4 configured “multi-rotor”  
(Image courtesy of Align)*

In New Zealand, there have been recent changes to legislation with respect to operating UAVs (Civil Aviation NZ, 2015). Broadly, unless a pilot has a specific exemption, all flights must be below 120m AGL and can only be conducted within line of sight and during daylight hours. Flights cannot be conducted over people without their express permission which includes gaining permission from any land owner. Special conditions apply if flights are within four kilometres of an aerodrome. UAVs must also be less than five kilograms without specific approval. Further legislation changes are likely due to the significant increase UAV numbers.

Aerial remote sensing using a UAV typically requires capturing many overlapping images to create a single orthomosaic image. Orthomosaic images are becoming an important tool in agriculture (Gómez-Candón, De Castro, & López-Granados, 2014).

The key advantages of using a UAV to capture remote sensing images is the relatively low setup cost and associated operating costs. Lower operating costs mean higher temporal resolution can be obtained more economically. Taking images from low altitudes (<120m) usually means that higher spatial resolutions are also possible compared to manned aircraft or satellites. The ground coverage of a single pixel can be typically be less than 10 cm<sup>2</sup> (Berg-Jürgens, 2015). In this study, spatial resolution was approximately 8 cm<sup>2</sup>.

The disadvantages of using UAVs include relatively short flight times due to battery life, relatively inaccurate camera calibration, complexity associated with establishing Ground Control Points (GCP) and health and safety issues associated with flying near to people and property. Using UAVs as a platform for very expensive sensors such as hyperspectral cameras and LIDAR sensors which can cost more than NZD\$100,000 is also inherently risky and beyond the resources of most private UAV operators. Some UAVs themselves can cost between NZD\$30,000 and \$75,000, although consumer-grade UAVs are typically much less. Pilot error continues to be a significant cause of UAV crashes world-wide and despite their apparent simplicity, incidents are very common say New Zealand UAV insurance underwriters.

## 3 Methods

---

Chapter 3 is divided into four sections:

### 3.1. Design:

The first section describes the overall trial design and the reasons behind the site selection and the layout of ground-truth (sample) plants.

### 3.2. Data Collection:

The second section outlines how the MicaSense multi-spectrum camera was used to collect raw images. It describes how the raw ground-truth data was collected using a dual sensor Licor LAI 2200C meter and a handheld Minolta SPAD meter. Laboratory procedures for extraction and measurement of chlorophyll and sampling procedures for leaf nutrition analysis are discussed. The workflow for extracting topography data using GIS software (ArcMap) is also outlined.

### 3.3. Data Processing:

The third section in this chapter looks at how the raw images were processed to extract the spectral data using GIS techniques and how LAI was calculated using proprietary FV2200 software. Calculations of chlorophyll content using absorption data obtained in the laboratory are also discussed.

### 3.4. Statistical Analysis:

Having consolidated the data from all sources, the final section discusses the statistical methods used to analyse the data and to summarise the findings.

---

### 3.1 Design

The primary objective of the study design was to observe and record as much natural variability in G3 kiwifruit canopy vigour as possible. Consideration was given to travelling times within the Bay of Plenty and to finding a grower willing to expose their orchard to detailed scrutiny over an extended period. External health and safety considerations were also a factor in the final site selection.

Three candidate orchards were chosen for initial consideration. One orchard was in Katikati and two in Paengaroa. Each orchard was assessed for historical canopy variability using aerial images taken in 2008 by the Bay of Plenty Regional Council (BOPRC) as part of a regional aerial mapping exercise. A canopy vigour index was created for each orchard (Figure 3-1) using the Plant Vigour Ratio Index (PVR) described above.

Topography of each orchard was also analysed using Lidar data provided by the BOPRC. Contours were calculated for each orchard and slope and aspect maps created using ArcMap. Site visits were conducted to gain a better appreciation of the geographic context of each orchard and interviews were conducted with orchard owners/managers. Details of this preliminary assessment were reported as part of a separate assignment (Hull, 2015) and are summarised here.

From the preliminary canopy and topography assessments, two areas of “concentrated” variability were identified within each Paengaroa orchard and one area in the Katikati candidate orchard. These “Areas of Interest” (AOI) were each limited to approximately 1.5 hectares to ensure that each could be surveyed in a single UAV flight.

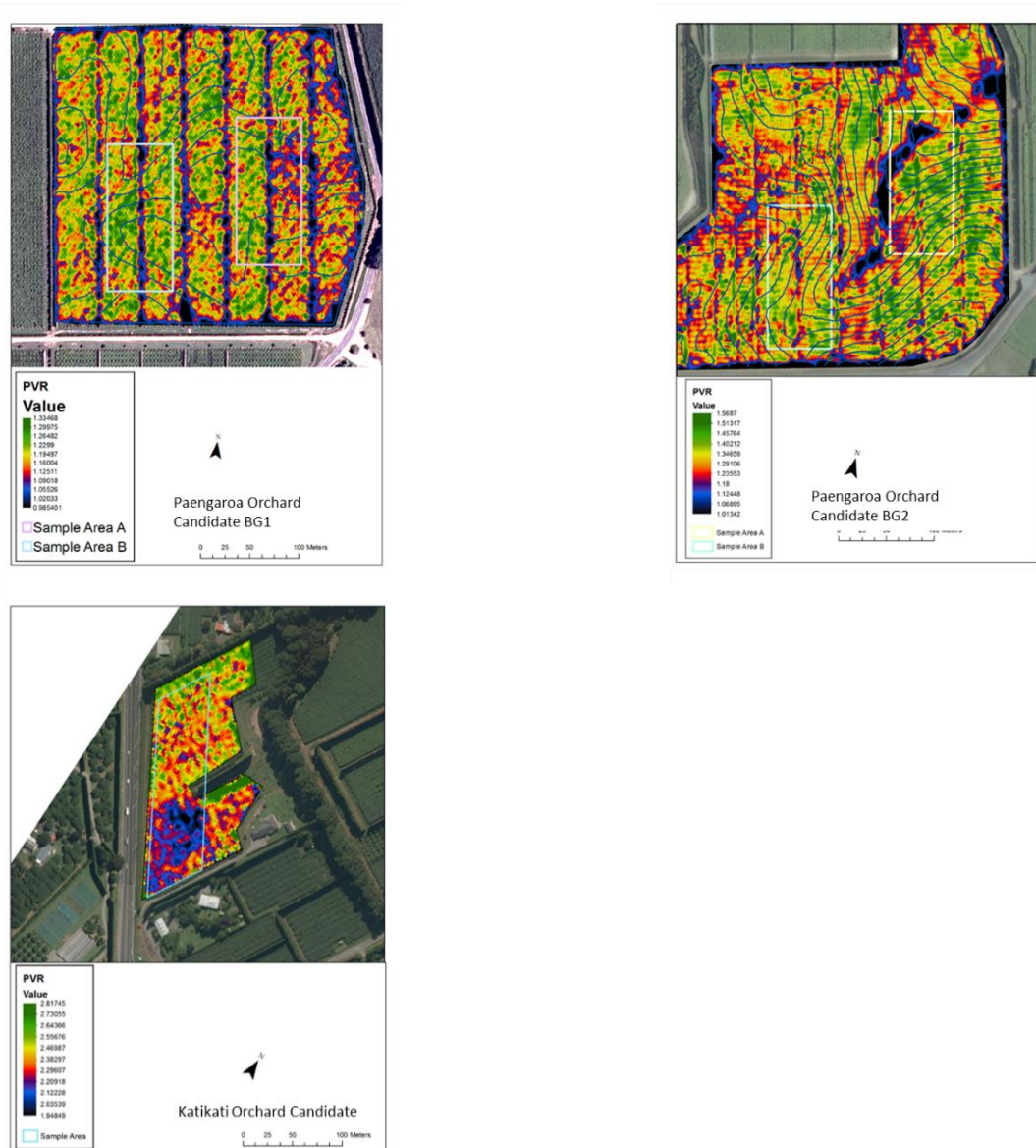


Figure 3-1 PVR maps for each of the 3 candidate orchards showing a total of five Areas of Interest

To ensure that the findings would be statistically robust, fifty (50) plants were selected for ground-truth measurements using a random stratified approach (Brewer, 1999). These are referred to as “sample plants” in this report. However, placing fifty (50) sample plants within such a small (<1.5 ha) area limited the physical distance between each plant. Tobler’s first law of Geography states “everything is related to everything else, but near things are more related than distant things” (Sui, 2004). As the study was looking to maximise variability, it was

decided to increase the distance between sample plants by using two AOI, each containing twenty-five (25) sample plants.

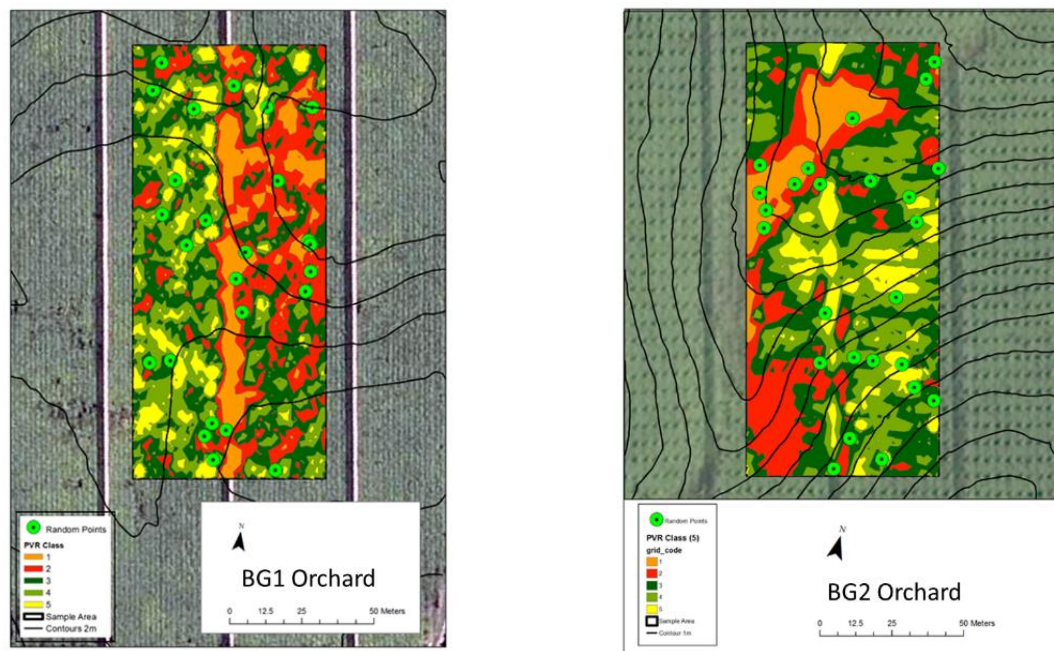


Figure 3-2 Segmented Areas of Interest showing random ground-truth sample points (5 per segment)

The two Paengaroa orchards were chosen for the study. There were three key reasons for eliminating the Katikati orchard. Firstly, this orchard is located adjacent to a main state highway which significantly increased the risk of an incident involving distracted motorists or a “downed” UAV. Secondly, the Katikati orchard is significantly smaller than the other two orchards and a large percentage of the AOI was potentially shaded by large shelter trees at certain times of the day. The final reason for eliminating the Katikati orchard was that it would have required significant traveling between Paengaroa and Katikati to survey two AOI as discussed above.

Of the four (4) remaining AOI candidates, one was selected from each of the Paengaroa orchards. Each AOI was classified into five (5) zones and five random points chosen from within each class (Brewer, 1999). This provided a total of 50 sample plants across two AOIs in two different orchards (Figure 3-2).

## 3.2 Data Collection

### 3.2.1 Multispectral Images

All images were captured using a MicaSense multi-spectrum camera mounted on a UAV (Figure 3-3) flying at approximately 120m above ground level (Figure 3-4). All surveys were flown without the aid of automated mission planning. No camera gimbal was used.



*Figure 3-3 MicaSense camera mounted on a “480-size” quadcopter.  
Note the down-welling light sensor (small red object centre left above camera) was not used in the study.*

Aerial surveys were conducted at four time periods on October 20, November 1, November 18 and December 2, 2015. These times were each assigned the value T1-T4, respectively.

Light conditions, within and between days, varied from completely overcast to no cloud at all. The most difficult light condition was a mixture of bright blue sky and large white cumulus clouds. An experimental downwelling light sensor (Figure 3-3), which measures changing light conditions due to clouds, was trialled but not used in this study. Before and after every flight, the camera was calibrated using a proprietary calibration board (Figure 3-5).



*Figure 3-4 UAV ascending to target altitude of 120m*



*Figure 3-5 Camera Calibration Board  
(Image courtesy of MicaSense Inc.)*

Most surveys were conducted between 10.00 am and 2.00 pm to minimise the effects of shadows on the canopy from shelterbelts and artificial shelter. Surveys were conducted by manually flying a series of near-parallel lines in the same direction as the rows of kiwifruit.

The camera was set up to take one image every two seconds provided altitude was greater than seventy (70) metres. Speed was manually controlled and estimated to give at least 80% overlap of each image along the row. Each parallel line was estimated to give at least a 70% image overlap but in practice the overlap between rows was greater than this.

Typically, each survey required a flight time of approximately thirteen (13) minutes which was the maximum safe limit with the UAV in this configuration. Before and after each survey, the camera was calibrated using a calibration board. This process is intended to help standardise reflectance values within and between flights.

During each flight the camera typically captured 800 – 1000 images with each image comprising five (5) separate spectral bands (Figure 3-6, to Figure 3-10). All images were automatically geotagged with GPS coordinates and altitude for use in the post-processing phase.

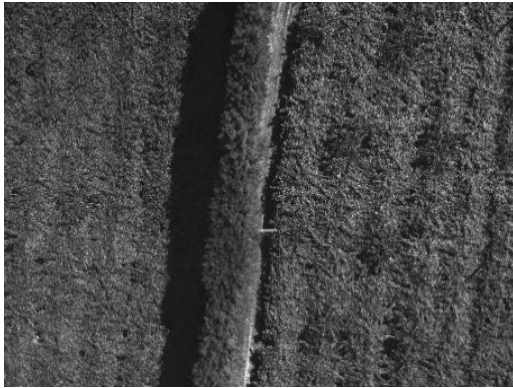


*Figure 3-6 Band 1 Blue*

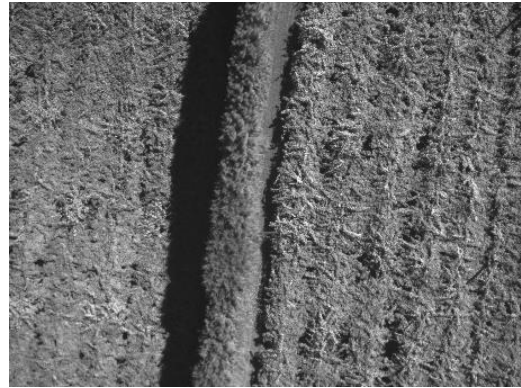


*Figure 3-9 Band 4 Red Edge*

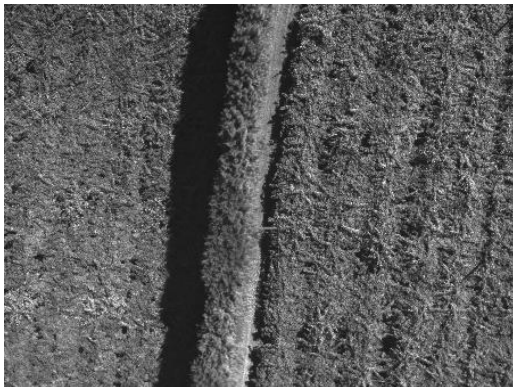


*Figure 3-7 Band 2 Green*

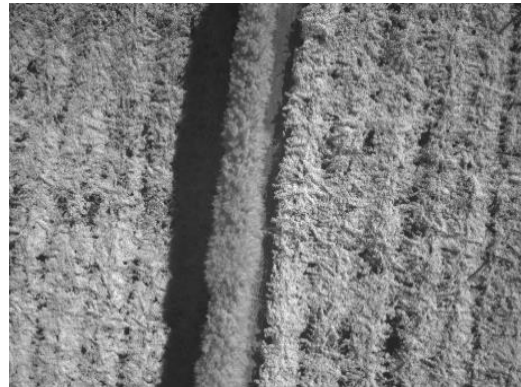


*Figure 3-10 Band 5 Near infrared*

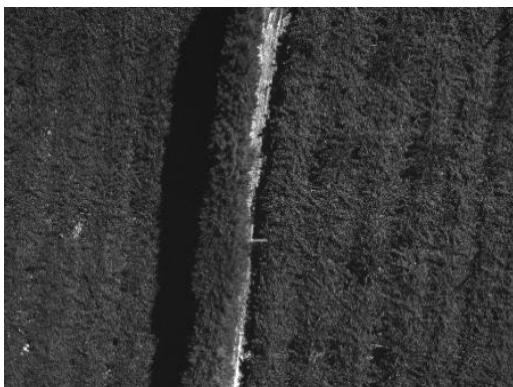


*Figure 3-8 Band 3 Red*

### 3.2.2 Chlorophyll Measurement – Field

1. All chlorophyll measurements in the field were taken using a Minolta SPAD meter
2. Non-destructive leaf chlorophyll measurements were taken at four time periods approximately two weeks apart (Oct 16, Nov 3, Nov 17, Dec 3 2015) These times were assigned the value T1-T4. respectively.
3. Leaves were sampled at random from three zones on each side of the main leader as shown in Figure 3-11.
4. Forty (40) measurements in total were taken from each of the fifty (50) sample plants on both G3 orchards (BG1 and BG2). Twenty measurements were taken from the eastern side of the main leader and the mean value was recorded. Twenty measurements were then taken from the western side of the main leader and the mean value recorded. The mean of these two values was then calculated and recorded.

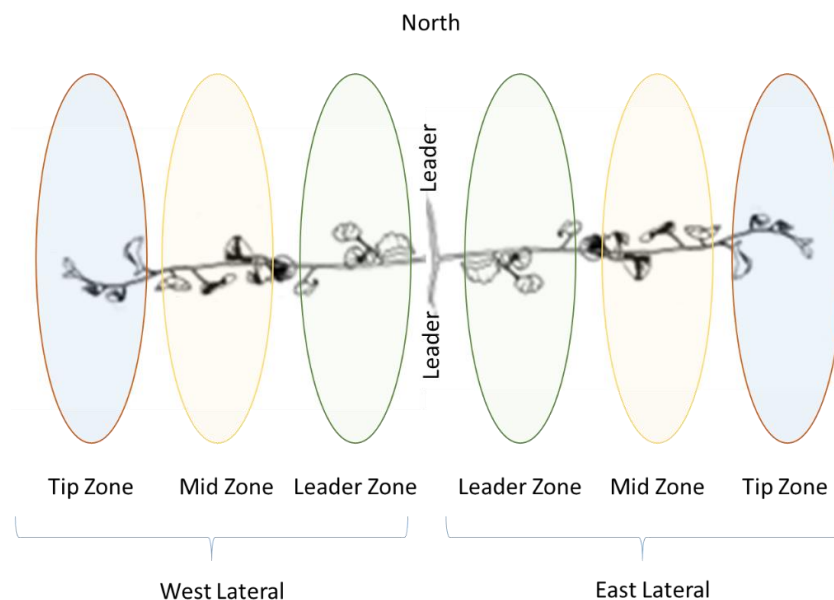


Figure 3-11 Sampling zones for leaf chlorophyll measurements.

### 3.2.3 Chlorophyll a + b Measurement – Laboratory

Twelve leaves were collected from each of the two G3 kiwifruit blocks BG1 and BG2 (24 leaves in total) on November 29, 2015. Leaves were selected from sample plants with the aim of obtaining a broad cross section of colour and maturity typical of the variation seen during the previous Minolta SPAD surveys. Leaves from each orchard were stored in separate plastic bags which were labelled at the time of collection to avoid identification errors. Collection of all leaves was completed within 24 hours of laboratory testing and leaves were refrigerated overnight.

Laboratory analysis was undertaken at the Plant Physiology Laboratory at the University of Waikato in Hamilton (Figure 3-13) under the supervision of a laboratory technician. Prior to chlorophyll extraction each leaf was measured using a Minolta SPAD. The method used for chlorophyll extraction and measurement is summarised below and was provided in the form of a Laboratory Guide (University of Waikato, 2016). This extraction procedure is based on published literature which validates the accuracy of this method against atomic absorption spectrophotometry (Porra, Thompson, & Kriedemann, 1989).

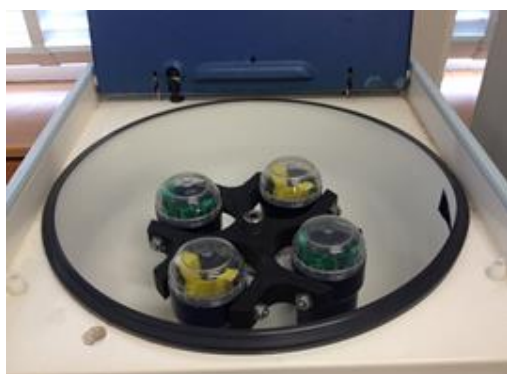


Figure 3-12 Leaf samples with 1cm<sup>2</sup> cork-borer and Minolta SPAD

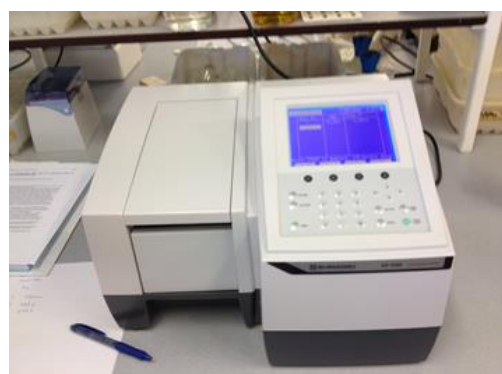


Figure 3-13 University of Waikato Laboratory

1. Using a 1 cm<sup>2</sup> cork borer as shown in Figure 3-12, one disc was taken from each leaf midway between the main rib and the leaf edge. Care was taken to avoid major leaf veins and any unhealthy tissue. Chlorophyll from each leaf disc was extracted and measured independently to produce twenty-four (24) data points.
2. Each disc was ground with approximately 3 ml of extraction solvent (buffered 80% aqueous acetone) using a mortar and pestle until all chlorophyll was in solution.
3. The extract was poured into a centrifuging tube, rinsing the mortar with extra solvent to ensure all chlorophyll was transferred into the tube. The volume was made up to 8ml and 10ml for BG1 and BG2 samples, respectively. Samples were centrifuged at 3900 rpm in batches of four for ten minutes.



*Figure 3-14 Centrifuge*



*Figure 3-15 Shimadzu UV-1280 spectrophotometer*

4. After centrifuging samples were wrapped in tin foil to shield from the light.
5. Each sample was individually placed in a Shimadzu UV-1280 spectrophotometer to measure absorption at three wavelengths (663.6, 646.6 and 750.0 nm). This gave a measurement for chlorophyll *a*, chlorophyll *b* and background turbidity, respectively (Porra et al., 1989). Raw data and calculated results can be found in Appendix 7.

### 3.2.4 Leaf Area Index Measurement

1. All Leaf Area Index readings from below the canopy were taken with a LI-COR 2200C instrument as shown in Figure 3-16. Two identical sensors were “matched” prior to any measurements in the field and a “match file” created for all subsequent measurements.



*Figure 3-16 LI-COR 2200C Instrument*

*(Image courtesy of Licor Biosciences)*

2. Leaf Area Index measurements were taken from all fifty (50) sample plants at four time periods approximately two weeks apart (Oct 20, Nov 3, Nov 17, Dec 2 2015). These times were assigned the value T1-T4, respectively.
3. The Licor instrument was configured with two sensors as prescribed in the User Instruction Manual (Brandenburg, 2012). Each sensor was fitted with a 45-degree lens cap oriented with the widest opening directly ahead to restrict the field of view.

- Both sensors were time synchronised and calibrated for the prevailing light conditions immediately before and after each survey on each orchard.



*Figure 3-17 Base sensor mounted on tripod with roving sensor in foreground*



*Figure 3-18 Sample plants marked with red/white tape.*

*NB These plants are separated by shelter cloth below the canopy.*

- The base sensor was mounted level on a tripod outside the canopy and in clear view of the sky but constrained by the 45-degree lens cap (Figure 3-17). The base sensor was aligned in a northerly direction and parallel to the kiwifruit rows to mirror the roving sensor. The roving sensor was carried manually and levelled by eye using the spirit-level on the instrument. The roving sensor was carried so that the sensor was approximately 1.5 m below the level of the kiwifruit canopy.
- Each sample plant was measured at three locations (locations 1, 2 and 3) on the eastern side of the main leader, facing in a northerly direction and the process was repeated on the west side of the main leader (locations 4, 5 and 6) as shown in Figure 3-19. The six readings were then saved internally as a single measurement with a file name that identified the sample plant for post-processing analysis.

7. Where the sample plant had artificial-shelter cloth running below the canopy along the length of the main leader (Figure 3-18), the measurements taken on the eastern side of the leader (locations 1-3) were saved separately to those taken on the western side of the leader (locations 4-6). These two measurements were processed separately and later combined to calculate the mean for that plant.
8. At the completion of each survey, data captured by the base sensor was transferred to the Licor unit before leaving the site.

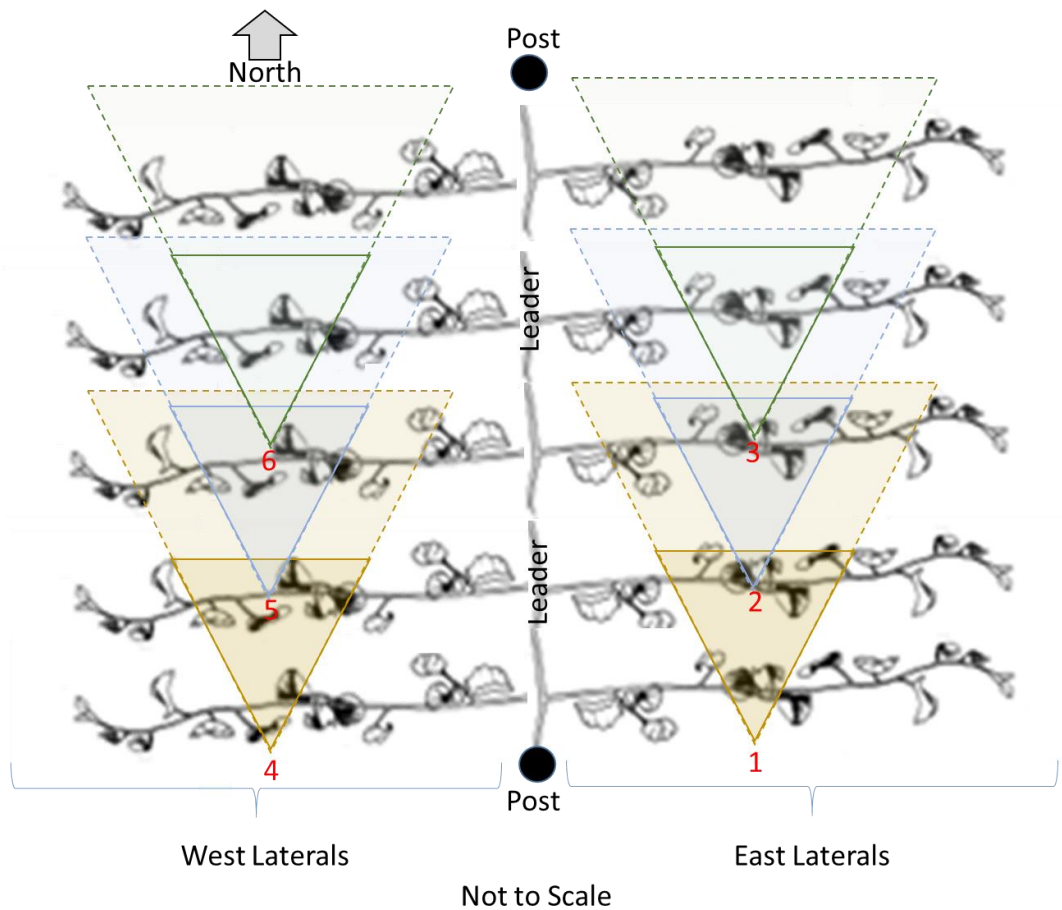


Figure 3-19 Locations 1-6 indicate where Licor readings were taken  
(Not to Scale)

### 3.2.5 Orchard Topography Measurements

An ESRI shapefile (.shp) containing land contours was downloaded from the Bay of Plenty Regional Council's FTP server (Bay of Plenty Regional Council, 2015). This data was created from an aerial LIDAR survey of the Bay of Plenty region, in 2011.

Using ArcMap (GIS) software, a Digital Elevation Model (DEM) was created from the contours for each orchard (Figure 3-20 and Figure 3-21) and their immediate surroundings. A DEM is a georeferenced raster layer. Each pixel in a DEM, contains a value of the elevation at a given location. By manually georeferencing (overlying) the orthomosaic multi-spectrum images of each orchard onto its respective DEM, the mean elevation of each sample plant was calculated using the ArcMap Raster Calculator.

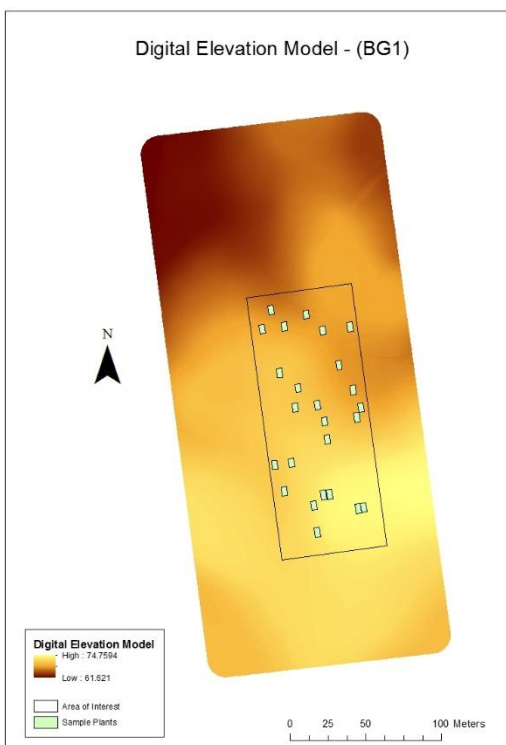


Figure 3-20 Digital Elevation Model (BG1)

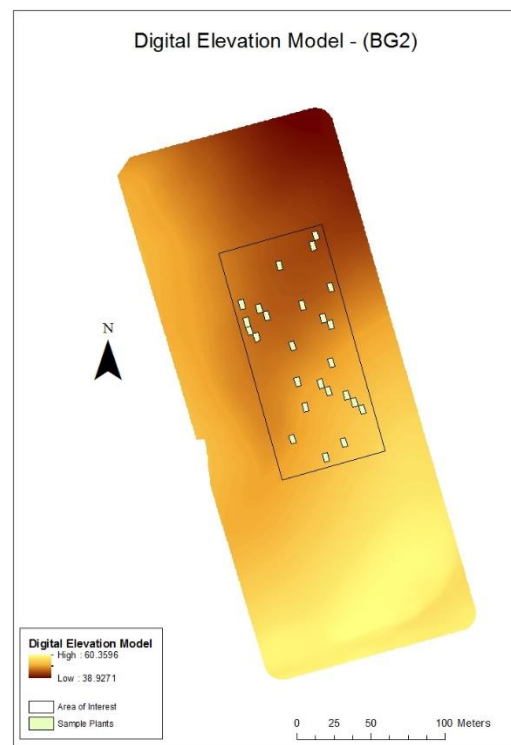


Figure 3-21 Digital Elevation Model (BG2)

Similarly, Relative Elevation was calculated at 5m, 10m, 20m and 50m scales. Relative Elevation is the elevation of each sample plant relative to its surrounding terrain. It is represented by the equation:

*Relative Elevation = Mean Elevation of Sample Plant / Mean Elevation of the surrounding (x) metres, (where (x) = the scale).*

An alternative measure of terrain was also calculated at the 50 metre scale only. Elevation difference (Elevation  $\Delta$ ) is also a measure of where a sample plant is located relative to its surrounding terrain. It is represented by the formula:

*Elevation  $\Delta$  = Mean Elevation of the sample plant – Mean Elevation of the surrounding 50 metres.*

Both Relative Elevation and Elevation  $\Delta$ , measure if a sample plant is in a low-lying area, on a raised area, or on constantly sloping ground (including flat ground). The reason for using two measures of terrain is that Relative Elevation is affected by the elevation of the orchard above sea level whereas Elevation  $\Delta$  is not.

### 3.3 Data Processing

#### 3.3.1 Image Post-processing

Raw images from each survey were stitched and georeferenced using a reputable cloud-based service provider. The resulting orthomosaic images were downloaded for further processing and data extraction using ESRI ArcMap software.

Survey images from the two orchards (BG1 and BG2) were manually georeferenced to ensure that the sample plants were accurately aligned in each round of images. The first survey in each orchard was used as the base reference layer against which all subsequent surveys were then georeferenced. These images were converted to NZTM projections.

Contamination from background reflectance associated with grass, weeds, soil and other objects that were not kiwifruit canopy had to be removed from all images. ArcMap's unsupervised (ISO) classification tool was used to create ten (10) classes of which the first five classes were identified as not being kiwifruit canopy in T1. In later rounds, the number of bands allocated to kiwifruit canopy was specific to each survey to get the most accurate mask possible.

Once unsupervised classification was completed a binary map was created and used to exclude anything from the images that was not classed as kiwifruit canopy prior to data extraction. Six (6) Vegetation Indices as described in section 2.5.3 were created for each survey. Respective binary masks were applied to remove unwanted reflectance data. The ArcMap Zonal statistics tool was used to calculate the mean pixel values within the allocated sample plant bay. These were then exported to a spreadsheet for further statistical analysis.

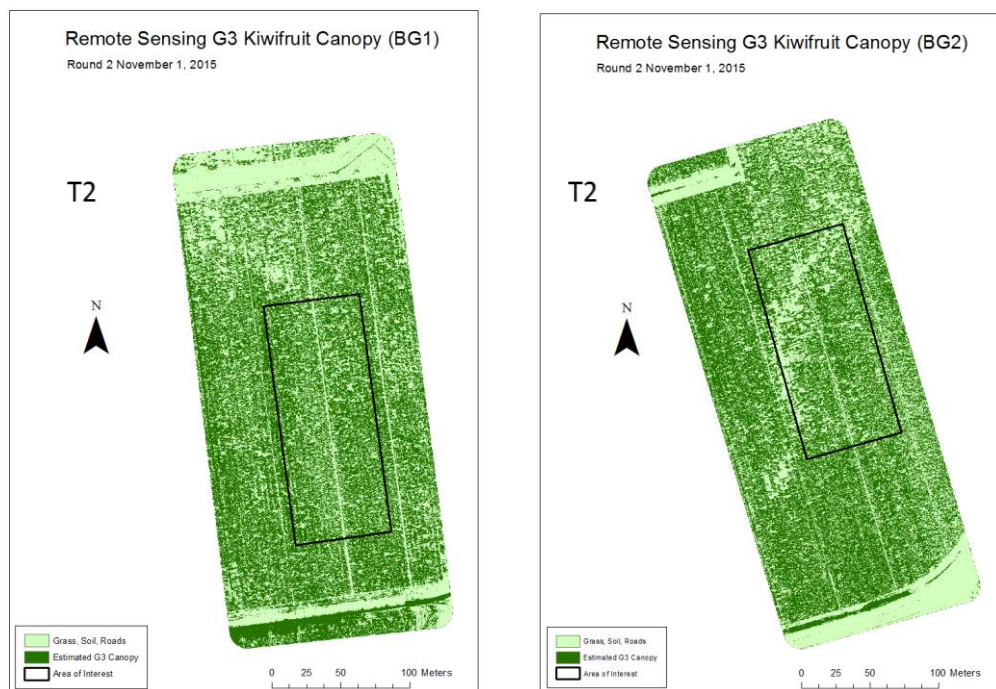


Figure 3-22 Examples of Binary Canopy Maps after exclusion of non-canopy background

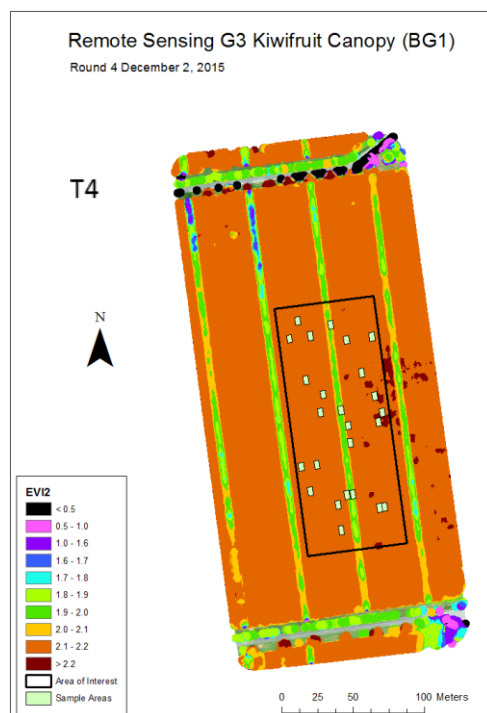
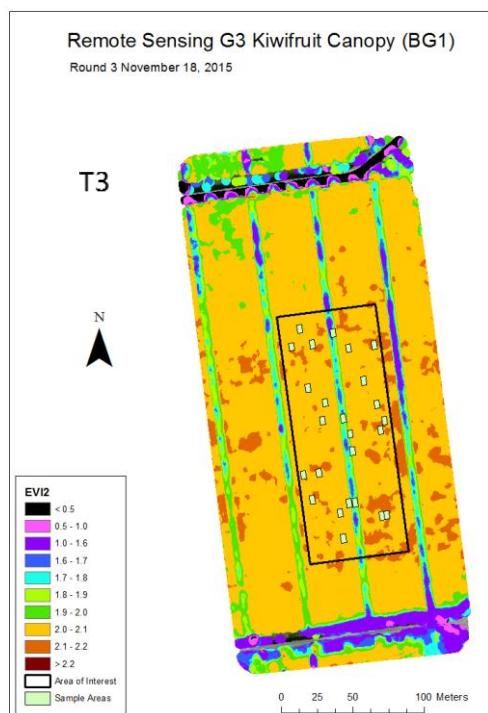
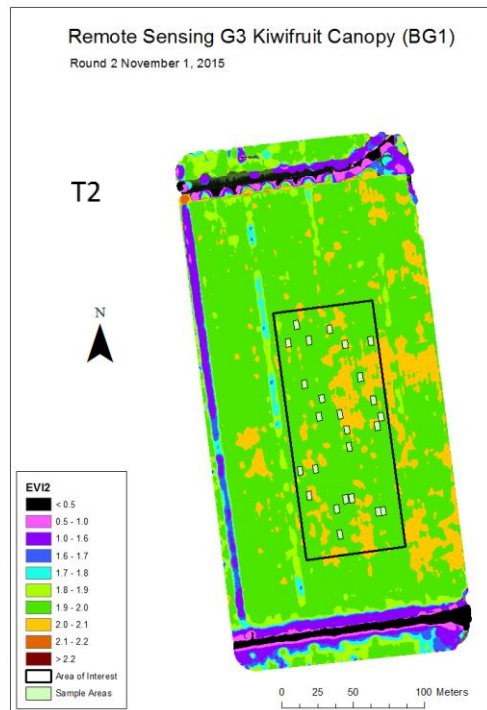
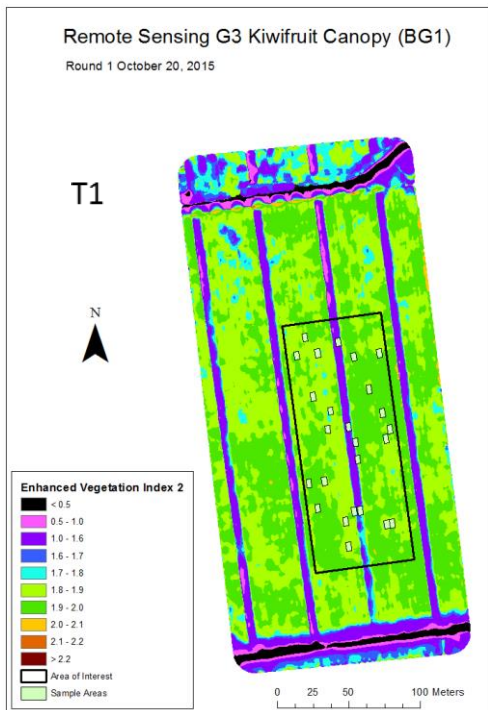


Figure 3-23 Examples of Vegetation Indices (EVI2) created for T1-T4 on BG1 orchard

N.B. The same colour scale is used in all images highlighting changes from one survey to the next over time.

### 3.3.2 Leaf Chlorophyll Measurement

No data processing was required for the non-destructive chlorophyll measurements in the field. All calculations are performed internally within the Minolta SPAD instrument. Raw data results are tabulated in Appendix 1.

For the comparative laboratory based chlorophyll extraction and measurement, the equations provided in the Laboratory Guide (University of Waikato, 2016) were applied as follows:

Corrected Absorbance was first calculated as:

$$\text{Corrected } A^{663.6} = A^{663.6} - A^{750}$$

$$\text{Corrected } A^{646.6} = A^{646.6} - A^{750}$$

Total chlorophyll content of each leaf disc ( $\mu\text{g cm}^2$ ) was calculated using these corrected values as:

$$\text{Chl } a = (12.24 A^{663.6} - 2.55 A^{646.6}) \times 10 \text{ ml (or } \times 8 \text{ ml for BG1 leaf samples)}$$

$$\text{Chl } b = (20.31 A^{646.6} - 4.91 A^{663.6}) \times 10 \text{ ml (or } \times 8 \text{ ml for BG1 leaf samples)}$$

$$\text{Chl } a + b = (17.76 A^{646.6} + 7.34 A^{663.6}) \times 10 \text{ ml (or } \times 8 \text{ ml for BG1 leaf samples)}$$

These equations represent the chlorophyll content of the solution ( $\text{mg ml}^{-1}$ ; coefficients from Porra et al. 1989) multiplied by 10ml and 8ml for BG2 and BG1 leaf sample, respectively, divided by 1 cm of leaf tissue per disc. The result is therefore chlorophyll content per unit leaf area (University of Waikato, 2016).

### 3.3.3 Leaf Area Index Measurement

Processing of the raw data captured by the Licor 2200C instrument was performed on a PC using FV2200 software provided by the instrument manufacturer. A detailed instruction manual was provided (Li-Cor, 2014). The following is a summary of the key steps performed during the data analysis phase.

1. Transfer files from the Licor instrument to a computer using a USB connection;
2. Identify and link sensor match file (M file) created earlier to correct any discrepancies between sensors;
3. Match above canopy data (A files) and below canopy data (B files) based on exact time synchronisation;
4. Create a “K file” (scatter correction) based on the calibration files collected in field before each survey. Apply the scatter correction to the raw data;
5. Specify the number of bands to use in the calculation. In this study, this was set to three bands ( $7^\circ$ ,  $23^\circ$  and  $38^\circ$ ) which approximates the extent of the canopy occupied by one sample plant;  
(N.B. incorporating more than three bands in the equation would likely have included canopy beyond the sample plant)
6. Run Leaf Area Index calculations for each sample plant and save the resulting file. Sample plants can be processed individually or in batches. Both methods were used in this study; and
7. Export Mean LAI values to a spreadsheet for further statistical analysis.

Orchard = A = BG1  
 Sample Plant 1 (side A & B)  
 (Split records due to shelter cloth)

Number Above  
Canopy Records

Number Below  
Canopy Records

Scatter Correction  
(K values)

Sample Plant 3  
(single record)

LAI File	Date	TransComp	Model	Records	ScattCorr	LAI
1117A1A	20151117 10:35:01	c-p-s	Horizontal	3A 3B 3K 3G	0.015	4.23
1117A1B	20151117 10:48:20	c-p-s	Horizontal	3A 3B 2K 3G	0.028	4.54
1117A2A	20151117 10:37:46	c-p-s	Horizontal	3A 3B 2K 3G	0.019	3.47
1117A2B	20151117 10:45:44	c-p-s	Horizontal	3A 3B 2K 3G	0.011	4.07
1117A3	20151117 10:39:34	c-p-s	Horizontal	6A 6B 4K 6G	0.0038	4.16
1117A4	20151117 10:40:58	c-p-s	Horizontal	6A 6B 4K 6G	0.0065	3.86
1117A5	20151117 10:42:46	c-p-s	Horizontal	6A 6B 3K 6G	0.019	1.87
1117A6	20151117 10:44:02	c-p-s	Horizontal	6A 6B 3K 6G	0.0027	3.22
1117A7	20151117 10:46:48	c-p-s	Horizontal	6A 6B 3K 6G	0.014	2.77
1117A8A	20151117 10:52:19	c-p-s	Horizontal	3A 3B 2K 3G	0.0028	2.51
1117A8B	20151117 11:10:21	c-p-s	Horizontal	3A 3B 3K 3G	0.018	4.54
1117A9	20151117 10:53:19	c-p-s	Horizontal	6A 6B 3K 6G	0.012	4.00
1117A10A	20151117 10:55:00	c-p-s	Horizontal	3A 3B 2K 3G	0.02	3.88
1117A10B	20151117 11:05:37	c-p-s	Horizontal	3A 3B 2K 3G	0.036	5.15
1117A11	20151117 10:55:47	c-p-s	Horizontal	6A 6B 3K 6G	0.02	4.58
1117A12	20151117 10:57:05	c-p-s	Horizontal	6A 6B 3K 6G	0.0091	3.96
1117A13A	20151117 10:58:39	c-p-s	Horizontal	3A 3B 2K 3G	0.025	2.43
1113B	20151117 11:03:56	c-p-s	Horizontal	3A 3B 3K 3G	0.02	4.54
1117A14	20151117 10:59:45	c-p-s	Horizontal	6A 6B 4K 6G	0.0099	3.19
1117A15	20151117 11:01:05	c-p-s	Horizontal	6A 6B 3K 6G	0.0039	3.33
1117A16	20151117 11:02:17	c-p-s	Horizontal	6A 6B 4K 6G	0.013	2.65
1117A17A	20151117 11:08:45	c-p-s	Horizontal	3A 3B 2K 3G	0.013	4.15
1117A17B	20151117 11:22:06	c-p-s	Horizontal	3A 3B 2K 3G	0.016	3.07
1117A18	20151117 11:07:08	c-p-s	Horizontal	6A 6B 3K 6G	0.0038	3.40

Plant 1  
Leaf Area Index  
(mean 2 readings)

Plant 3  
Leaf Area Index

Figure 3-24 FV2200 Screen shot showing examples of “split” and single observations for each sample plant.

### 3.4 Statistical Analysis

Data collected and exported from the six Vegetation Indices, the Leaf Area Index calculations, and leaf Chlorophyll measurements described above were all tabulated for each of the four rounds of observations. Mean values for T1-T4 were also calculated. Data from each orchard were consolidated into a single data set. These are provided in the Appendices.

The consolidated data set was imported into Statistica software for statistical analysis as follows. N.B. The steps outlined are iterative rather than sequential:

1. A descriptive analysis including:
  - performing a Summary Statistics Analysis of mean (T1-T4) values to determine Mean, Maximum, Minimum, Standard Deviation, Normal-P plot and distribution histogram for each of the sample plants;
  - creating box and whisker plots of key variables to show trending changes over time;
  - calculating Analysis of Variance for key variables of interest (ANOVA Repeated Measure Analysis) to determine the significance of observed changes over time; and
  - creating Correlation Matrices for all measured variables and calculated variables (“derived variables”) using mean values (T1-T4) to identify areas of interest for further targeted investigation.
2. A series of Stepwise Multiple Regressions were calculated using different combinations of measured and derived variables as the dependent and Predictor variables. The aim of this step was twofold:
  - a) To determine which variable or variables were the best proxy for plant vigour (the dependent variable); and
  - b) To determine which variable or variables best explain the dependent variable chosen in 2a and to what extent.
3. An analysis of errors was undertaken on models of interest to determine if errors were normally distributed. Outliers were identified and removed where justifiably warranted. The steps above were repeated until the three “best” models were obtained.

## 4 Results

---

This chapter is divided into four (4) sections. Each section only includes the significant results. Other relevant data, not included in this chapter, can be found in the appendices.

Section 4.1 Canopy Vigour Measurements

Section 4.2 Remote Sensing and GIS Measurements

Section 4.3 Correlations

Section 4.3 Multiple Regressions

---

Section 4.1 includes an Analysis of Variance for Leaf Area Index (LAI) and Leaf Chlorophyll (Chl\_SPAD). Each table provides a measure of how significantly different the observations are, over the course of the study. Box and Whisker Plots illustrate changes in each variable from T1 to T4. A summary of the differences (Mean T1-T4) between the sample plants is provided. Finally, there is a comparison of laboratory-based chlorophyll measurements (destructive) with field-based measurements (non-destructive) using a proximal sensor (Minolta SPAD).

Section 4.2 analyses remotely-sensed, canopy reflectance, in the same way that the previous section looked at canopy vigour. This section also tables orchard topography data extracted using GIS tools.

Important correlations are illustrated with Scatter Plots in Section 4.3 and the final section (Section 4.4), tables three multiple regression models. Each model explains canopy vigour using 1, 2 or 3 remotely sensed measurements. The dependent variable in all multiple regression equations is LAI x Chl\_SPAD. These multiple regression models underpin the discussion in Chapter 5.

## 4.1 Canopy Vigour Measurements

### 4.1.1 Leaf Area Index Measurements

Changes in Leaf Area Index with time.

Table 4-1 Analysis of Variance Table - Leaf Area Index

Repeated Measures Analysis of Variance (Summary Mean LAI in Dataset_Summary_Master_V2 2018)					
Sigma-restricted parameterization					
Effective hypothesis decomposition					
Effect	SS	Degr. of Freedom	MS	F	p
Intercept	1696.313	1	1696.313	460.4486	0.00
Error	139.994	38	3.684		
TIME	223.214	3	74.405	126.2577	0.00
Error	67.181	114	0.589		

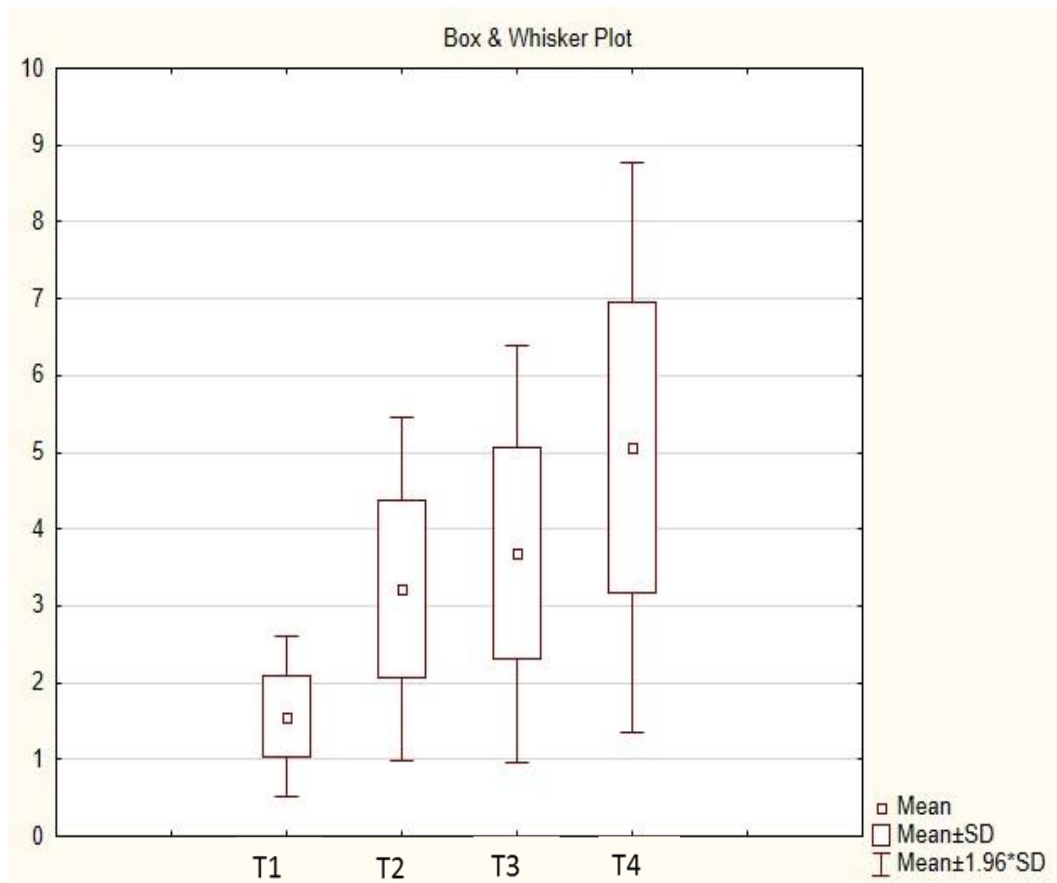


Figure 4-1 Box & Whisker plot illustrates significant increase in LAI across the four sampling periods.

Plot includes all cases including outliers.

- Mean Leaf Area Index differs strongly across time. Mean values increase steadily as the season progresses.

Differences in Mean LAI between plants (T1 - T4).

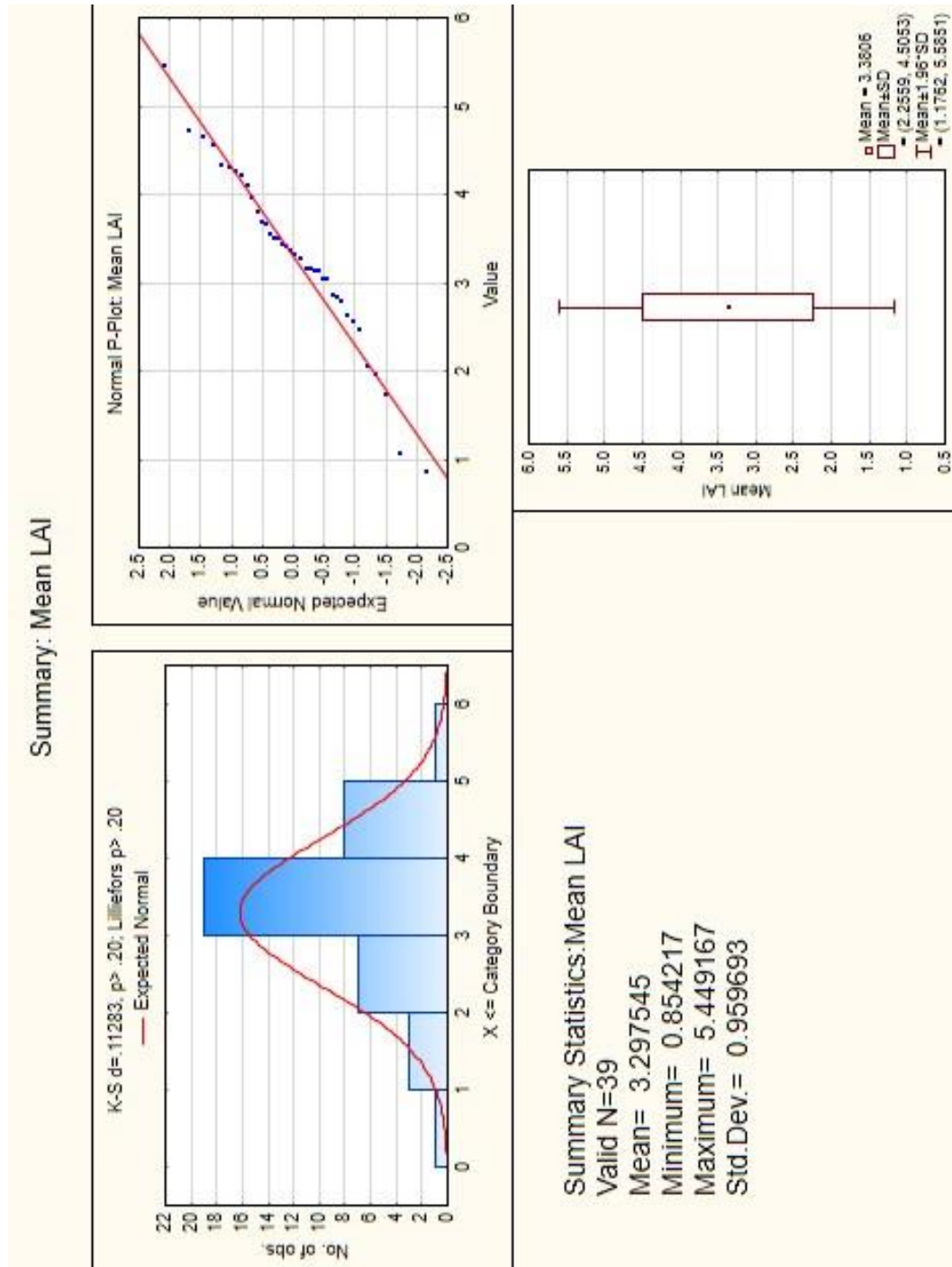


Figure 4-2 Histogram, Scatterplot and Box & Whisker graphs illustrate summary statistics for Mean Leaf Area Index (T1-T4)

## 4.1.2 Chlorophyll Measurements

### Changes in Chlorophyll with time

Table 4-2 Analysis of Variance Table - Leaf Chlorophyll

Repeated Measures Analysis of Variance (Summary Chlorophyll in Dataset_Summary_Master_V2.2 Sigma-restricted parameterization Effective hypothesis decomposition)					
Effect	SS	Degr. of Freedom	MS	F	p
Intercept	215871.6	1	215871.6	15679.27	0.00
Error	523.2	38	13.8		
TIME	2360.7	3	786.9	720.41	0.00
Error	124.5	114	1.1		

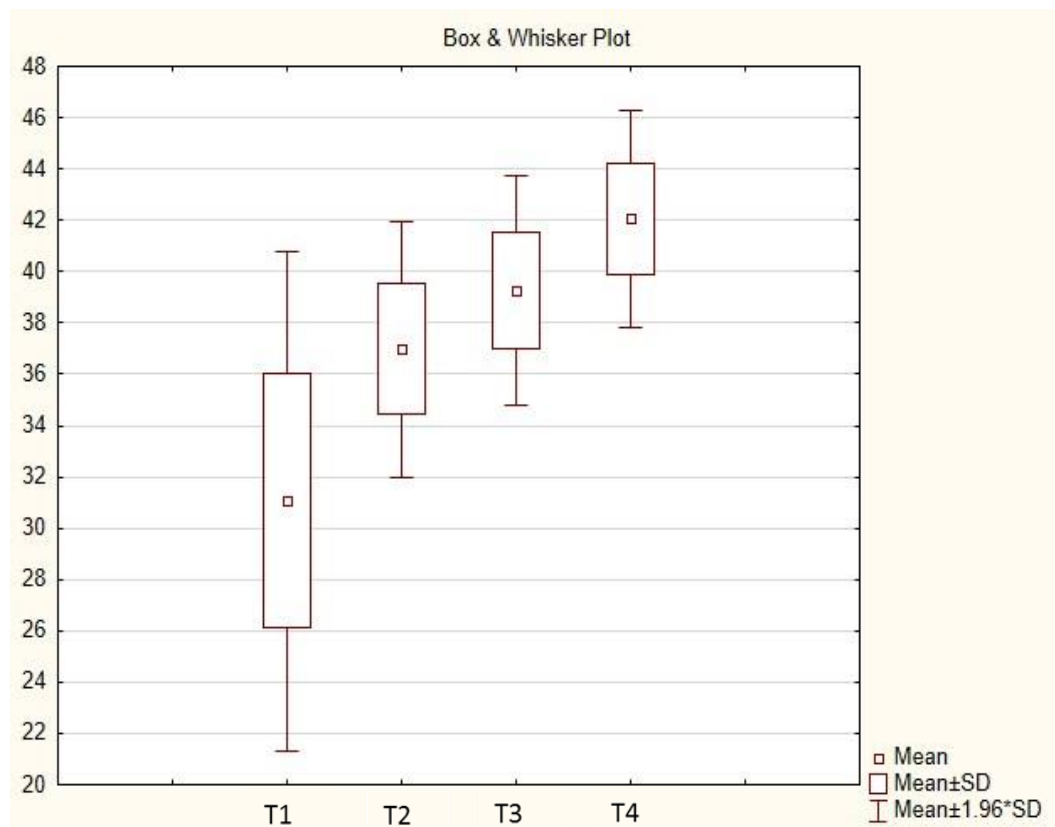


Figure 4-3 Box & Whisker plot illustrates significant increase in Leaf Chlorophyll across the four sampling periods.

Plot includes all cases including outliers.

- Chlorophyll differs strongly across time. Mean values increase steadily as the season progresses.
- Note the greater variability between Sample Plants in period T1.

Differences in Mean Chlorophyll between plants (T1 - T4).

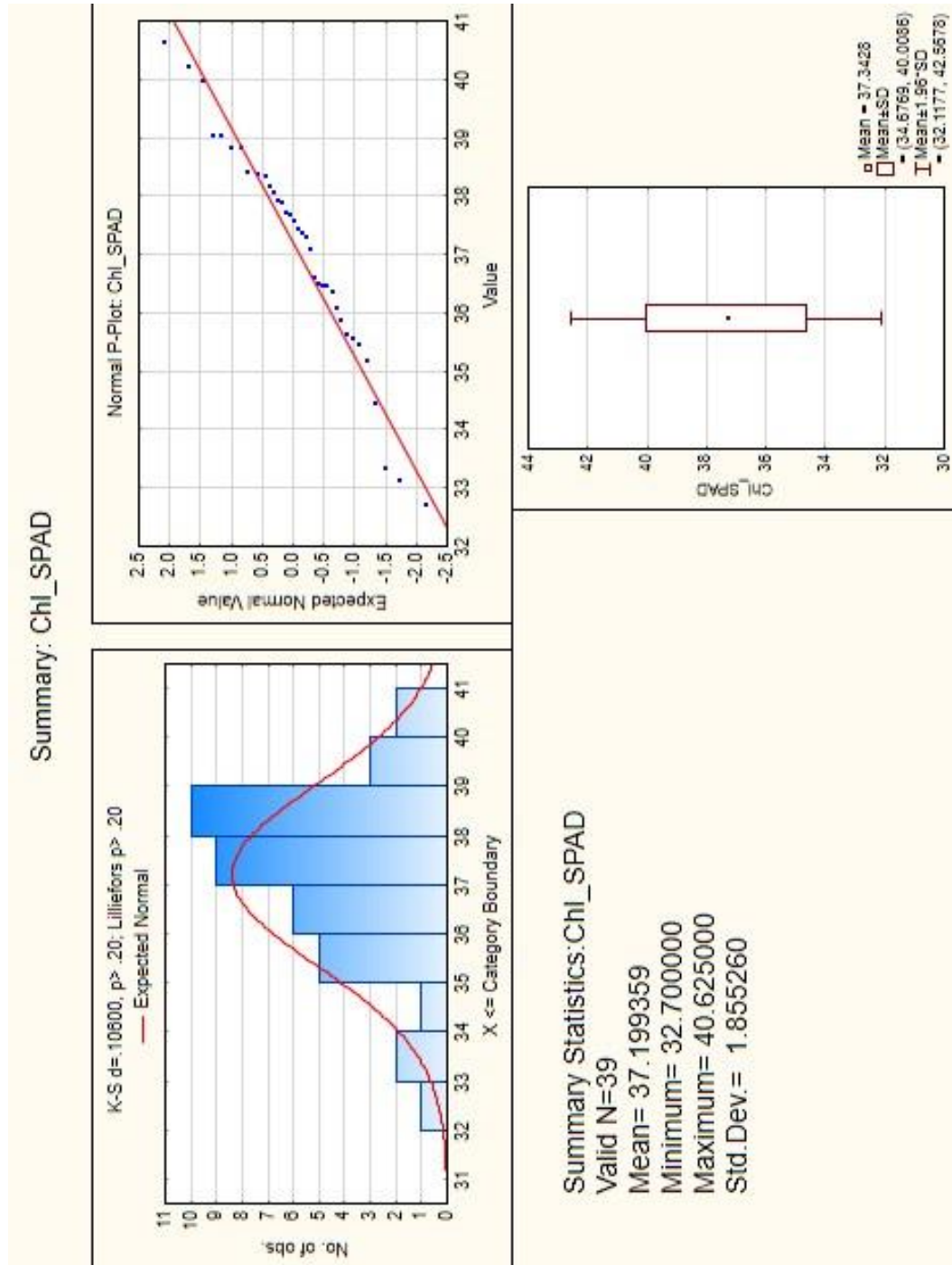


Figure 4-4 Histogram, Scatterplot and Box & Whisker graphs illustrate summary statistics for Mean Leaf Chlorophyll (T1-T4)

## Comparison of Laboratory vs Minolta SPAD chlorophyll measurements

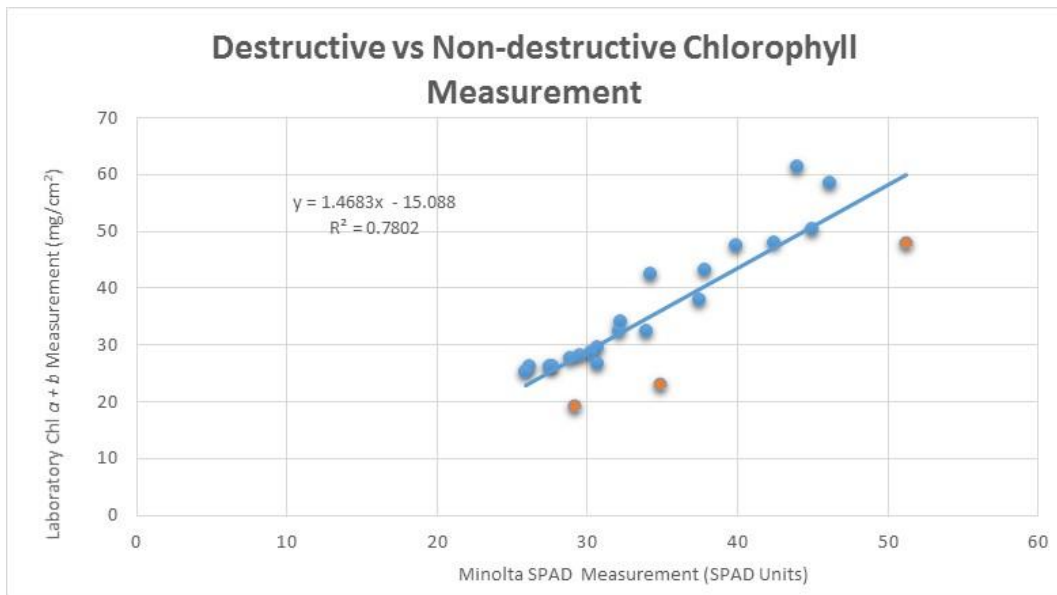


Figure 4-5 Scatter plot illustrates correlation between laboratory & field chlorophyll measurements\*

\*Before removal of outliers (marked in orange)

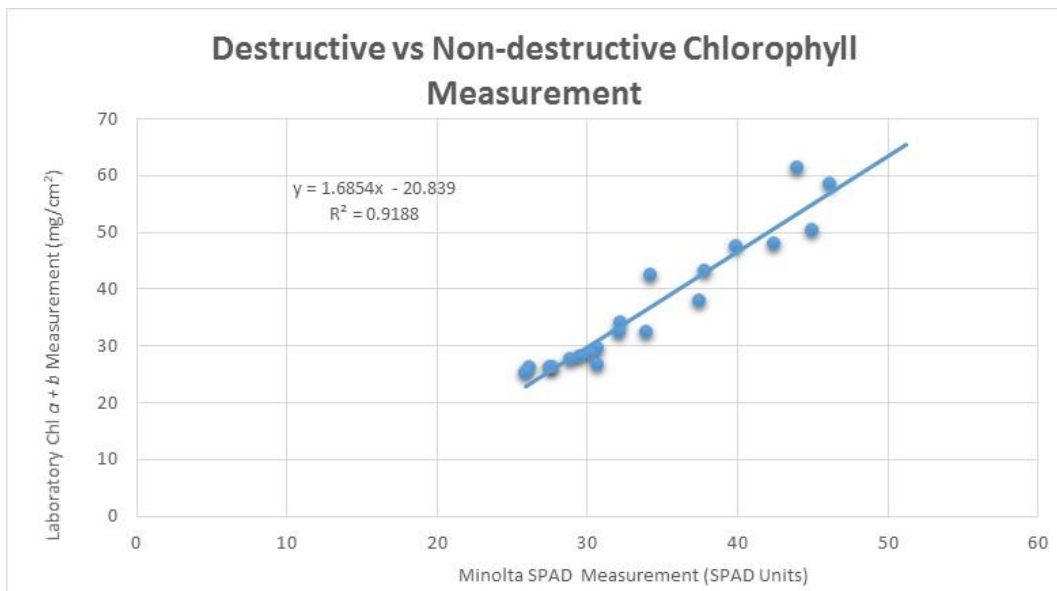


Figure 4-6 Scatter plot illustrates correlation between laboratory & field chlorophyll measurements\*.

\*After removal of outliers

## 4.2 Remote Sensing and GIS Measurements

### 4.2.1 Canopy Reflectance Measurements

#### 4.2.1.1 NDVI

Table 4-3 Analysis of Variance Table - NDVI

Repeated Measures Analysis of Variance (Summary NDVI in Dataset_Summary_Master_V2 20 Sigma-restricted parameterization Effective hypothesis decomposition)					
Effect	SS	Degr. of Freedom	MS	F	p
Intercept	119.4500	1	119.4500	448310.6	0.00
Error	0.0101	38	0.0003		
TIME	0.1772	3	0.0591	1221.5	0.00
Error	0.0055	114	0.0000		

NB Plot includes all cases including outliers.

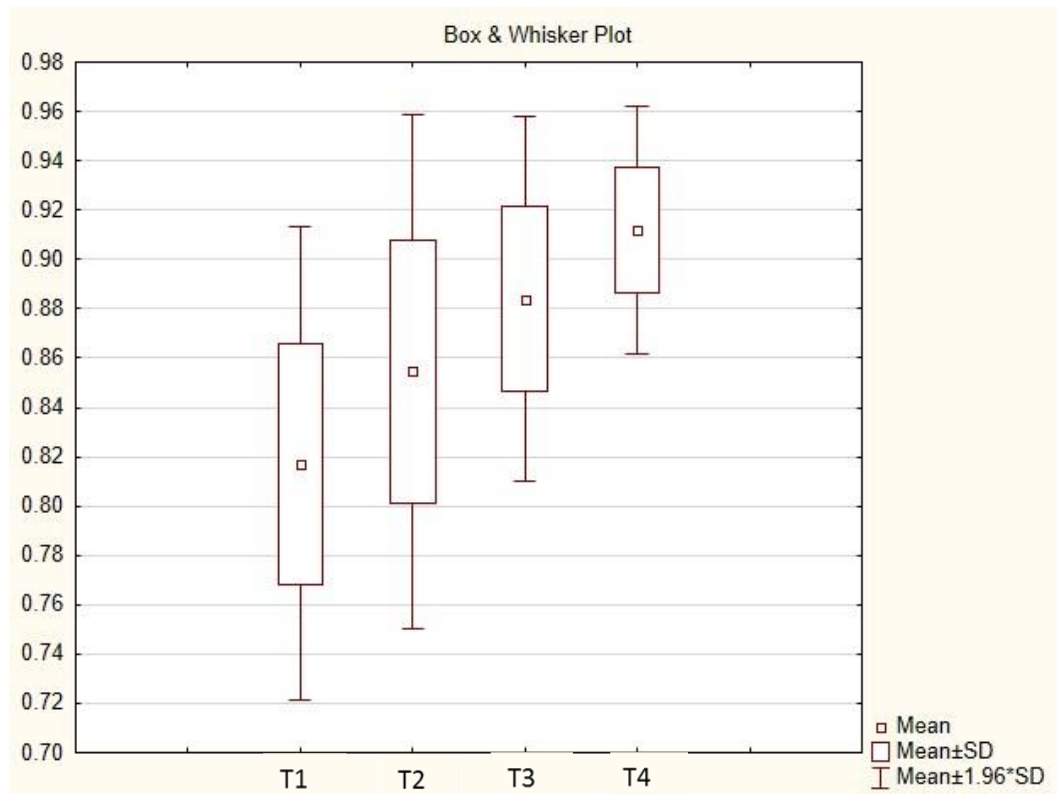


Figure 4-7 Box & Whisker plot illustrates significant increase in NDVI across the four sampling periods

- NDVI differs strongly across time. Mean values increase steadily as the season progresses.

Differences in Mean NDVI between plants (T1 - T4).

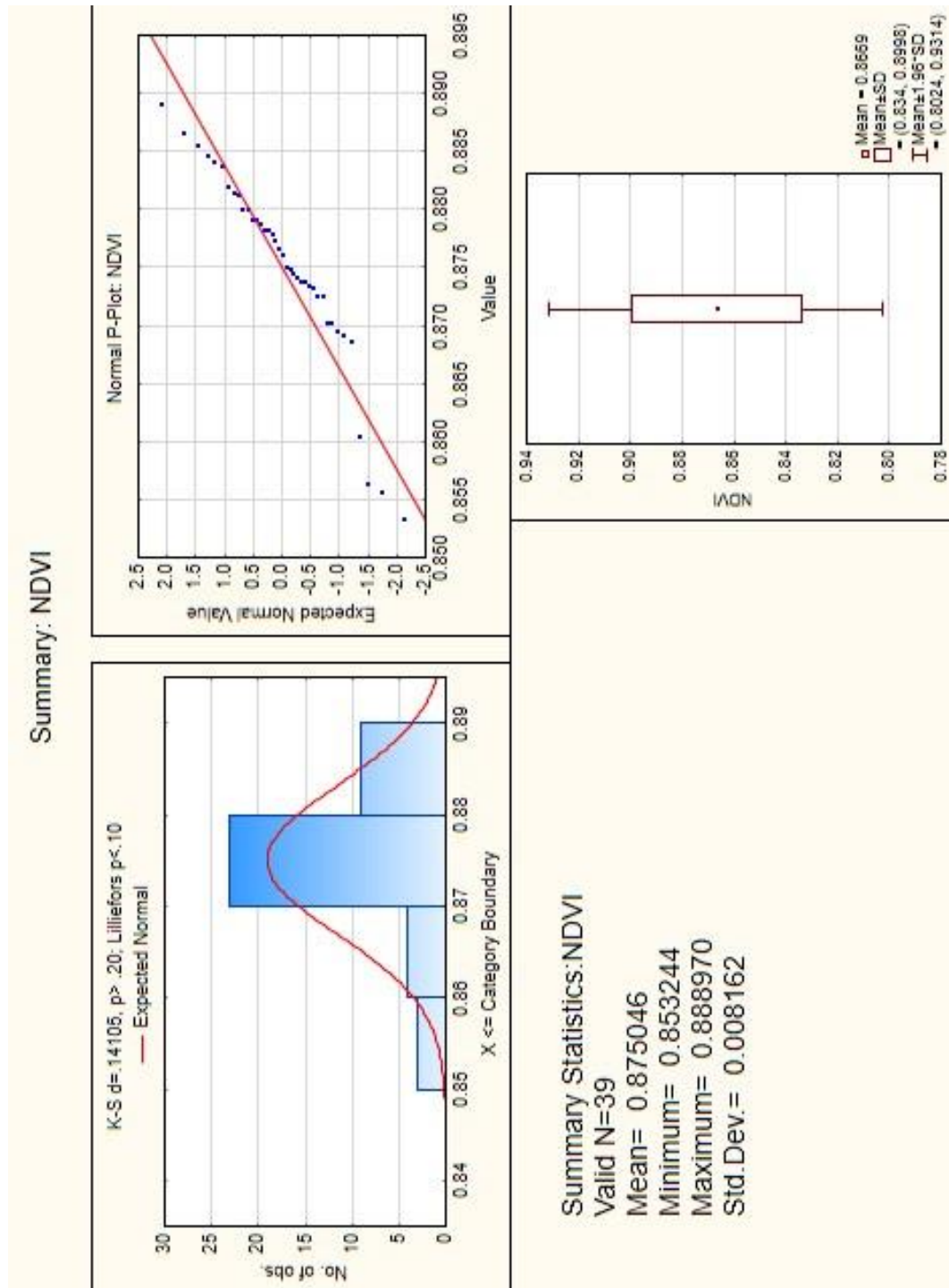


Figure 4-8 Histogram, Scatterplot and Box & Whisker graphs illustrate summary statistics for Mean NDVI (T1-T4)

#### 4.2.1.2 EVI2

Table 4-4 Analysis of Variance Table - EVI2

Repeated Measures Analysis of Variance (Summary EVI2 in Dataset_Summary_Master_V2 20: Sigma-restricted parameterization Effective hypothesis decomposition					
Effect	SS	Degr. of Freedom	MS	F	p
Intercept	633.9422	1	633.9422	200645.6	0.00
Error	0.1201	38	0.0032		
TIME	2.2323	3	0.7441	1370.8	0.00
Error	0.0619	114	0.0005		

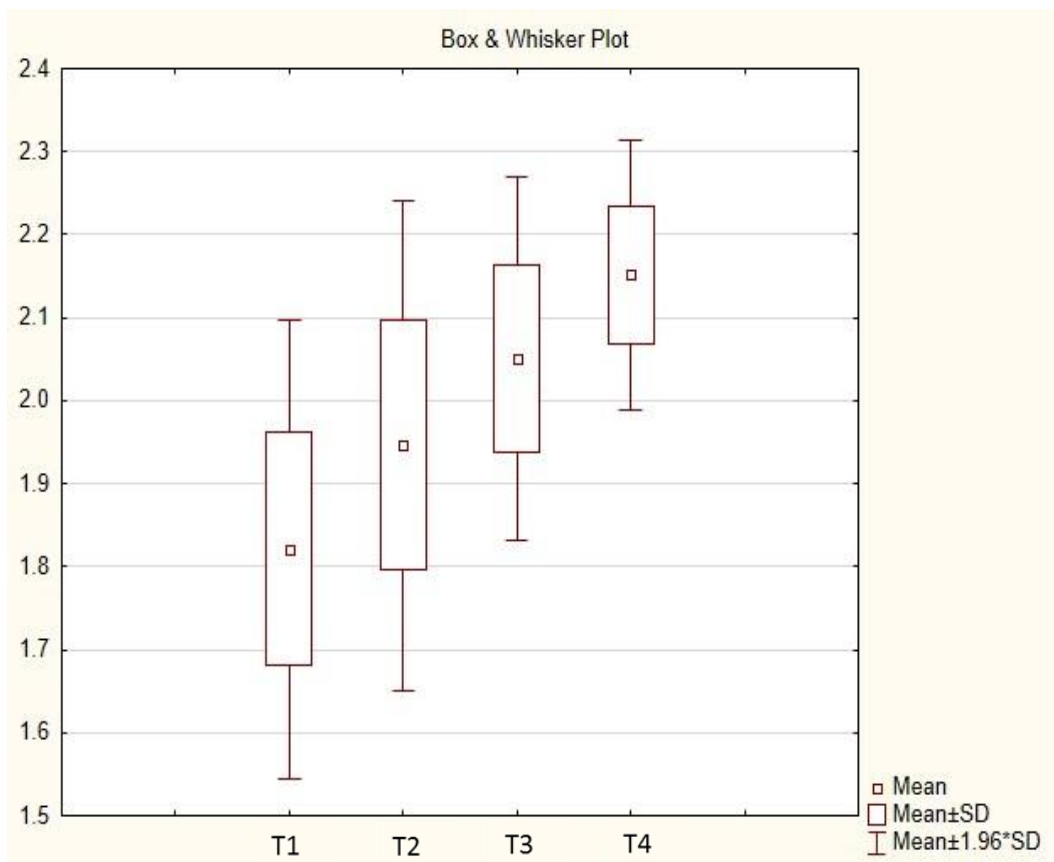


Figure 4-9 Box & Whisker plot illustrates significant increase in EVI2 across the four sampling periods.

NB Plot includes all cases including outliers

- EVI2 differs strongly across time. Mean values increase steadily as the season progresses.

Differences in Mean EVI2 between plants (T1 - T4).

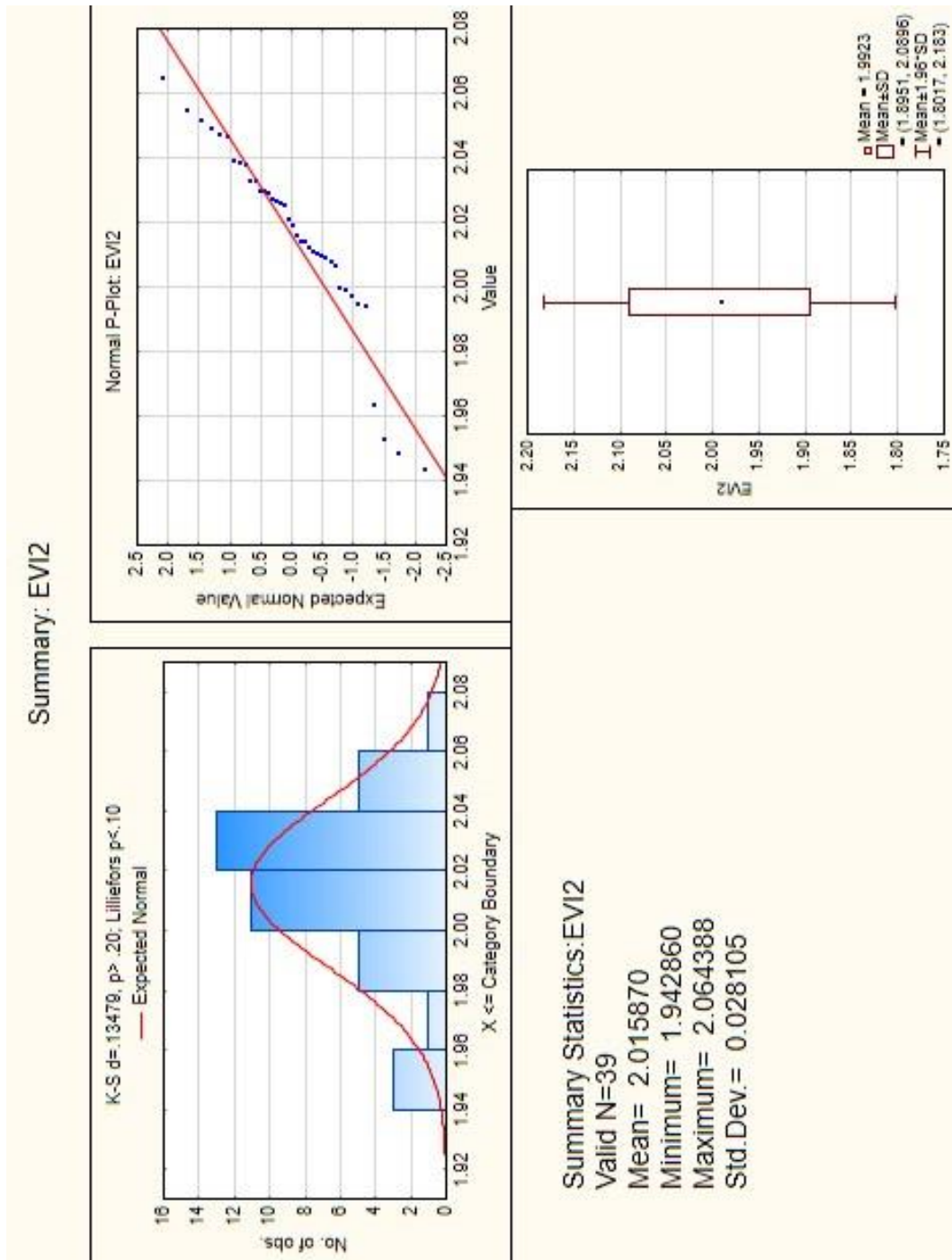


Figure 4-10 Histogram, Scatterplot and Box & Whisker graphs illustrate summary statistics for Mean EVI2 (T1-T4)

### 4.2.1.3 PVR

Table 4-5 Analysis of Variance Table - PVR

Repeated Measures Analysis of Variance (Summary PVR in Dataset_Summary_Master_V2 20: Sigma-restricted parameterization Effective hypothesis decomposition					
Effect	SS	Degr. of Freedom	MS	F	p
Intercept	1590.446	1	1590.446	20699.77	0.00
Error	2.920	38	0.077		
TIME	33.419	3	11.140	1146.21	0.00
Error	1.108	114	0.010		

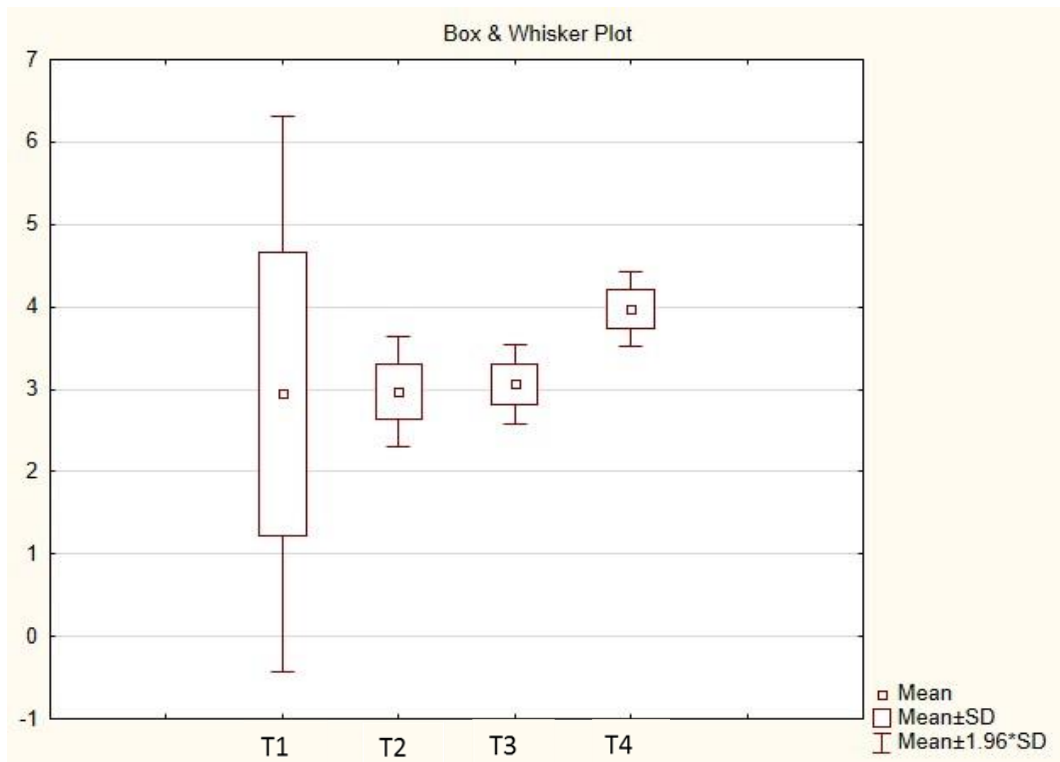


Figure 4-11 Box & Whisker plot illustrates minimal increase in Mean PVR across the first three sampling periods.

NB Plot includes all cases including outliers. Note the greater variability in Sample Plants in period T1.

- PVR differs moderately across time. Mean values remain steady from T1 to T3 and then increase in T4.

Differences in Mean PVR between plants (T1 - T4).

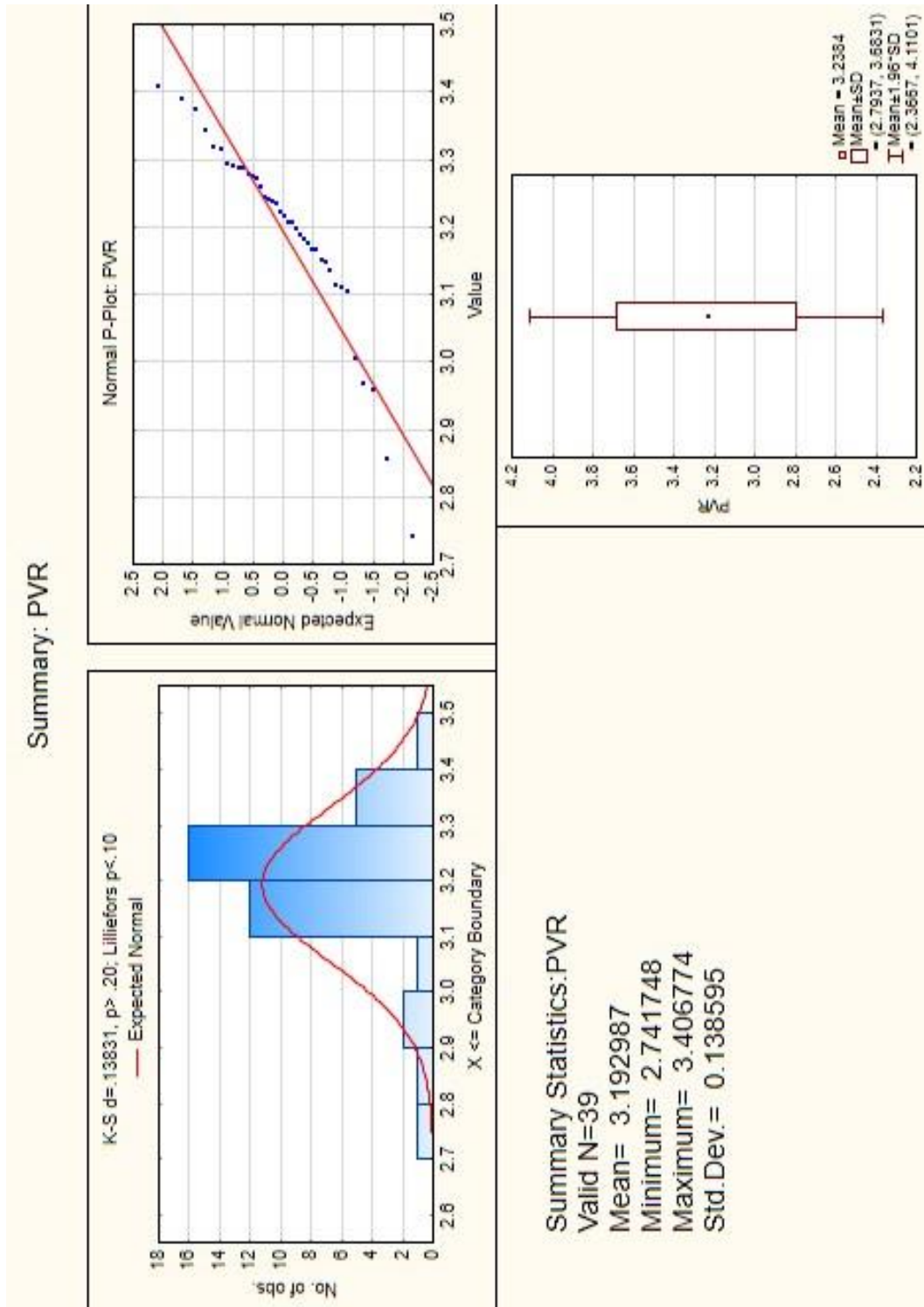


Figure 4-12 Histogram, Scatterplot and Box & Whisker graphs illustrate summary statistics for Mean PVR (T1-T4)

#### 4.2.1.4 NDRE

Table 4-6 Analysis of Variance Table - NDRE

Repeated Measures Analysis of Variance (Summary NDRE in Dataset_Summary_Master_V2 : Sigma-restricted parameterization Effective hypothesis decomposition					
Effect	SS	Degr. of Freedom	MS	F	p
Intercept	16.38042	1	16.38042	30434.70	0.00
Error	0.02045	38	0.00054		
TIME	0.47231	3	0.15744	1476.80	0.00
Error	0.01215	114	0.00011		

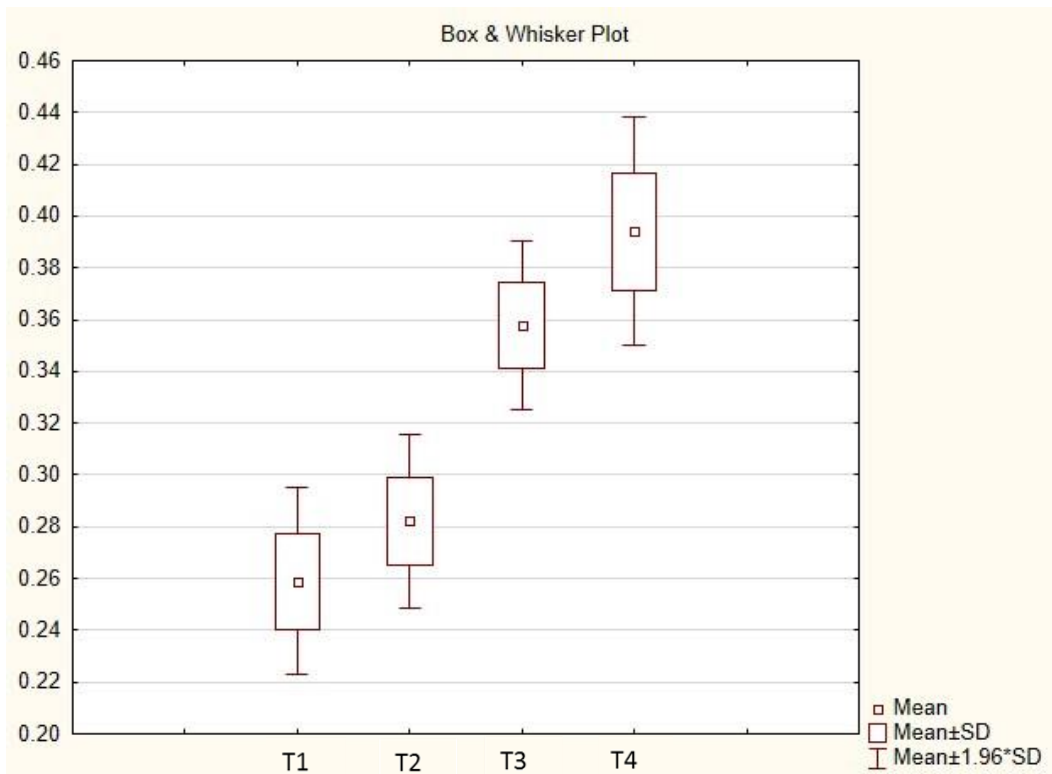


Figure 4-13 Box & Whisker plot illustrates significant increase in NDRE across the four sampling periods.

NB Plot includes all cases including outliers.

- NDRE differs strongly across time. Mean values increase steadily as the season progresses.

Differences in Mean NDRE between plants (T1 - T4).

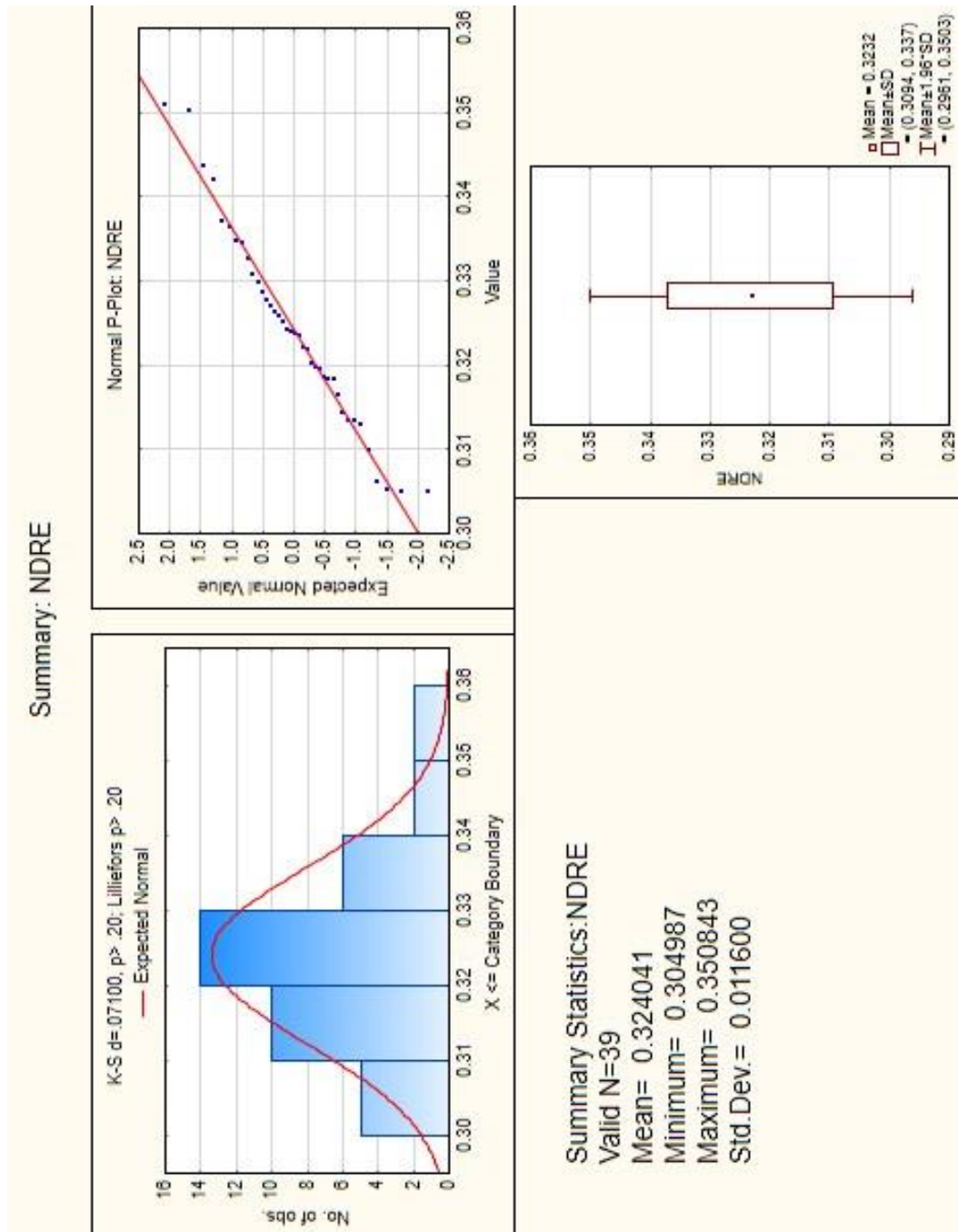


Figure 4-14 Histogram, Scatterplot and Box & Whisker graphs illustrate summary statistics for Mean NDRE (T1-T4)

#### 4.2.1.5 GCI

Table 4-7 Analysis of Variance Table - GCI

Effect	Repeated Measures Analysis of Variance (Summary GCI in Dataset_Summary_Master_V2 2 Sigma-restricted parameterization Effective hypothesis decomposition)				
	SS	Degr. of Freedom	MS	F	p
Intercept	2682.616	1	2682.616	19487.25	0.00
Error	5.231	38	0.138		
TIME	103.804	3	34.601	1267.93	0.00
Error	3.111	114	0.027		

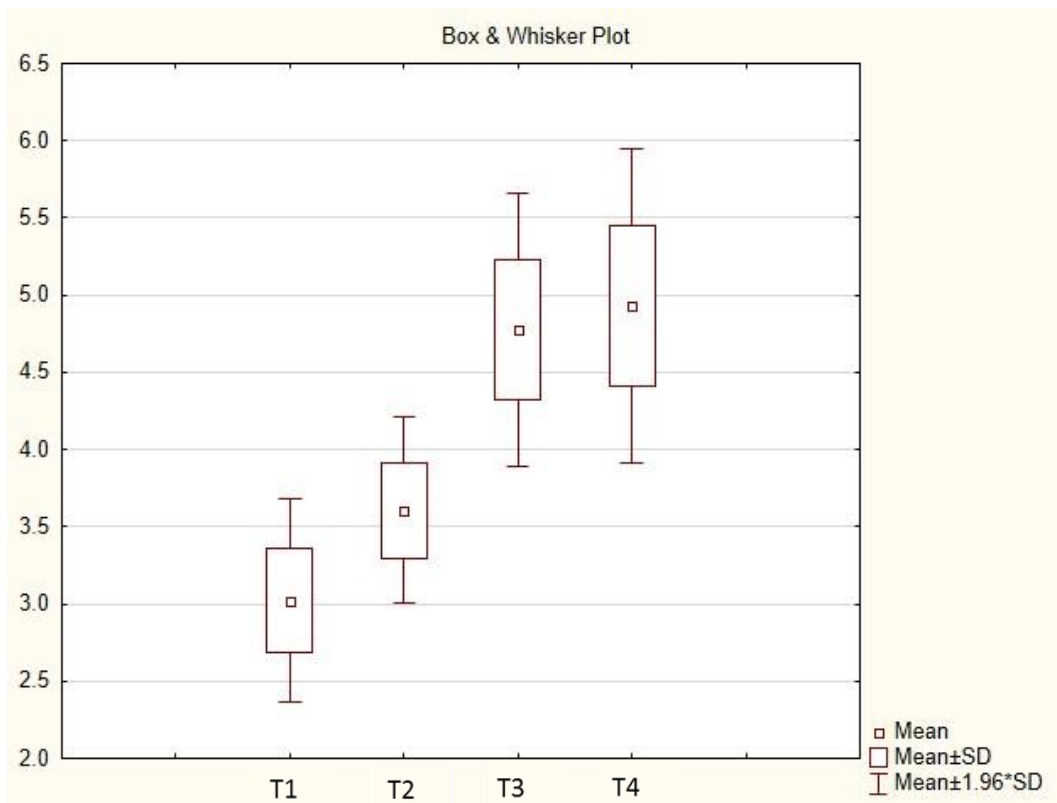


Figure 4-15 Box & Whisker plot illustrates significant increase in GCI across the four sampling periods. NB Plot includes all cases including outliers.

- GCI differs strongly across time. Mean values increase steadily as the season progresses.

Differences in Mean GCI between plants (T1 - T4).

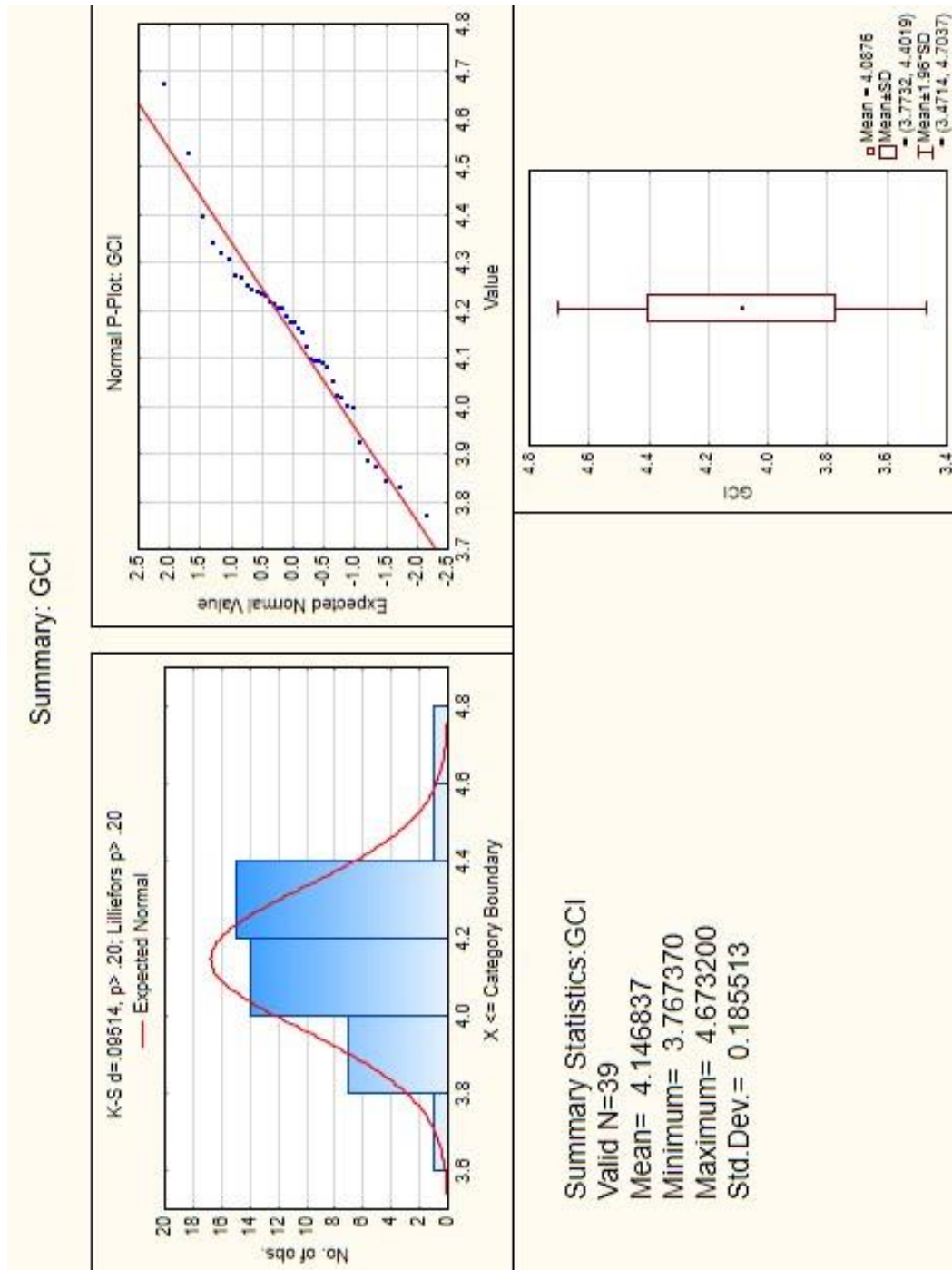


Figure 4-16 Histogram, Scatterplot and Box & Whisker graphs illustrate summary statistics for Mean GCI (T1-T4)

#### 4.2.1.6 RECI

Table 4-8 Analysis of Variance Table - RECI

Effect	Repeated Measures Analysis of Variance (Summary RECI in Dataset_Summary_Master_V2 ; Sigma-restricted parameterization Effective hypothesis decomposition)				
	SS	Degr. of Freedom	MS	F	p
Intercept	151.4881	1	151.4881	13401.22	0.00
Error	0.4296	38	0.0113		
TIME	9.4901	3	3.1634	1573.12	0.00
Error	0.2292	114	0.0020		

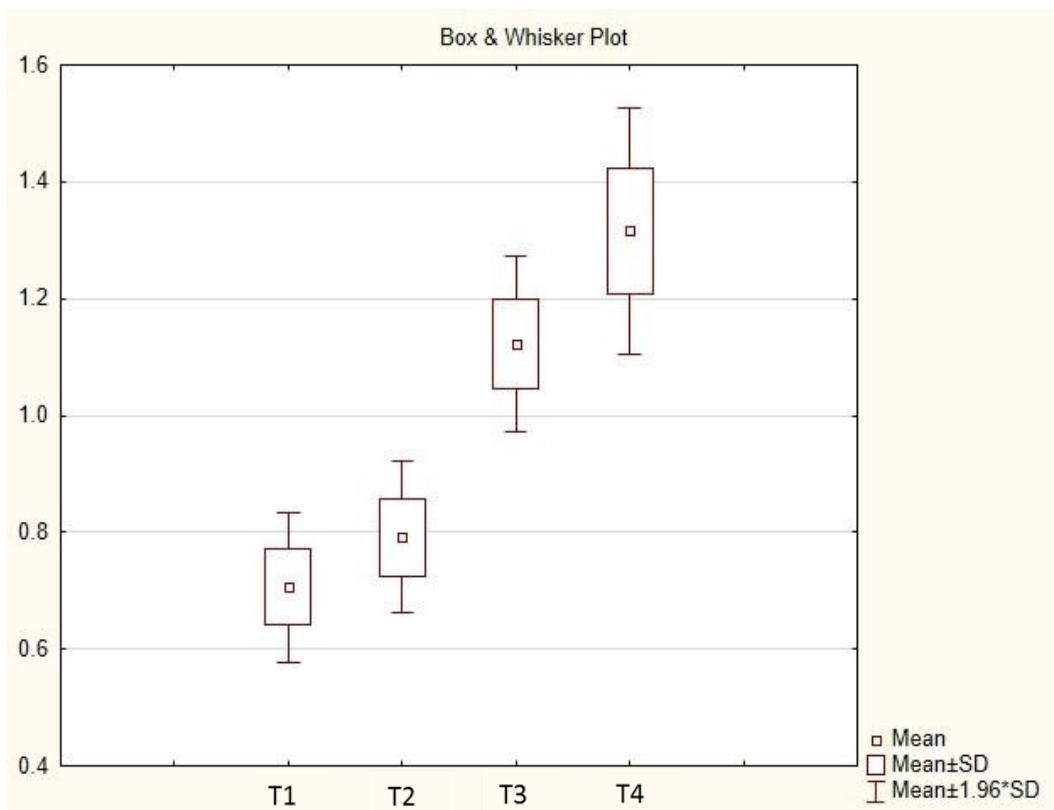


Figure 4-17 Box & Whisker plot illustrates significant increase in RECI across the four sampling periods

NB Plot includes all cases including outliers.

- RECI differs strongly across time. Mean values increase steadily as the season progresses.

Differences in Mean RECI between plants (T1 - T4).

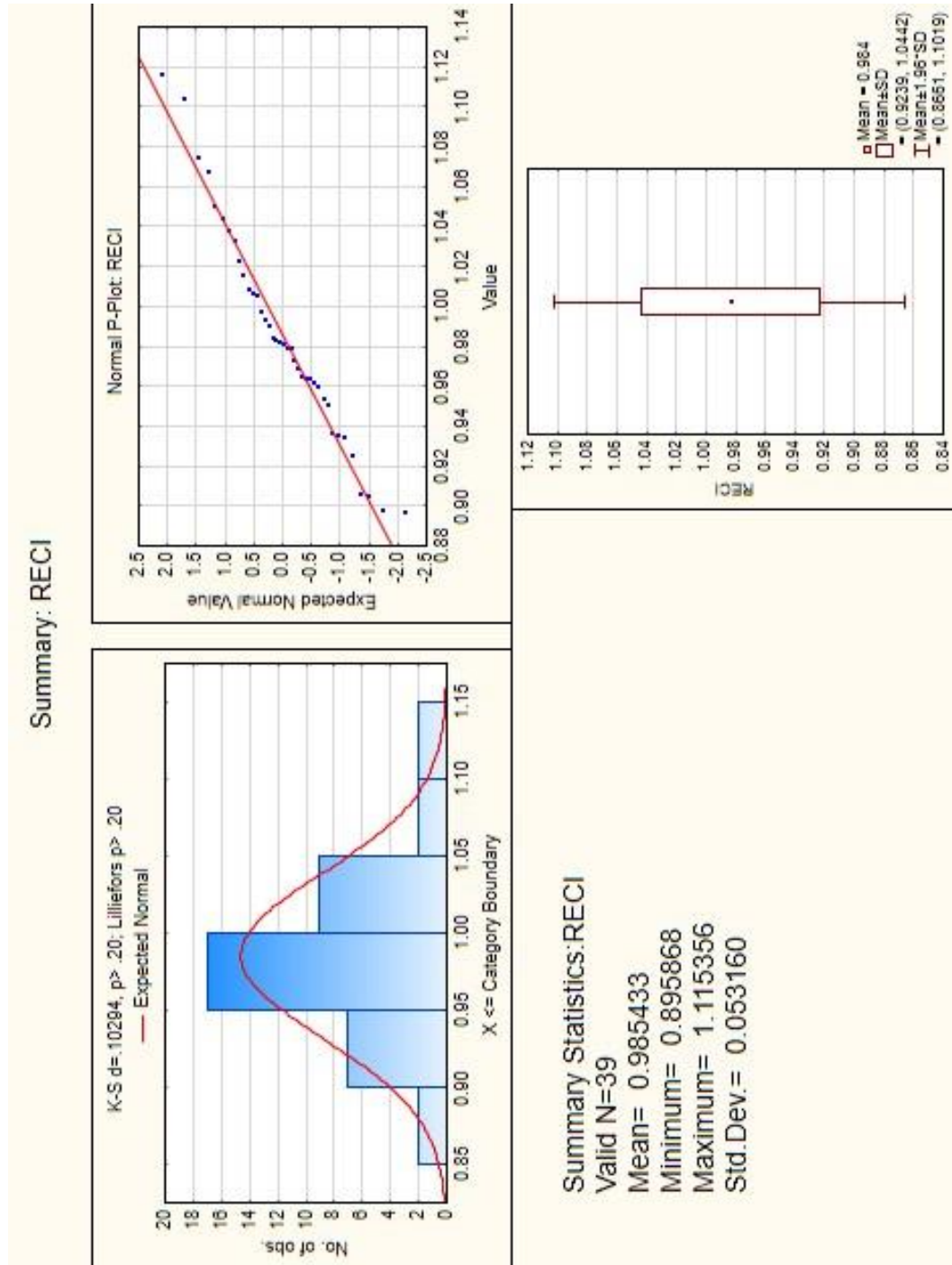


Figure 4-18 Histogram, Scatterplot and Box & Whisker graphs illustrate summary statistics for Mean RECI (T1-T4)

#### 4.2.1.7 Summary - Mean Vegetation Indices (T1 – T4)

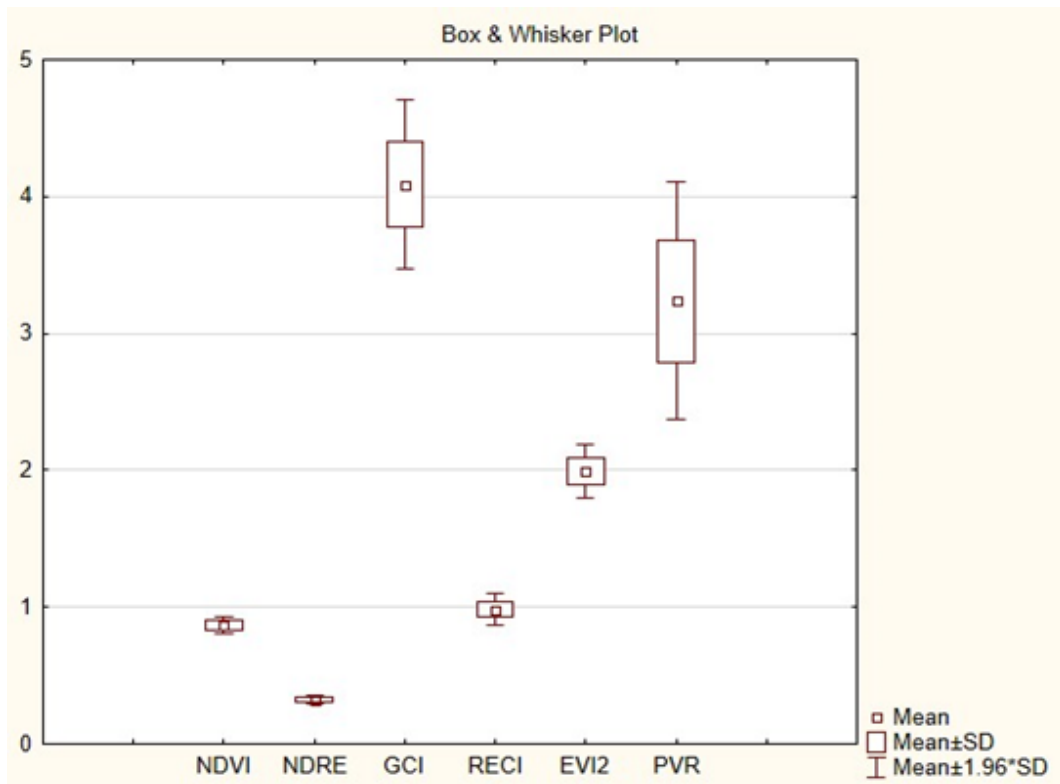


Figure 4-19 Box & Whisker plot illustrates differences in overall Mean Vegetation Index values.

Note differences in variability between indices.

- PVR and GCI are both significantly more variable than other indices over the duration of the study.
- NDRE is the least variable index over the duration of the study.

## 4.2.2 Orchard Topography Measurements

Table 4-9 Table of Orchard Topography for each sample plant.

Point Name	Block	Mean Elevation	Relative Elevation-5m	Relative Elevation-10m	Relative Elevation-20m	Relative Elevation-50m	Mean Slope 50m	Slope (Rise/Run)	Rise (Slope x Run)	Elevation Delta 50m
A1	BG1	67.9180	1.0000	1.0001	0.9998	0.9985	6.7400	1.9971	3.3700	-0.0993
A2	BG1	68.6008	0.9996	0.9985	0.9946	0.9790	9.3049	1.9580	4.6524	-1.4714
A3	BG1	74.4185	1.0002	1.0006	1.0023	1.0145	5.9268	2.0289	2.9634	1.0602
A4	BG1	74.4265	1.0001	1.0006	1.0020	1.0136	6.0502	2.0272	3.0251	1.0002
A5	BG1	69.5342	1.0000	0.9996	0.9974	0.9858	8.9175	1.9716	4.4587	-1.0022
A6	BG1	67.8796	0.9996	0.9984	0.9942	0.9783	8.6530	1.9566	4.3265	-1.5071
A7	BG1	67.8401	0.9997	0.9987	0.9954	0.9864	7.3607	1.9727	3.6803	-0.9373
A8	BG1	67.4263	0.9992	0.9979	0.9959	0.9920	7.2402	1.9840	3.6201	-0.5426
A9	BG1	68.0163	1.0000	0.9998	0.9986	0.9962	6.5915	1.9925	3.2958	-0.2573
A10	BG1	70.3113	1.0000	1.0000	1.0004	1.0017	6.9381	2.0035	3.4690	0.1226
A11	BG1	70.8367	1.0001	1.0002	1.0010	1.0018	7.3621	2.0036	3.6810	0.1288
A12	BG1	71.7284	1.0001	1.0005	1.0015	1.0055	7.4794	2.0110	3.7397	0.3907
A13	BG1	73.9314	1.0004	1.0013	1.0043	1.0158	6.0991	2.0316	3.0495	1.1483
A14	BG1	73.1536	1.0001	1.0005	1.0020	1.0049	4.3074	2.0097	2.1537	0.3545
A15	BG1	73.1540	1.0001	1.0005	1.0020	1.0067	5.2374	2.0134	2.6187	0.4857
A16	BG1	73.6479	1.0003	1.0011	1.0036	1.0131	5.9156	2.0261	2.9578	0.9502
A17	BG1	70.8825	1.0000	1.0002	1.0009	1.0071	6.1847	2.0142	3.0924	0.4995
A18	BG1	70.5687	1.0001	1.0005	1.0021	1.0104	6.3115	2.0209	3.1558	0.7281
A19	BG1	68.0069	0.9994	0.9986	0.9973	0.9977	7.7258	1.9953	3.8629	-0.1590
A20	BG1	66.9124	0.9998	0.9992	0.9970	0.9912	8.5202	1.9824	4.2601	-0.5943
A21	BG1	68.6403	1.0001	1.0004	1.0022	1.0083	8.2305	2.0166	4.1152	0.5646
A22	BG1	70.6488	1.0002	1.0007	1.0032	1.0159	6.6740	2.0319	3.3370	1.1075
A23	BG1	71.8398	1.0002	1.0007	1.0015	1.0018	5.9103	2.0035	2.9551	0.1260
A24	BG1	71.3860	0.9997	0.9988	0.9960	0.9899	5.1659	1.9797	2.5830	-0.7317
A25	BG1	71.1434	0.9998	0.9993	0.9978	0.9938	5.4046	1.9877	2.7023	-0.4414
B1	BG2	46.7166	1.0002	1.0000	0.9994	0.9918	7.7138	1.9835	3.8569	-0.3878
B2	BG2	46.3527	0.9995	0.9982	0.9942	0.9806	8.0112	1.9612	4.0056	-0.9182
B3	BG2	46.3421	0.9995	0.9982	0.9943	0.9780	8.2156	1.9560	4.1078	-1.0430
B4	BG2	46.1907	0.9993	0.9980	0.9943	0.9752	8.4065	1.9504	4.2032	-1.1754
B5	BG2	45.6851	0.9997	0.9988	0.9953	0.9794	7.7845	1.9588	3.8922	-0.9603
B6	BG2	45.5195	0.9997	0.9989	0.9949	0.9756	7.9910	1.9512	3.9955	-1.1388
B7	BG2	46.6478	0.9998	0.9986	0.9949	0.9813	8.8749	1.9626	4.4374	-0.8879
B8	BG2	48.8368	1.0005	1.0012	1.0029	0.9986	9.5141	1.9972	4.7570	-0.0686
B9	BG2	50.1270	1.0003	1.0011	1.0035	1.0012	9.9200	2.0025	4.9600	0.0621
B10	BG2	49.4261	0.9995	0.9986	0.9948	0.9756	10.0042	1.9511	5.0021	-1.2373
B11	BG2	52.5638	1.0000	0.9998	0.9994	0.9984	9.8435	1.9969	4.9218	-0.0826
B12	BG2	53.5051	1.0002	1.0006	1.0013	1.0064	9.6272	2.0129	4.8136	0.3417
B13	BG2	53.6285	1.0003	1.0010	1.0028	1.0134	9.3872	2.0269	4.6936	0.7111
B14	BG2	52.9739	1.0003	1.0010	1.0030	1.0130	9.7747	2.0261	4.8873	0.6820
B15	BG2	52.2235	1.0003	1.0011	1.0026	1.0117	10.0232	2.0234	5.0116	0.6046
B16	BG2	51.0105	1.0003	1.0010	1.0023	1.0094	9.9315	2.0188	4.9658	0.4744
B17	BG2	50.1713	1.0001	1.0003	1.0011	1.0058	9.7469	2.0115	4.8735	0.2879
B18	BG2	49.5912	1.0000	0.9998	0.9995	1.0019	9.9488	2.0037	4.9744	0.0925
B19	BG2	47.5586	1.0002	1.0003	1.0005	0.9974	9.4358	1.9949	4.7179	-0.1223
B20	BG2	46.7354	0.9999	0.9998	0.9990	0.9916	9.0748	1.9832	4.5374	-0.3952
B21	BG2	45.2496	0.9993	0.9980	0.9954	0.9863	8.5870	1.9727	4.2935	-0.6265
B22	BG2	45.1931	0.9996	0.9986	0.9951	0.9778	8.3574	1.9555	4.1787	-1.0276
B23	BG2	44.4072	0.9997	0.9989	0.9958	0.9842	7.4927	1.9683	3.7463	-0.7150
B24	BG2	43.5262	0.9996	0.9985	0.9962	0.9884	7.4793	1.9768	3.7396	-0.5108
B25	BG2	43.2523	0.9996	0.9985	0.9966	0.9916	7.3308	1.9832	3.6654	-0.3658

### 4.3 Correlations

#### 4.3.1 Correlations between Canopy Vigour and Orchard Topography

Table 4-10 Table of Correlations between Canopy Vigour and Orchard Topography

Variable	Correlations (Mean R1-R4 in Dataset_Summary_Master_V2 20161021.stw) Marked correlations (red) are significant at $p < .05000$ N=39 (Casewise deletion of missing data)					
	Mean Elevation	Relative Elevation 5m	Relative Elevation 10m	Relative Elevation 20m	Relative Elevation 50m	Elevation $\Delta$ 50m
Chl_SPAD	0.365532	0.632660	0.640118	0.624754	0.649811	0.576281
Mean LAI	0.111962	0.585873	0.559738	0.535833	0.543425	0.489294
Mean (Chl_SPAD x LAI)	0.135833	0.614909	0.592830	0.569701	0.580596	0.522262

#### 4.3.2 Correlation between Leaf Area Index and Chlorophyll

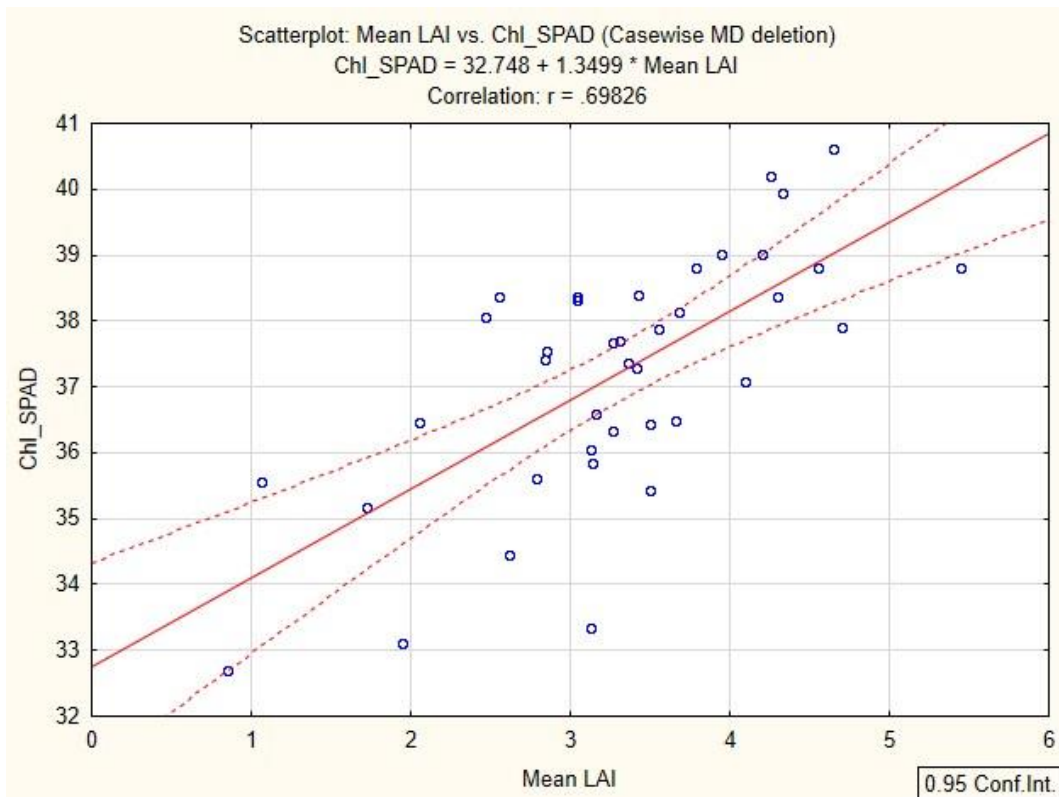


Figure 4-20 Scatterplot illustrates correlation between Leaf Chlorophyll and LAI (Mean T1-T4)

### 4.3.3 Correlations between Vegetation Indices

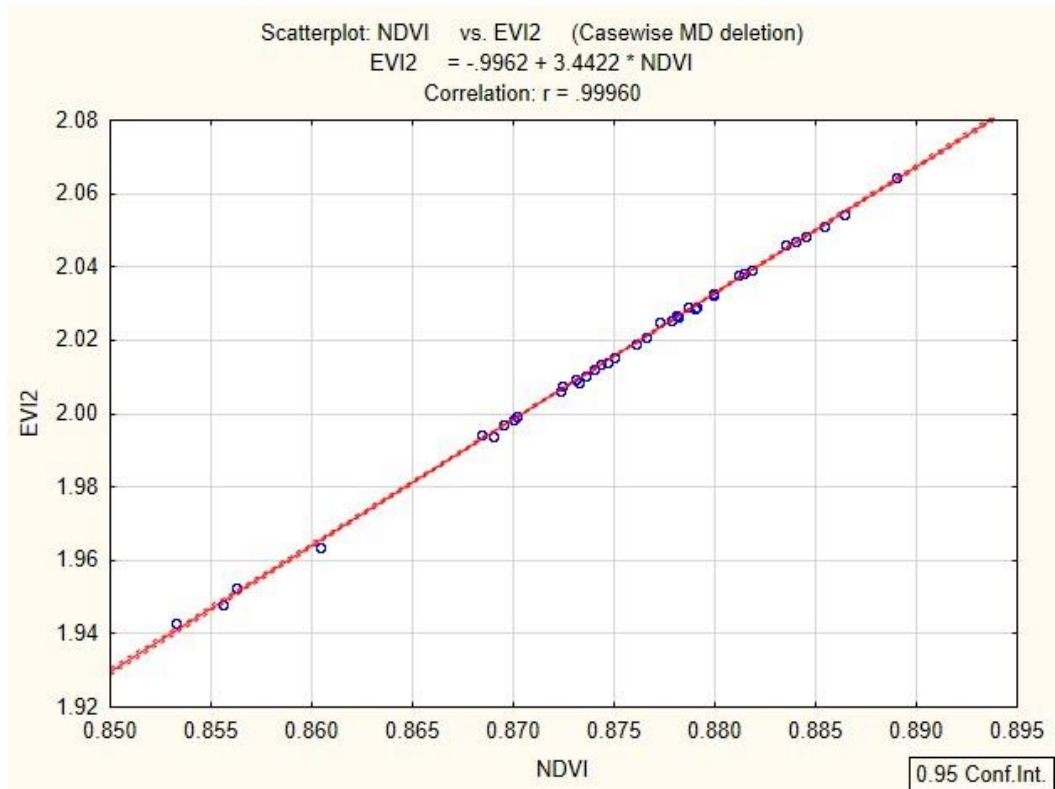


Figure 4-21 Scatterplot illustrates correlation between NDVI and EVI2 (Mean T1-T4)

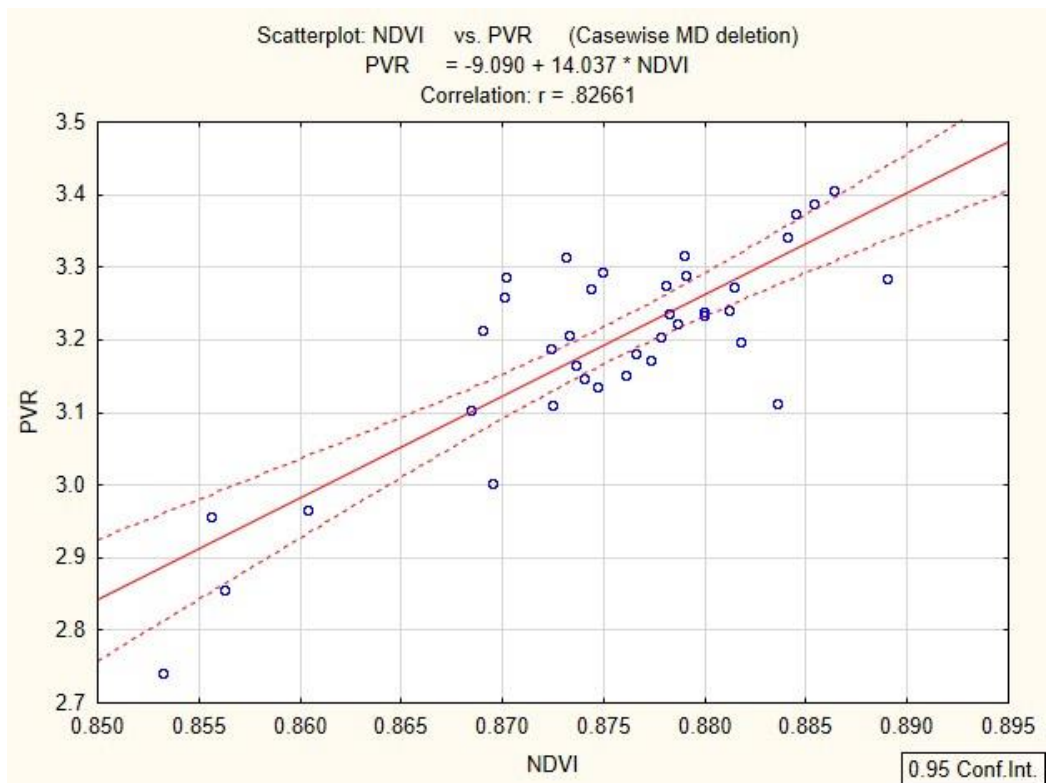


Figure 4-22 Scatterplot illustrates correlation between NDVI and PVR (Mean T1-T4)

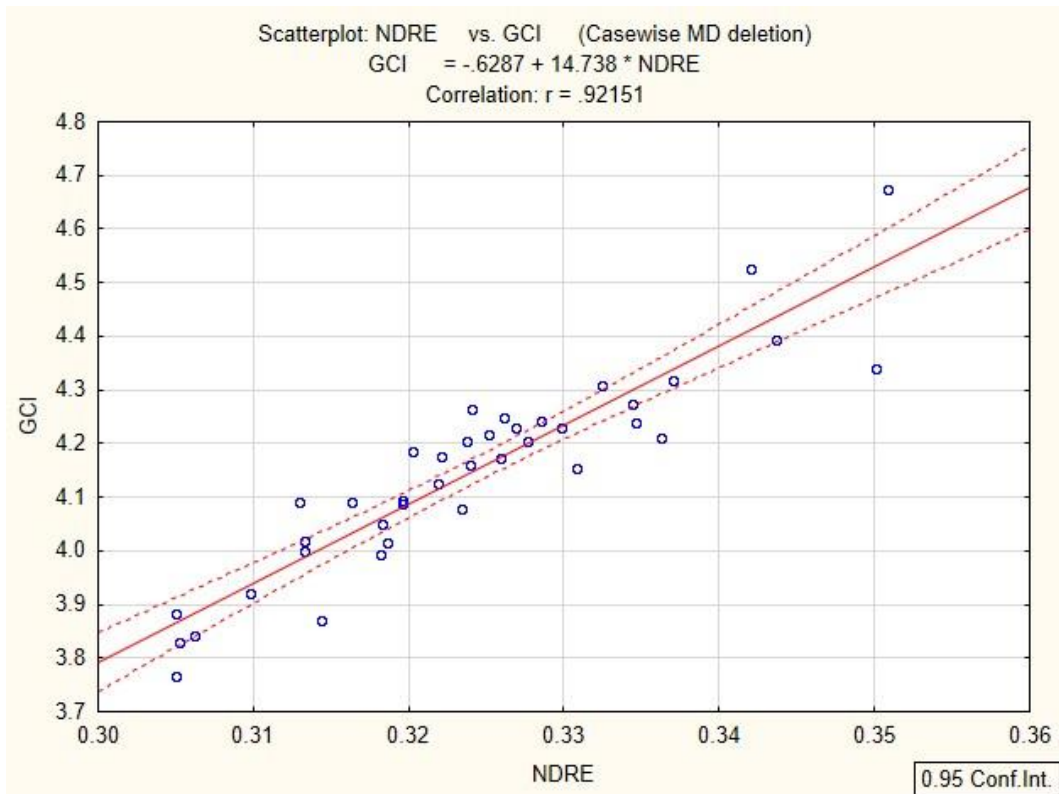


Figure 4-23 Scatterplot illustrates correlation between NDRE and GCI (Mean T1-T4)

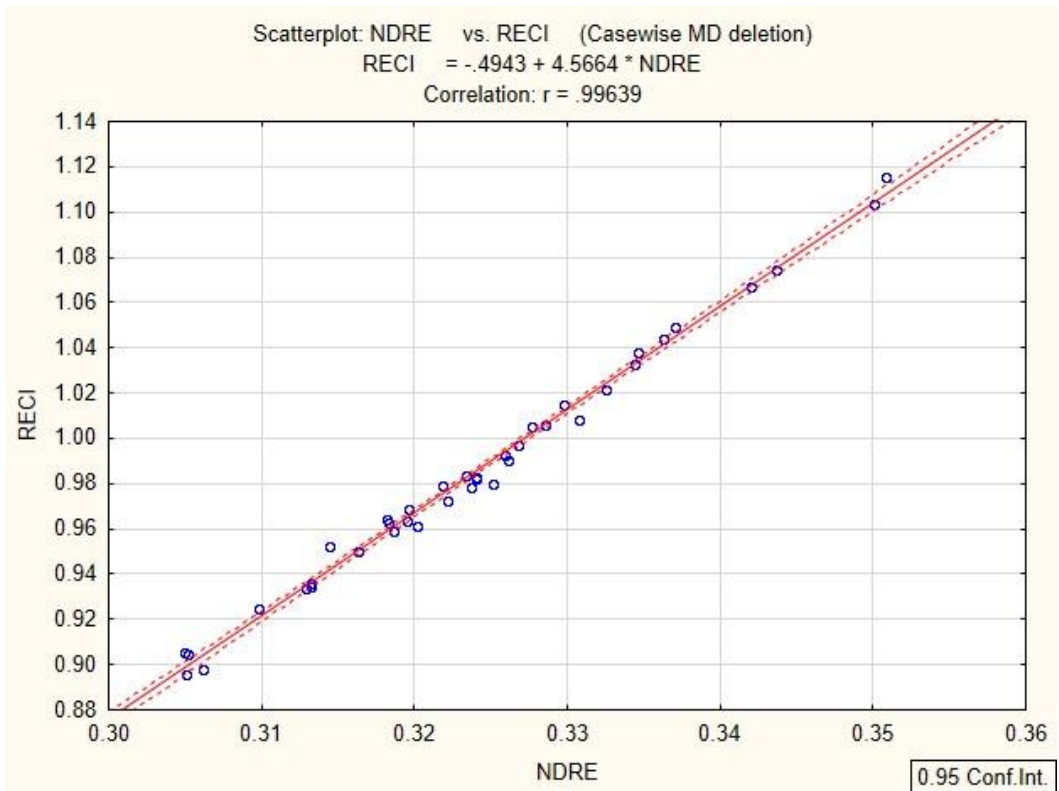


Figure 4-24 Scatterplot illustrates correlation between NDRE and RECI (Mean T1-T4)

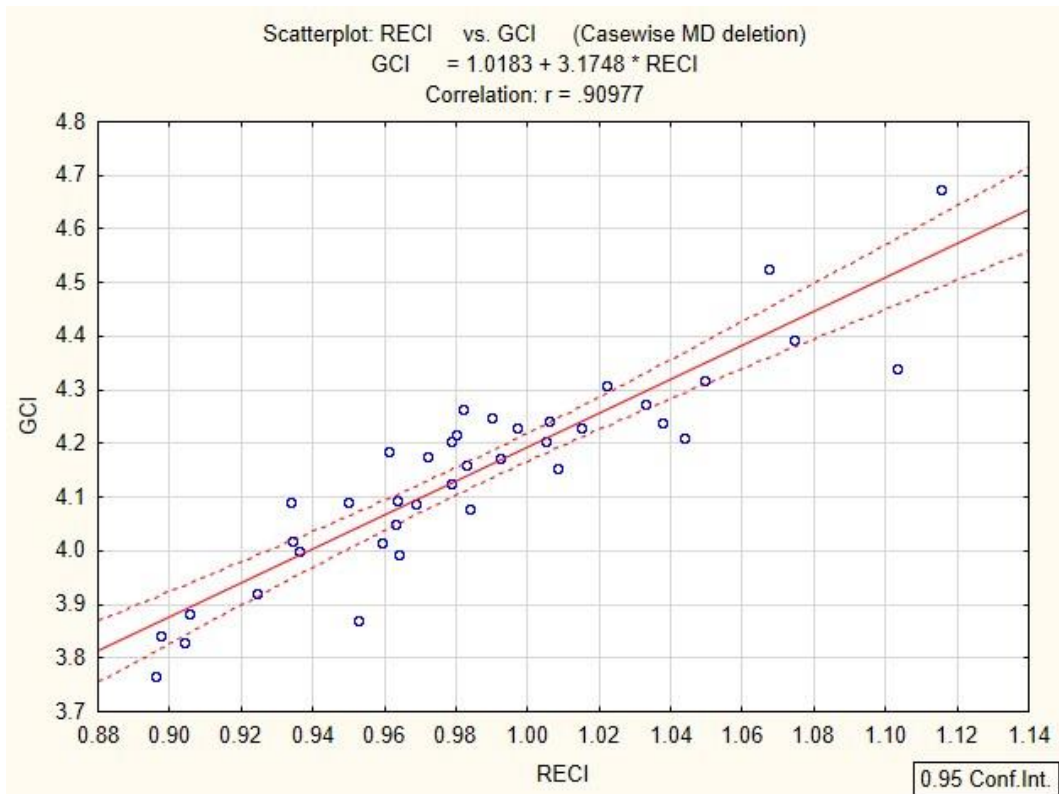


Figure 4-25 Scatterplot illustrates correlation between RECI and GCI (Mean T1-T4)

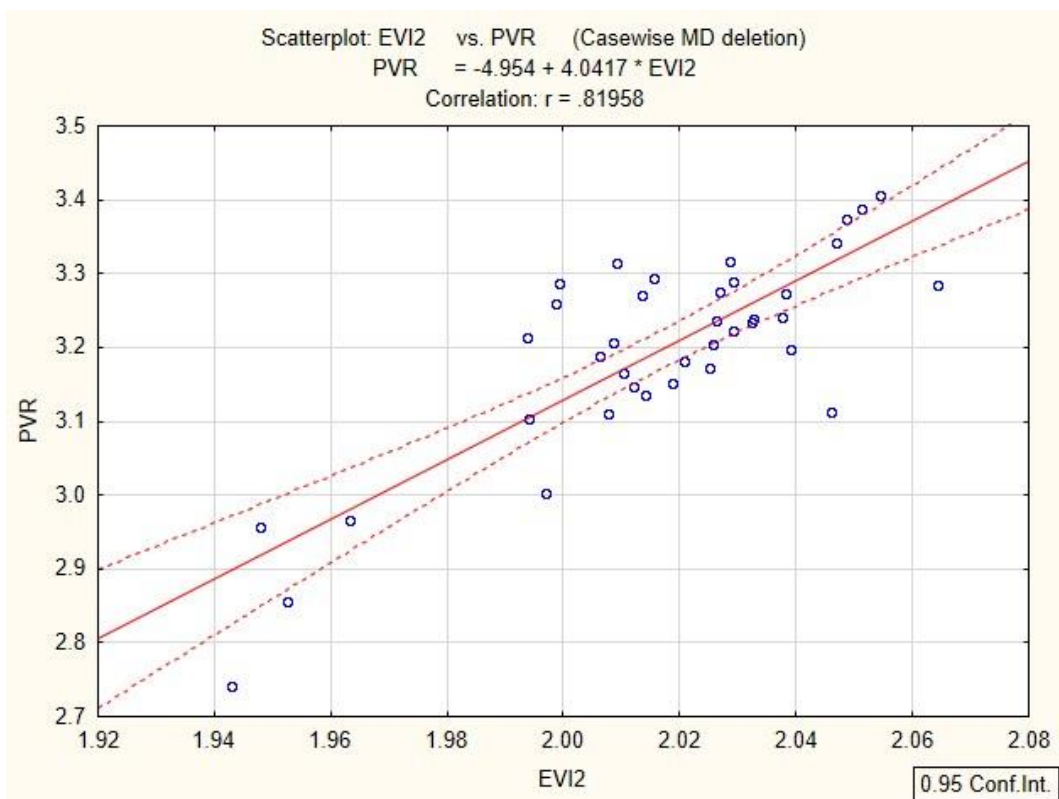


Figure 4-26 Scatterplot illustrates correlation between EVI2 and PVR (Mean T1-T4)

#### 4.3.4 Correlations between Canopy Vigour and Canopy Reflectance

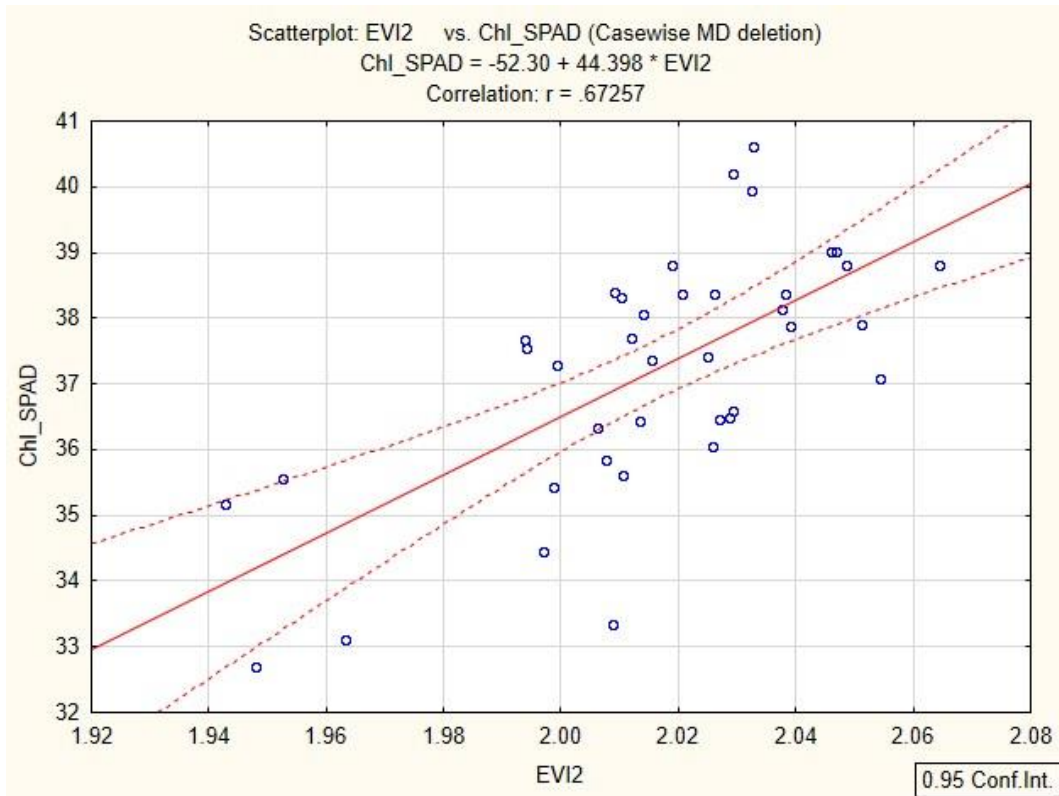


Figure 4-27 Scatterplot illustrates correlation between Leaf Chlorophyll and EVI2 (Mean T1-T4)

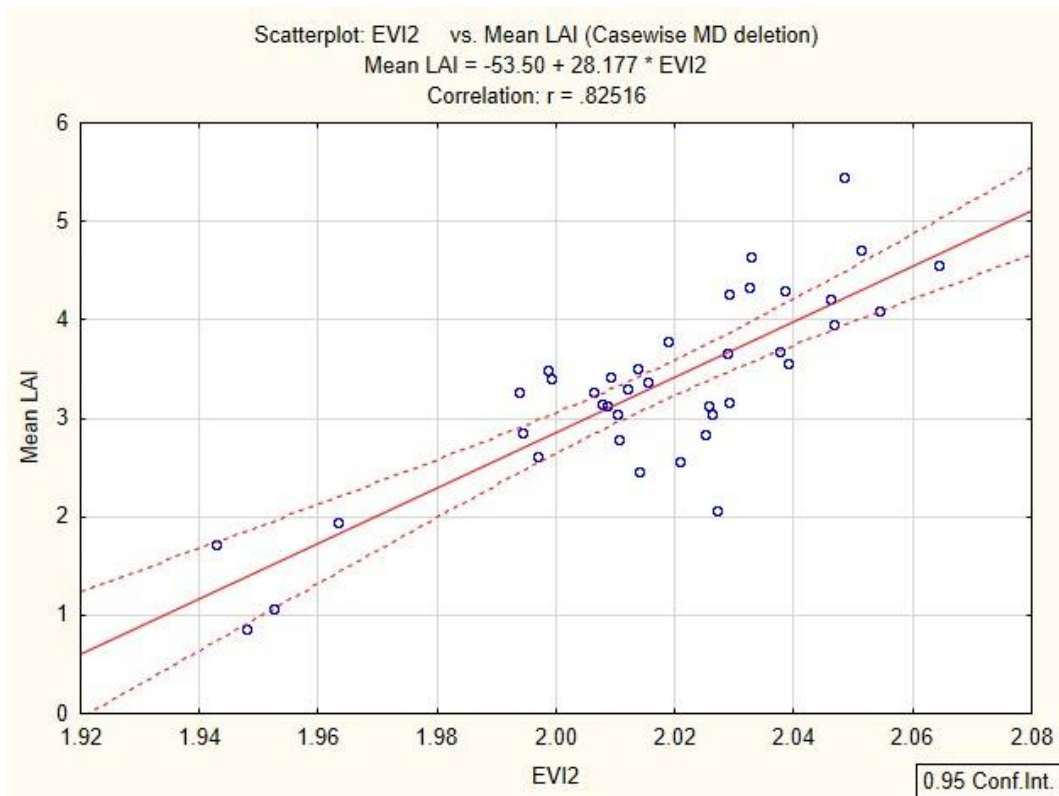


Figure 4-28 Scatterplot illustrates correlation between Leaf Area Index and EVI2 (Mean T1-T4)

## 4.4 Multiple Regressions

Table 4-11 Multiple Regression Summary – Model 1 (3 Variables)

Regression Summary for Dependent Variable: Mean (Chl_SPAD x LAI) (Mean R1-R4 in Dataset_Summary_Master_V2 20161021.stw)						
R= .92720415 R <sup>2</sup> = .85970753 Adjusted R <sup>2</sup> = .84768246						
F(3,35)=71.493 p<.00000 Std.Error of estimate: 15.469						
N=39	b*	Std.Err. of b*	b	Std.Err. of b	t(35)	p-value
Intercept			-2074.37	185.4100	-11.1880	0.000000
EVI2	0.792551	0.065926	1117.74	92.9767	12.0217	0.000000
Elevation Delta 50m	0.463587	0.069985	25.93	3.9142	6.6241	0.000000
Mean Elevation	-0.257516	0.070792	-0.89	0.2442	-3.6377	0.000878

Multiple Regression Equation:

$$\text{Canopy Chlorophyll Content} = (1117.74 * \text{EVI2}) + (25.93 * \text{Elevation } \Delta) - (0.89 * \text{Mean Elevation}) - 2074.37$$

Table 4-12 Multiple Regression Summary – Model 2 (2 Variables)

Regression Summary for Dependent Variable: Mean (Chl_SPAD x LAI) (Mean R1-R4 in Dataset_Summary_Master_V2 20161021.stw)						
R= .89814617 R <sup>2</sup> = .80666654 Adjusted R <sup>2</sup> = .79592579						
F(2, 36)=75.103 p<.00000 Std.Error of estimate: 17.906						
N=39	b*	Std.Err. of b*	b	Std.Err. of b	t(36)	p-value
Intercept			-1996.49	213.1756	-9.36549	0.000000
EVI2	0.747048	0.074923	1053.57	105.6650	9.97083	0.000000
Elevation Delta 50m	0.366790	0.074923	20.51	4.1904	4.89553	0.000021

Multiple Regression Equation:

$$\text{Canopy Chlorophyll Content} = (1053.57 * \text{EVI2}) + (20.51 * \text{Elevation } \Delta) - 1996.49$$

Table 4-13 Multiple Regression Summary – Model 3 (1 Variable)

Regression Summary for Dependent Variable: Mean (Chl_SPAD x LAI) (Mean R1-R4 in Dataset_Summary_Master_V2 20161021.stw)						
R= .82338263 R <sup>2</sup> = .67795896 Adjusted R <sup>2</sup> = .66925515						
F(1, 37)=77.892 p<.00000 Std.Error of estimate: 22.795						
N=39	b*	Std.Err. of b*	b	Std.Err. of b	t(37)	p-value
Intercept			-2217.00	265.2605	-8.35781	0.000000
EVI2	0.823383	0.093294	1161.22	131.5737	8.82566	0.000000

Regression Equation:

$$\text{Canopy Chlorophyll Content} = (1161.22 * \text{EVI2}) - 2217$$

#### 4.4.1 Analysis of Errors (Model 2)

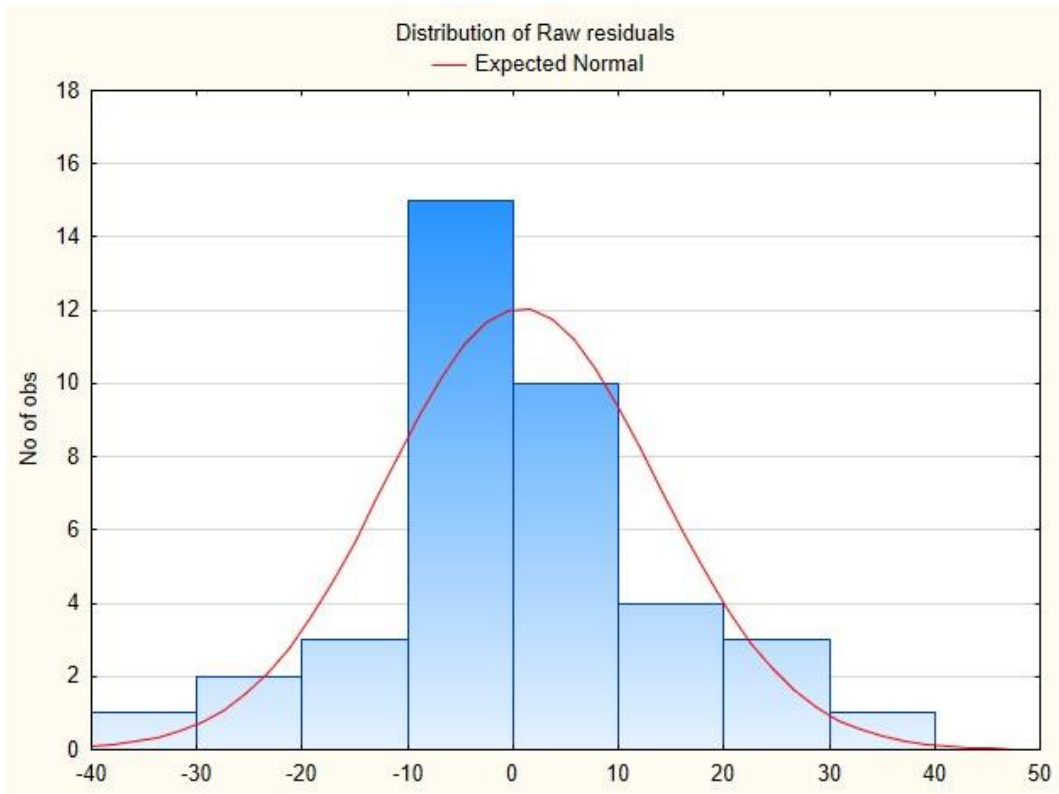


Figure 4-29 Histogram illustrates distribution of residuals compared to a normal distribution

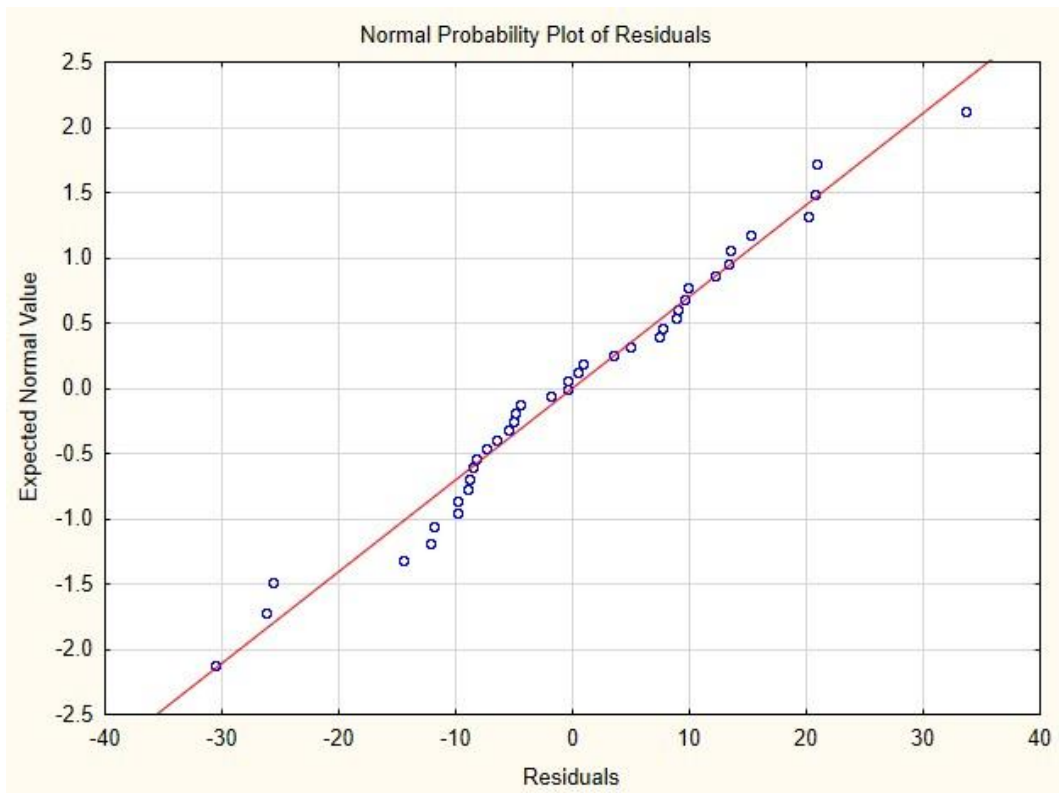


Figure 4-30 Scatter plot illustrates residual values against expected values

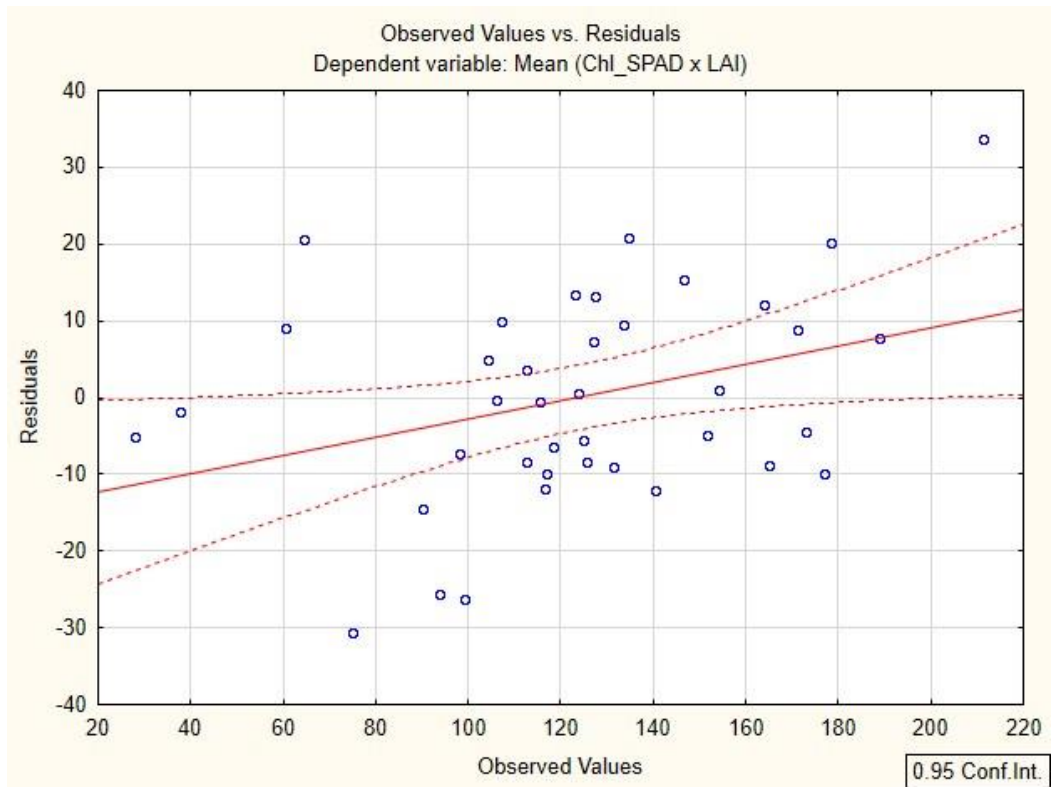


Figure 4-31 Scatter plot illustrates observed values compared to residual values

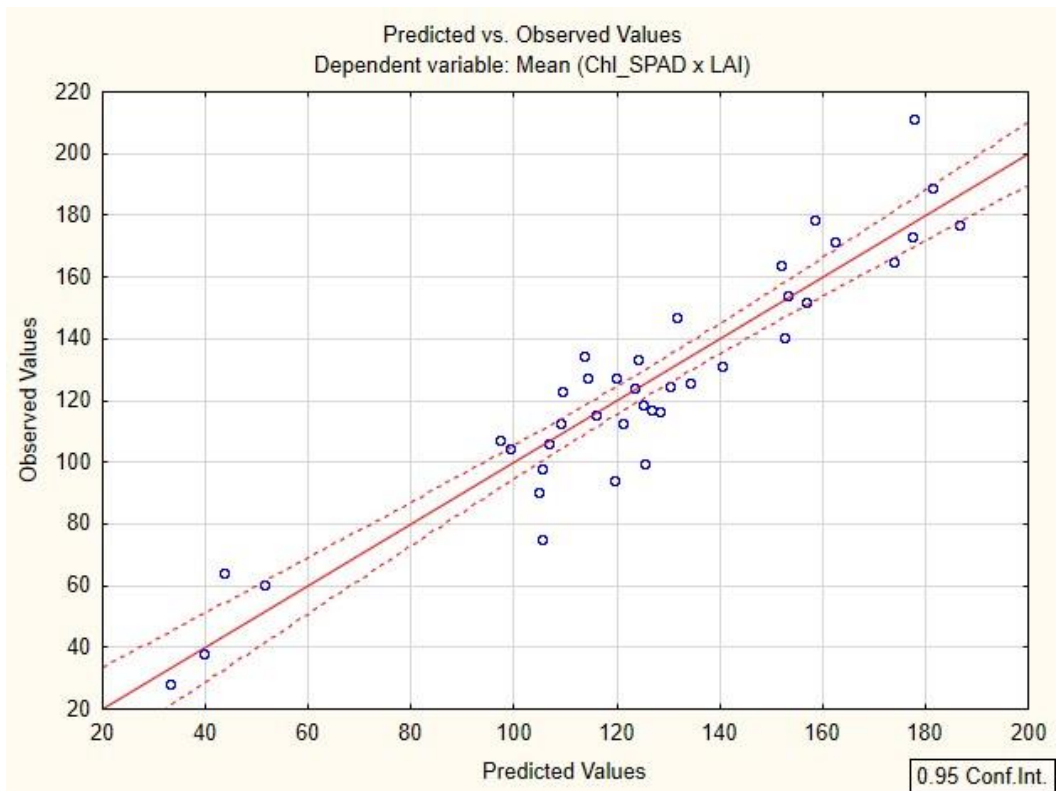


Figure 4-32 Scatter plot illustrates predicted values compared to observed values

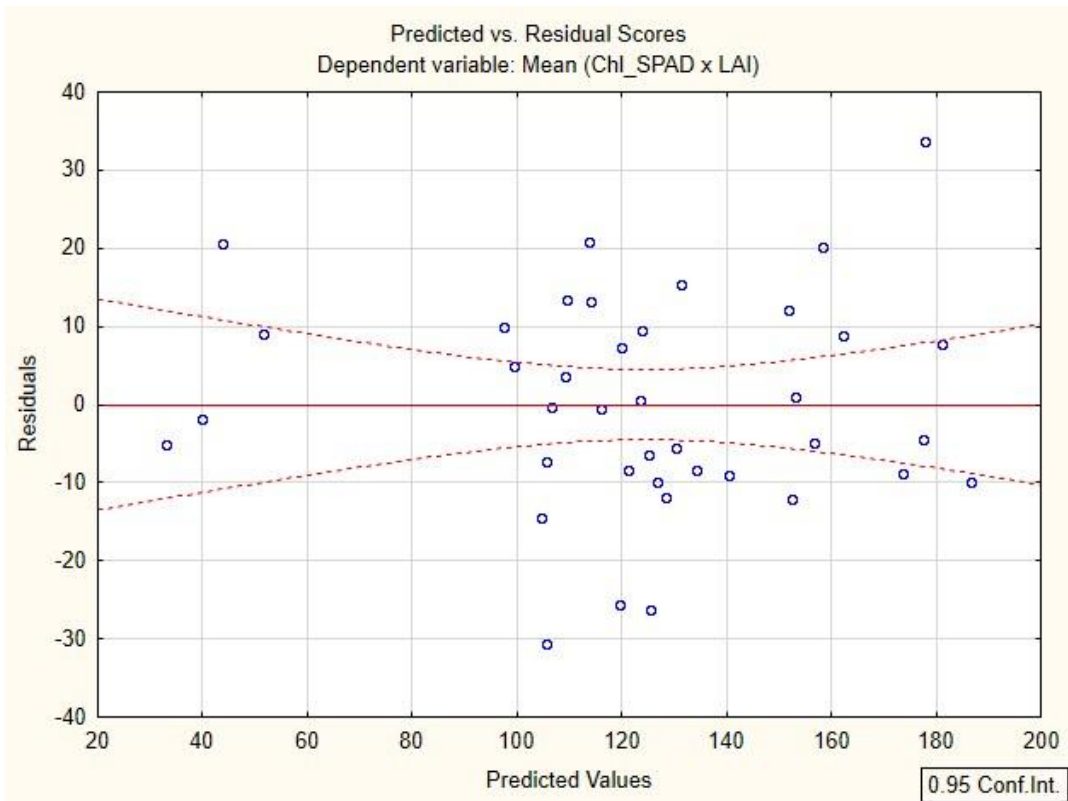


Figure 4-34 Scatter plot illustrates predicted values compared to residual values

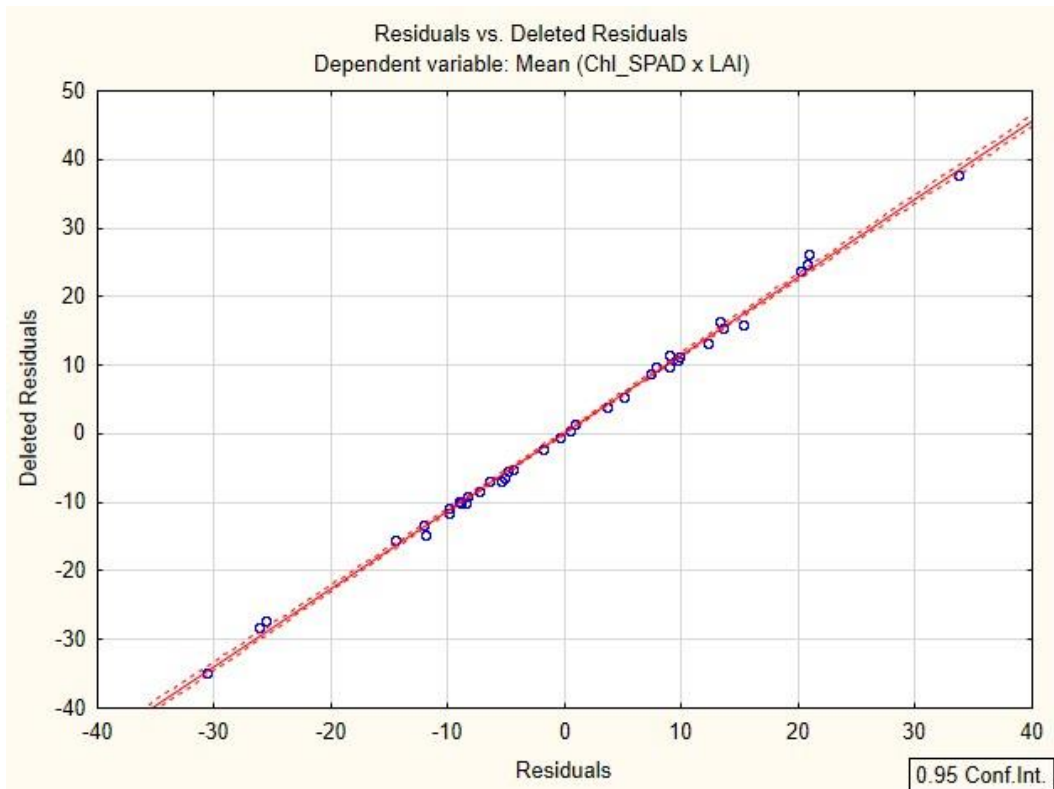


Figure 4-33 Scatter plot illustrates residual values compared to deleted residuals.

## 5 Discussion

---

This chapter discusses the results in two parts (Sections 5.1 and 5.2 ). The first, deals primarily with *interpreting* the results in the wider context of an orchard production system, rather than from a solely plant physiology perspective. The second part, discusses the limitations of the research from several angles. While the results are observational, and do not explain causality, this chapter does include some discussion about possible causes in the interests of promoting further inquiry.

---

Section 5.1 is divided into four sub-sections, starting with discussion about the orchard topography and the range of bio-physical conditions in which the plants are growing.

Section 5.1.2, deals primarily with canopy vigour; its spatial and temporal variability, as well its relationship with orchard terrain. This sub-section also looks at how field and laboratory measurements of chlorophyll differ and considers the implications for remote sensing.

Section 5.1.3, deals with canopy reflectance. A comparison of Vegetation Indices is made, including consideration of possible causes.

Finally, Section 5.1.4 discusses how canopy reflectance data is used to determine canopy vigour. Relationships between the two are considered. The strength of the results and how repeatable the findings are likely to be, is analysed from a statistical perspective. There is also discussion about how useful the multiple regression models are likely to be for predicting canopy vigour.

Section 5.2, considers the limitations of the research.

## 5.1 Interpretation of Results

### 5.1.1 Orchard Topography

This study was conducted on two, non-contiguous blocks (BG1 and BG2) within a two (2) kilometres radius of each other. The mean elevation of the sample plants in BG1 is 70.8m above sea level (asl), while the mean elevation of the sample plants in BG2 is 48.3m asl. The range of elevations on BG1 and BG2 is similar (7.6m and 10.3m respectively). However, the range in elevation for all sample plants across both blocks is 31.2 m. Orchard elevation is generally thought to affect fruit quality (Praat et al., 2003), but no evidence could be found in the literature, to suggest that differences of this magnitude, in the same general area, has any significant effect on kiwifruit canopy vigour.

The topography of the two blocks is quite different. BG1 can be described as flat to undulating, with narrow remnants of small watercourses running through it. In contrast, BG2 is a sloping block, with an aspect towards the north and a substantial, piped, watercourse winding through the lower third of the block. Sample plants in BG1 are on slopes ranging from 4.3 degrees to 8.9 degrees (Mean 6.7 degrees), while sample plants in BG2 are on slopes ranging from 7.3 degrees to 10.0 degrees (Mean 8.9 degrees).

More importantly, the location of the sample plants in relation to their surrounding 50m is very different. The mean Elevation  $\Delta$ , for plants in BG1 is 0.04m. This is 4cm above the surround terrain which reflects its flat to undulating nature. In contrast, plants in BG2 are on average, -0.3m or 30cm below their surrounding terrain. Some sample plants in both BG1 and BG2 are as much as 1.5m and 1.2m respectively, below their surround terrain.

Elevation  $\Delta$ , is likely to encompass other bio-physical characteristics not specifically measured in this study. Water accumulation, cold air movement, sedimentation, fertility transfer, to name a few, are all likely to be influenced by topography. Soil structure is also known to be affected by slope and soil moisture. The result, is what is known as a soil catena (Moore, Gessler, Nielson, & Peterson, 1993). Flatter ridges and gullies are more likely to have deeper soils, with more organic matter than adjacent, more steeply sloping areas.

### 5.1.2 Canopy Vigour

With just one exception, Leaf Area Index (LAI) and Chlorophyll (Chl\_SPAD) had significant correlations with all measures of topography, at all scales. The only exception, was that LAI did not have a significant correlation with Mean Elevation. Some of the strongest correlations for Chlorophyll and LAI were seen with Relative Elevation at the 5m scale ( $r = 0.63$  and  $r = 0.56$  respectively). This is an example of Tobler's first law of geography at work. Tobler said "everything is related to everything else, but near things are more related than distant things." (Tobler, 1970). In this example, Elevation  $\Delta$  at the 5m scale is geo-spatially located exactly where the LAI and Chl\_SPAD measurements are taken from.

Chlorophyll measurements increased significantly over the duration of the study. In the early part of the season (T1), variability between sample plants was high. This probably reflects variable bud-break timing and therefore, leaf age. Very young leaves, typically have low chlorophyll levels. Chlorophyll is strongly (positively) correlated with Elevation  $\Delta$ , which could be associated with earlier bud-break in elevated, warmer areas. As time progressed from T1 to T2, chlorophyll variability reduced greatly and then remained reasonably constant for the remainder of the study. Once past the initial bud-break period, chlorophyll levels became more

similar. Mean chlorophyll levels were also observed to increase in a non-linear way. This suggests, that at some point after T4, chlorophyll levels will probably plateau and eventually decrease with the onset of senescence.

In contrast, LAI measurements were considerably less variable between plants in the early part of the season (T1), compared to later measurements. While LAI increased significantly over all time periods, so too did variability. From T1 to T3, sample plants at the lower end of the LAI range are growing slowly while those sample plants at the upper end of the range, are rapidly growing more leaves. This has the effect of dragging up the mean LAI values. It suggests, that prior to canopy closure, plants are reasonably similar with only a small amount of leaf relative to the overall area allocated to each plant. As canopy closure is reached, some plants continue to grow ever increasing amounts of leaf, while other plants maintain a more constant leaf area.

Significant and moderately strong correlations ( $r = 0.70$ ) were observed between chlorophyll levels (Chl\_SPAD) and Leaf Area Index (LAI). This supports anecdotal evidence, that kiwifruit plants with more leaves, also appear greener and more vigorous.

It can be concluded, that in the context of an orchard production system, canopy vigour at a block level, starts slowly and somewhat variably depending on terrain within the block. Bud-break in low lying areas is later. As the season progresses beyond flowering, mean canopy vigour across the block continues to increase. However, at a plant level, some plants increase their biomass much faster than others. The result is that canopy vigour within the block becomes more variable. At the leaf level, chlorophyll content becomes more similar, as leaves on spring-breaking canes finish growing and mature. Reflecting on early research conducted

by Angela Snowball, on Hayward kiwifruit (Snowball, 1995), she found that later breaking canes grew longer and had larger leaves than spring-breaking canes. While Hayward and G3 kiwifruit are clearly different, vigorous G3 kiwifruit may also be producing more summer canes with larger leaves than less vigorous plants.

#### 5.1.2.1 Comparison of field and laboratory chlorophyll measurements

From a comparison of non-destructive leaf chlorophyll measurements using a Minolta SPAD and destructive leaf chlorophyll measurements in the laboratory, we established a strong and significant correlation between the two methods ( $r = 0.96$ ) after removal of outliers. The three outliers identified in Figure 4-5 were all due to small amounts of spillage of extract as it was passed from the mortar to the test tube.

These results highlight an important point to consider when comparing remote sensors with other measurement methods. Even the Minolta SPAD, which is considered an industry standard, does not give identical results to destructive measurement methods. The same principle will apply to LAI measurements taken with the LICOR meter. The LICOR measurements are likely to differ from measurements taken by removing all leaves from a plant and measuring the area of each leaf individually. When comparing canopy reflectance, measured with a remote sensor, and canopy vigour measured with a Minolta SPAD and LICOR meter, we are interested in the relative strength of their relationship. This is because, in all cases, we do not have an absolute value for canopy vigour.

### 5.1.3 Canopy Reflectance

All Vegetation Indices showed significant change over the duration of the study. Each index, is derived from just two (2) of the five (5) discrete bands as shown in Figure 5-1. GCI and PVR were the most variable indices (Figure 4-19) and it is noteworthy, that only these two indices use the green band in their formula. NDVI is often regarded as an industry standard, but is known to “saturate” at high LAI values which may explain a lower range of values. NDRE was the least variable index over the duration of the study. This may be associated with using the Red Edge band which occurs at a very steep and narrow part of the reflectance curve.

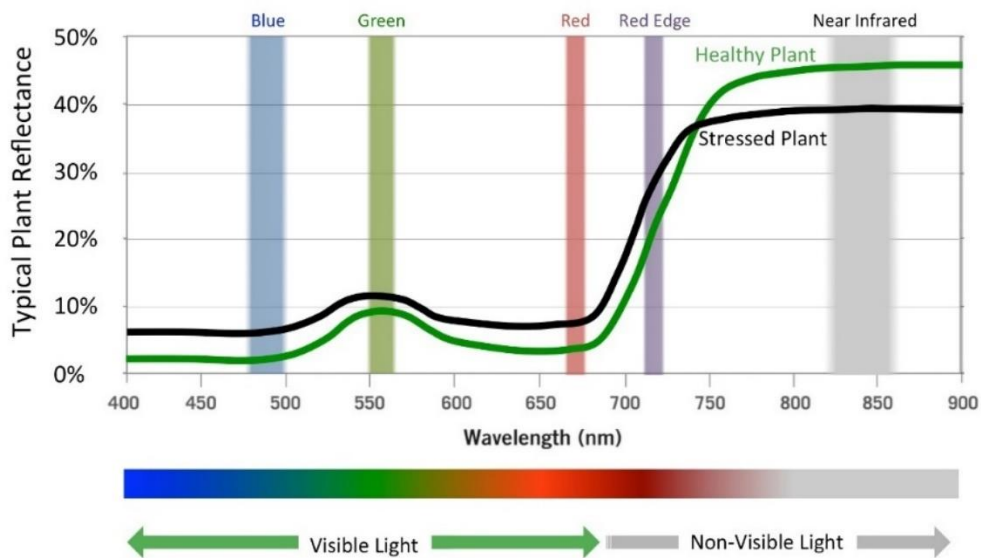


Figure 5-1 Image showing typical effect of plant vigour on reflectance.

(Courtesy MicaSense Inc.)

Increases in both RECI and GCI suggests that the total amount of chlorophyll in the canopy was increasing during the study. This is consistent with increasing chlorophyll measurements as illustrated in Figure 4-3 and increasing LAI measurements illustrated in Figure 4-1. Similarly, significant increases in the NDRE index shows that NIR reflectance is increasing relative to Red-edge. NIR

reflectance is typically influenced by leaf structure (Figure 2-5) rather than cell pigments or chlorophyll content. As leaves are becoming thicker and more mature we would expect to see increasing levels of NIR reflectance.

NDVI and EVI2 have been shown in other studies, including a study of Hayward kiwifruit in 2015 (Hull, 2016), to behave similarly to each other. This is seen again in this study of G3 kiwifruit. NDVI has a non-linear relationship with leaf area. It becomes unresponsive when LAI increases above 2 (A. Gitelson et al., 2003) which occurred shortly before T2 in this study. In contrast, EVI2 is thought to be more sensitive to increasing biomass than NDVI.

PVR behaved differently over time compared with the other indices in this study. While there was a moderately significant increase in PVR over the full duration of the study, this increase was not significant between all time periods. Specifically, between T2 and T3 there was no significant change in observed PVR values. The mean PVR measured in T1 was also very similar to that measured in T2 but the standard deviation was much greater in T1, resulting in a significant difference between T1 and T2. Constant mean PVR values between T1, T2 and T3 suggests that plant vigour is not changing. However, this differs from observations made on Hayward kiwifruit orchards in 2015-16 (Hull, 2016). On Hayward orchards, PVR was observed to decrease significantly between November and March. One explanation is that G3 kiwifruit may be more vigorous than Hayward kiwifruit during the first eight (8) weeks post bud-break. Another explanation for PVR behaving differently, is that kiwifruit leaves have a high red to green pigment ratio due to the presence of anthocyanins (Fraser et al., 2013). This may give the appearance that canopy vigour is constant, when in fact, red anthocyanin pigments may be “masking” the increasing levels of green chlorophyll.

It is not surprising that strong and significant correlations exist between the Vegetation Indices. They are all essentially ratios of two narrow reflectance bands. EVI2 is a derivative of NDVI and consequently shows the strongest correlation ( $r = 0.9996$ ). Similarly, RECI and NDRE both use the narrow red-edge band in their respective formulae resulting in a very strong correlation ( $r = 0.9964$ ). GCI and RECI are two indices that are both considered good indicators of chlorophyll content. They also have a strong correlation with each other ( $r = 0.91$ ). Even GCI and NDRE which come from different origins are observed to have a strong correlation ( $r = 0.92$ ). Again, the notable exception is the relationship between PVR and the other indices. PVR is the only index that does not use either NIR nor red-edge bands in its formula and it shows the lowest correlations with all other indices. In fact, PVR does not show any significant correlation with NDRE, GCI nor RECI. It does however have a reasonably strong correlation with NDVI ( $r = 0.83$ ) which is arguably the industry standard.

NDVI, EVI2 and PVR show significant correlations with orchard terrain ( $p < 0.05$ ). These correlations are all weak to moderate. They show, that plants in relatively low-lying areas, generally have lower canopy reflectance. This is also consistent with lower chlorophyll and LAI measurements, in low-lying areas.

What can be concluded about the Vegetation Indices, is that while there are strong correlations between indices, except for NDVI and EVI2 which are essentially the same, each index tells a slightly different story. None are inconsistent with what chlorophyll and LAI measurements are showing. Each is behaving in a way that can be explained in terms of basic plant physiology and the principles underpinning its formula.

#### 5.1.4 Determining Canopy Vigour using Canopy Reflectance and GIS

The following discussion, is at the heart of this thesis. The research question is, “To what extent, can canopy reflectance and orchard topography explain G3 kiwifruit canopy vigour?” As already noted, Leaf Area Index (LAI) and chlorophyll (Chl\_SPAD) were chosen as the two measures of canopy vigour and results show there is a moderately strong correlation between these two measures ( $r = 0.70$ ).

Firstly, several important relationships stand out between canopy vigour and some of the vegetation indices and with orchard topography. Chl\_SPAD and LAI show the same moderate to strong correlations with both NDVI and EVI2 ( $r = 0.67$  and  $r = 0.83$  respectively). They also have moderate to strong correlations with PVR ( $r = 0.50$  and  $r = 0.75$  respectively). Chl\_SPAD has a moderate correlation with RECI ( $r = 0.60$ ), reinforcing claims by Gitelson, Gritz and Merzlyak (Gitelson et al., 2003) that this index is a good predictor of chlorophyll. Finally, Chl\_SPAD and LAI both have moderate correlations with Relative Elevation at all scales and with Elevation  $\Delta$  at the 50m scale. All correlations noted above are significant ( $p < 0.05$ ).

These statistically significant correlations, are very unlikely to be random events. They are important because without them, determining canopy vigour with a multispectral camera would have been almost impossible. These results show, that there are moderate to strong correlations between measurements taken with remote sensors (Multispectral camera and LIDAR) and measurements taken with proximal sensors (Minolta SPAD and LICOR meter). However, correlations alone cannot determine which remotely sensed variable or variables, best explain canopy vigour and to what extent. Similarly, these correlations cannot determine which measure of canopy vigour, LAI or Chl\_SPAD, is most important, when it comes to prediction.

To definitively answer the research question, several stepwise multiple regressions were run on the most promising candidates (Independent or Predictor Variables), namely EVI2, NDVI, PVR, RECI, Mean Elevation, Relative Elevation (at all 4 scales) and Elevation  $\Delta$  at the 50m scale. For canopy vigour (the Dependent Variable), LAI, and Chl\_SPAD were used. A “wildcard” dependent variable (LAI x Chl\_SPAD) was also included.

The results show that in all cases, the wildcard, Chl\_SPAD x LAI rather than Chl\_SPAD or LAI on their own, produced models with the highest Adjusted  $R^2$  values. On further investigation, this variable is sometimes referred to in the literature as Canopy Chlorophyll Content (Darvishzadeh et al., 2008), because it represents the total amount of chlorophyll in the canopy rather than chlorophyll concentration in the leaf. Interestingly in this study, Canopy Chlorophyll Content (CCC) is very strongly correlated with LAI ( $r = 0.99$ ) which makes it an equally good proxy for canopy vigour. This was an unexpected outcome of the analysis.

In all cases, Elevation  $\Delta$  at the 50m scale, rather than Relative Elevation was the better measure of terrain. Elevation  $\Delta$  is the *difference* in elevation (in meters) and is not influenced by an orchard’s elevation above sea level. In contrast, an orchard’s elevation does affect Relative Elevation, because it is a ratio. For example, an orchard of a given slope located well above sea level, will have larger relative elevations than an orchard of the same slope near sea level.

The model that best explained canopy vigour, included three (3) predictor variables; Mean Elevation, Elevation  $\Delta$  at 50m scale and EVI2. All predictor variables can be measured with remote sensors or calculated using GIS tools. This model (Table 4-11) had an Adjusted  $R^2 = 0.85$ ,  $p < 0.00001$ ,  $rsd = 15.47$ . Adjusted  $R^2$  values were used rather than  $R^2$  to remove the temptation to including too many variables.

Model 2 (Table 4-12) had the second highest Adjusted  $R^2$  value using only two predictor variables. Mean Elevation was forcibly excluded. As with Model 1, both remaining variables can be measured with either a remote sensor or calculated using GIS tools. Neither variable is influenced by the elevation of the orchard, which potentially makes it more useful than Model 1, on a regional scale. Model 2 had an Adjusted  $R^2 = 0.80$  and  $p < 0.0001$ .

Finally, a third model was developed using just the vegetation index EVI2. Model 3 (Table 4-13) had an Adjusted  $R^2 = 0.67$  and  $p < 0.0001$ . Mean Elevation and Elevation  $\Delta$  were forcibly excluded. The purpose of Model 3, was to see how much extra information was contained within the orchard topography data. It was found that while EVI2 alone explains approximately 67% of canopy vigour (Canopy Chlorophyll Content), by adding terrain information, the explanatory power of the model was increased to almost 80%. In other words, the Elevation  $\Delta$  is accounting for approximately 13% of the variability in canopy vigour. Anecdotally, kiwifruit orchardists have long believed that plants in low-lying areas do not “do as well” and these results, quantitatively reinforce that view. A subsequent review of the literature, also reveals that kiwifruit plants in colder conditions, (as often found in low-lying areas) produce wound-healing tissues more slowly and are therefore more susceptible to diseases such as Psa (Froud, Everett,

Tyson, Beresford, & Cogger, 2015). This adds further weight to these results showing plants in low-lying areas are less vigorous.

In summary, there are moderate to strong correlations between canopy vigour measurements taken with remote and proximal sensors. The best regression model (Model 1), shows that canopy reflectance and orchard topography, together explain approximately 85% of the variability in canopy vigour (Adjusted  $R^2 = 0.85$ ). This is a strong relationship and the very low p value ( $p < 0.00001$ ), indicates that it should be very repeatable. In other words, the chances that these results are a random event, is very low. Finally, the residual standard deviation ( $rsd = 15.47$ ) reveals how useful the model is likely to be in practice. Prediction error is approximately  $\pm 2rsd$ . With Canopy Chlorophyll Content ranging from 27.93 to 211.5 and a mean value of 123.88, we would expect Model 1 to have a prediction error of approximately  $\pm 30.9$ . It is reasonable to conclude, that Model 1, is a useful predictor of canopy vigour, using a multispectral camera and GIS tools, rather than a Minolta SPAD and LICOR meter.

#### 5.1.4.1 Analysis of Errors

Multiple Regressions assume that the residuals are normally distributed. Where there are small sample sizes ( $< 100$  observations), outliers can have a significant influence on the eventual regression line (Dell Inc., 2016). An analysis of the residuals for Model 2 was performed after data from eleven (11) sample plants had been removed:

- i. The distribution of residuals histogram (Figure 4-29) shows that residual values are close to the expected normal distribution. There are slightly more residual values in the 0 to -10 range than would normally be expected.

- ii. Similarly, the scatter plot of Residuals against Expected normal values (Figure 4-30) shows that most residuals have values close to the expected normal values. A small number sit above and below the line.
- iii. The scatter plot of Observed values against Residuals (Figure 4-31) shows that residual values are generally larger for high values of Canopy Chlorophyll Content (Chl\_SPAD x LAI). Ideally this should be a horizontal line with residuals spread evenly along the line.
- iv. The scatter plot of Predicted Values against Observed Values (Figure 4-32) shows most observations sitting reasonably close to the Predicted values line. This does not indicate any cluster of outliers which were not well predicted.
- v. The scatter plot of Predicted Values against Residuals (Figure 4-34) shows that most residuals form a cloud either side of the horizontal line. There is a group of three (3) notable exceptions sitting well below the line and one sitting well above the line. This suggests that the overall relationship between Canopy Chlorophyll Content (Chl\_SPAD x LAI) is linear in relation to the Predictor variables used in Model 2.
- vi. The scatter plot of Residuals against Deleted Residuals (Figure 4-33) suggests that there are no serious outliers (not already removed) that would change the regression line significantly if removed. In summary, the analysis of errors does not suggest any serious violations of normality. No further outlying data were removed, as there was insufficient evidence for doing so.

## 5.2 Research Limitations

### 5.2.1 Design Limitations

With the benefit of hindsight, the method used to randomly select the sample plants resulted in a relatively large number of outliers (11 from 50) that were later discarded during statistical analysis. It is believed that this was caused by the extra light reflectance associated with both overhead and below-canopy white artificial shelter which was close to some of the chosen sample plants. The problem was noticeably more pronounced in BG1 compared to BG2.

Where randomly selected sample plants were situated directly adjacent and below overhead shelter, this affected both multispectral data captured with the UAV and the LAI measurements captured with the Licor meter. Below-canopy artificial shelter did not affect the multispectral images to the same extent but did affect the Licor readings. Artificial shelter did not affect the Chl\_SPAD measurements.

The fact that BG1 and BG2 were not contiguous areas of land and that they were managed by two different orchard managers means that analysis of the effect of mean elevation could not be reliably interpreted. While some significant correlations between mean elevation and leaf chlorophyll levels were observed, the trial design may have contributed to the appearance that the sample plants are from two different populations which cannot be ruled out.

### 5.2.2 Data Capture Limitations

This study used a multispectral camera with five discrete spectral bands. Measuring and comparing spectral variability over time and/or space across the two Areas of Interest requires accurate instrument calibration which is not yet available in the MicaSense camera. To some degree, using spectral ratios (Vegetation Indices) does mitigate this problem, but it does not solve the issue entirely. Real-

time measurement of prevailing light conditions is a technique currently under investigation by the camera manufacturer using a down-welling light sensor (DLS), and should be incorporated into future studies, once proven.

Physical orchard structures such as artificial shelter can create difficulties in collecting reliable canopy data. The trend towards horizontal overhead shelter is likely to be particularly challenging, both in terms of light quality and the physical constraints of flying under an overhead structure.

While the collection of kiwifruit canopy data with a remote sensor was significantly more cost effective than ground-based proximal sensors, the cost of aerial surveying each orchard individually is still relatively inefficient. This is due to the large amount of time necessary for survey pre-planning and on-site setup compared to the actual flight time. Health and safety requirements and CAA documentation are both becoming increasingly onerous for UAV operators.

Using UAVs as a platform for remote sensing equipment is revolutionising the survey world. However, the legislative framework is still under development in New Zealand and many questions remain unanswered or untested. Unlike manned aircraft, UAVs must be flown within visual line of sight and require permission from landowners and/or people who are flown over. This limits the opportunity for large scale surveys and the associated economies of scale normally associated with manned aerial surveying.

### 5.2.3 Processing Limitations

Cloud-based pre-processing of images into orthomosaic images is both cost effective and timely on the scale of this study. Several providers offer this service. For this type of analysis, it is unlikely that in-house processing is warranted unless very large numbers of surveys are required in a very short timeframe.

Extracting reflectance data from survey images can be successfully achieved using either public domain or commercially available GIS software. The workflow does require segmentation and classification techniques which can be time consuming and subject to accuracy errors. Specifically, the accuracy of the canopy mask used to remove background reflectance of grass, weed etc. can vary depending on operator experience and software used. Alternative software options are available that may extract data more efficiently and accurately. However, specialist software is typically more expensive to purchase and they often incur annual maintenance fees. There is no evidence to suggest that different software would have altered the results of this study.

#### 5.2.4 Analysis Limitations

Observations were made at four (4) time periods between October and December. However, the results show that mean values across all four periods (T1 - T4), usually produced stronger correlations than data from a single time-period. This may be due to mean values over time, being more normally distributed than a smaller sample size drawn from a single time-period. Regardless, it has practical implications for modelling canopy vigour from a single measurement.

The Predictive Models (Section 4.4) all have very low p values ( $p < 0.0001$ ) which suggests the results should be very repeatable. However, because the regression models used mean values and not values from each time-period, a validation study may be necessary to measure how each Model performs at specific times during the season. Before any Model is used commercially as a prediction tool, it should ideally be ground-truthed against plants that were not used to develop the model. This was not done as part of this study.

## 6 Conclusions

---

This chapter reflects on the primary motivation for conducting this study. Consideration is given to the major findings and to definitively answering the research question. Most importantly, this chapter looks at how this study has created new knowledge and/or validated previous work. It looks at how this study can be used as a platform, for further research.

---

### 6.1 Opportunities for Remote Sensing and GIS

This study has important implications from a Precision Agriculture perspective. Currently, proximal sensors are expensive to acquire, often difficult use, and time-consuming to implement at a commercial scale. Consequently, few if any kiwifruit orchardists, routinely and quantitatively measure and monitor canopy vigour. Precision Agriculture is not yet a reality in the New Zealand kiwifruit industry.

The remote sensors and GIS tools used in this study, were cost effective and easy to use on a commercial-scale. Multi-spectrum cameras have sufficient spectral and spatial resolution to distinguish much of the variability found within kiwifruit canopies. Using a low cost, mid-sized UAV as a platform, enabled greater temporal resolution, than would normally be possible using proximal sensors. This study showed the “Align UAV” to be reliable, across a range of typical weather conditions. GIS tools enabled freely available LIDAR data to be exploited. Data capture should become more cost effective, with wider industry adoption over time.

Data processing and map creation remains reasonably complex and requires a degree of operator proficiency to achieve consistent outputs with high  $R^2$  values. A good understanding of Geographic Information Systems (GIS) is certainly a pre-

requisite for anyone doing their own processing. However, third party processing is fast becoming a reality for orchardists without the necessary skills or time. These findings are an important, enabling step, towards industry-wide adoption of Precision Agriculture.

## 6.2 Contribution to Knowledge

This study has pushed many boundaries with respect to what was known about G3 kiwifruit canopy reflectance. G3 is a new commercial variety and almost all previous literature about canopy physiology, relates to Hayward or Hort16A varieties. G3 kiwifruit, has very different growth habits from Hayward kiwifruit.

Many of the results of this study, support or reinforce previous research findings. The observed behaviour of the vegetation indices for example, confirmed RECI as a good predictor of chlorophyll and NDVI as a good all-round performer, albeit that after canopy closure, it struggles to measure increasing LAI. The unique behaviour of PVR was somewhat unexpected. It seems to be affected by the high anthocyanin levels, known to be in kiwifruit leaves. The results of this study, have also produced quantitative evidence, for what growers have known anecdotally for some time. Plants in low-lying areas often appear less vigorous and now it is known that they tend to have measurably lower LAI and chlorophyll levels too.

This study has also resulted in some new understandings. For example, a new method was developed for measuring LAI on an overhead kiwifruit canopy structure (Figure 3-19). No previous literature was available to describe a method for measuring LAI in kiwifruit. It was also found that calculating three LAI measurements using 7°, 23° and 38° bands (Figure 2-1) and then taking the mean of all three estimates, produced the best estimation of the LAI within a single kiwifruit bay. Using the 53° and 68° bands produced inferior results. This is useful

information for anyone wanting to use a LICOR meter to measure LAI of kiwifruit grown on pergola structures.

Unexpectedly, Canopy Chlorophyll Content (CCC) was found to be a better dependent variable than LAI or leaf chlorophyll in regression models. Canopy Chlorophyll Content is an indicator of the total photosynthetic potential of the canopy. Because Canopy Chlorophyll Content and LAI have a very strong correlation ( $r = 0.99$ ), it is considered an equally valid proxy for canopy vigour and should be included in future studies of this nature.

Most importantly, this study definitively showed the extent to which canopy reflectance and orchard topography can explain G3 kiwifruit canopy vigour. The EVI2 index on its own explains about 67% of the observed variability in canopy vigour as measured by CCC. Adding simple terrain data, significantly increases the explanatory power by adding another 13%, taking the total to approximately 80%. This is new knowledge, that enables remote sensing data to be used with more confidence, as a viable alternative to proximal sensors.

## 6.3 Future Research

### 6.3.1 Model Validation

Having established three multiple regression models for Canopy Vigour (Adjusted  $R^2 = 0.85, 0.80$  and  $0.67$  respectively), canopy vigour maps can now be created to represent the predicted canopy vigour beyond the sample plants. Examples of canopy vigour maps, created using Model 2 and data collected in this study, are illustrated in Figure 6-1 and Figure 6-2. Further research is required to validate models like these, using new season, canopy reflectance data. Random areas should be selected from within newly created canopy vigour maps and validated with ground-truth measurements. A new study, will ideally be conducted

in multiple areas within the Bay of Plenty. Comparisons between G3 orchards and Hayward orchards should also be made, once the validity is established on G3 orchards.

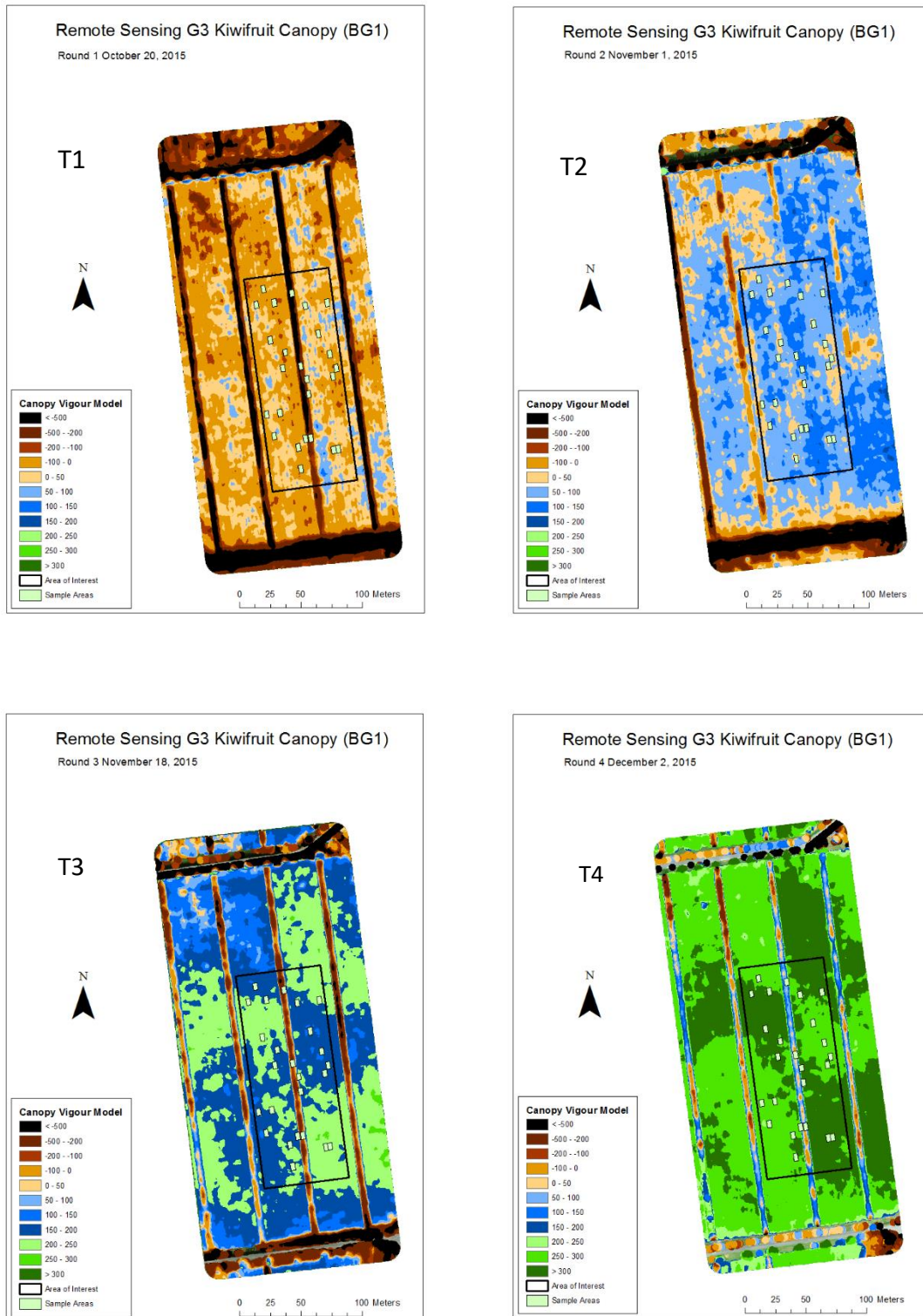


Figure 6-1 Examples of Canopy Vigour Maps based on Multiple Regression Model 2 for Orchard BG1 and Time Periods T1- T4

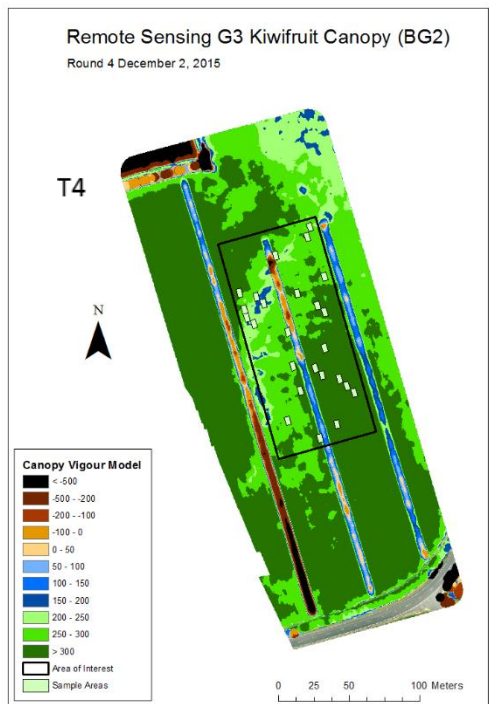
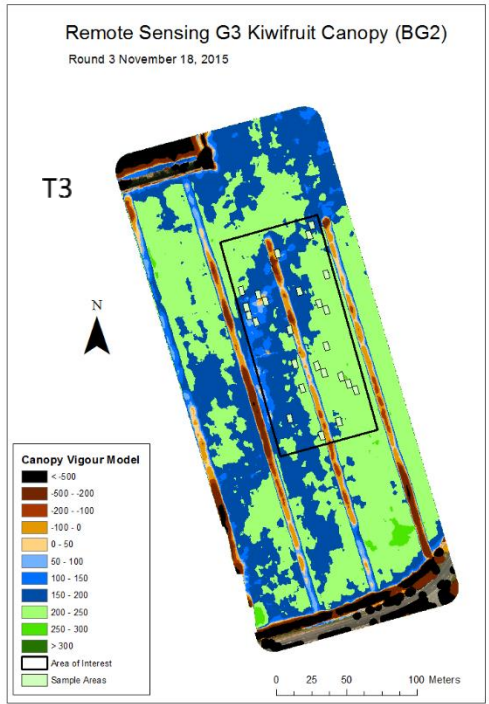
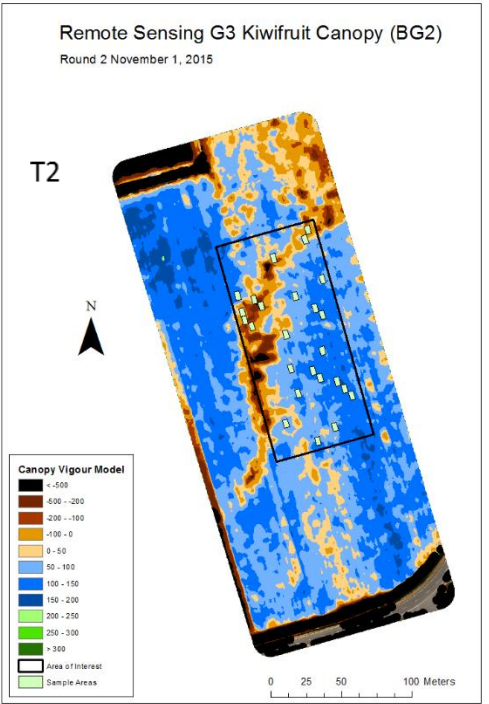
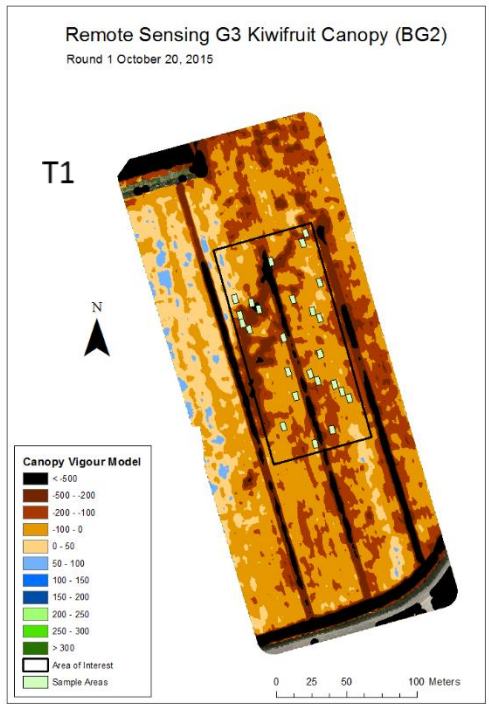


Figure 6-2 Examples of Canopy Vigour Maps based on Multiple Regression Model 2 for Orchard BG2 and Time Periods T1- T4

### 6.3.2 Advanced Terrain Modelling

Simple terrain data, in the form of Elevation  $\Delta$  and Relative Elevation at several scales, made a valuable contribution to the explanatory power of the models developed in this study. These rather crude measures of terrain, almost certainly contain information about water accumulation, cold air movement, sedimentation, fertility transfer and soil structure. Further research is required to determine if more sophisticated models of terrain can improve on the predictive power of the current models. These “advanced terrain models”, including hydrology models, could be applied to existing DEM datasets, without the need for further data collection in the field. Alternatively, they could also include new datasets such as air temperature and soil moisture probes, if future funding permits.

### 6.3.3 Relationship between Canopy Vigour, Fruit Quality and Yield

It is evident from discussions with kiwifruit growers, that predicting and mapping canopy vigour is not sufficient on its own, for most orchardists to modify their management practices, or to adopt Precision Agriculture per se. While plant health and vigour are generally associated with good yields, the relationships between canopy vigour, fruit quality and yield is not necessarily linear, or even positively correlated. Before growers are likely to find predictive maps useful, the relationships between orchard gate return (OGR), determined largely by yield and fruit dry matter, and canopy vigour, needs to be better understood. Yield was not measured in this study and should be incorporated into future studies of this nature

#### 6.3.4 Variable Rate Plant and Equipment

Physical and/or digital maps, do not easily translate into something that growers can use in a practical way on their orchards. Future development of decision support tools and the ability to export remote sensing data into orchard plant and equipment such as variable rate fertiliser spreaders and irrigation systems will be key. Before any remote sensing technology can be commercially exploited, further consideration also needs to be given to economies of scale. To this end, aerial surveying using manned aircraft should be considered. This will require further studies into the effects of surveying at higher altitudes and therefore lower spatial resolutions.

#### 6.3.5 Summary

In summary, this study has demonstrated that remote sensing and GIS have many advantages over traditional sensors. While they are not necessarily a replacement for all proximal sensors, the results suggest, that they are a viable alternative to the Minolta SPAD and LICOR meter, for use in kiwifruit. The interactions observed, between topography, soils, vegetation and management, all highlight the natural synergy between Geography and mainstream Science. There are significant opportunities, for greater integration between these disciplines. Further research is still required to understanding the three-way relationship between canopy vigour, fruit quality and OGR. However, the kiwifruit industry can now cost effectively, measure and monitor the first of these. This is an important first step, towards implementing Precision Agriculture in the New Zealand kiwifruit industry.

## 7 References

- 
- Adam, E., Mutanga, O., & Rugege, D. (2010). Multispectral and hyperspectral remote sensing for identification and mapping of wetland vegetation: A review. *Wetlands Ecology and Management*, 18(3), 281–296. <http://doi.org/10.1007/s11273-009-9169-z>
- Agisoft PhotoScan. (2017). Retrieved February 28, 2017, from <http://www.agisoft.com/>
- Annunziata, A., & Scarpato, D. (2014). Factors affecting consumer attitudes towards food products with sustainable attributes. *Agricultural Economics (Czech Republic)*, 60(8), 353–363.
- Aqeel-Ur-Rehman, Abbasi, A. Z., Islam, N., & Shaikh, Z. A. (2014). A review of wireless sensors and networks' applications in agriculture. *Computer Standards and Interfaces*, 36(2), 263–270. <http://doi.org/10.1016/j.csi.2011.03.004>
- Barsi, J. A., Schott, J. R., Hook, S. J., Raqueno, N. G., Markham, B. L., & Radocinski, R. G. (2014). Landsat-8 thermal infrared sensor (TIRS) vicarious radiometric calibration. *Remote Sensing*, 6(11), 11607–11626. <http://doi.org/10.3390/rs61111607>
- Bastiaanssen, W. G. M., Molden, D. J., & Makin, I. W. (2000). Remote sensing for irrigated agriculture: Examples from research and possible applications. *Agricultural Water Management*, 46(2), 137–155. [http://doi.org/10.1016/S0378-3774\(00\)00080-9](http://doi.org/10.1016/S0378-3774(00)00080-9)
- Bay of Plenty Regional Council. (2015). BOPRC - FTP Server. Retrieved August 1, 2015, from <ftp://files.boprc.govt.nz/Public/>
- Bellvert, J., Zarco-Tejada, P. J., Girona, J., & Fereres, E. (2014). Mapping crop water stress index in a Pinot-noir vineyard: Comparing ground measurements with thermal remote sensing imagery from an unmanned aerial vehicle. *Precision Agriculture*, 15(4), 361–376. <http://doi.org/10.1007/s11119-013-9334-5>
- Berg-Jürgens, N. L. and J. (2015). Accuracy of Orthomosaic Generated by Different Methods in Example of UAV Platform MUST Q. *IOP Conference Series: Materials Science and Engineering*, 96(1), 12041. <http://doi.org/10.1088/1757-899X/96/1/012041>
- Blaschke, T., Hay, G. J., Kelly, M., Lang, S., Hofmann, P., Addink, E., ... Tiede, D. (2014). Geographic Object-Based Image Analysis - Towards a new paradigm. *ISPRS Journal of Photogrammetry and Remote Sensing*, 87, 180–191. <http://doi.org/10.1016/j.isprsjprs.2013.09.014>
- Boike, J., Grüber, M., Langer, M., Piel, K., & Scheritz, M. (2012). Orthomosaic of Samoylov Island, Lena Delta, Siberia. *Pangaea*, (Appendix C), 0–2. <http://doi.org/10.1594/PANGAEA.786073>
- Brandenburg, D.-. (2012). *Licor 2200 Instruction manual. System*. <http://doi.org/10.1016/B978-1-4832-1312-5.50007-9>
- Brewer, K. R. W. (1999). Design-Based or Prediction-Based Inference? Stratified Random vs Stratified Balanced Sampling. *International Statistical Review / Revue Internationale de Statistique*, 67(1), 35–47.

- Broge, N. H., & Leblanc, E. (2001). Comparing prediction power and stability of broadband and hyperspectral vegetation indices for estimation of green leaf area index and canopy chlorophyll density. *Remote Sensing of Environment*, 76(2), 156–172. [http://doi.org/10.1016/S0034-4257\(00\)00197-8](http://doi.org/10.1016/S0034-4257(00)00197-8)
- Buxton, K. N. (2005). *Preharvest Practices Affecting Postharvest Quality of*. Massey University. Retrieved from <http://mro.massey.ac.nz/handle/10179/1630>
- Christian, N. (2002). Exploring Geographic Information Systems, 12–82. <http://doi.org/10.1108/jd.2002.58.3.339.9>
- Civil Aviation NZ. Gyrogliders and Parasails, Unmanned Aircraft (including Balloons), Kites, and Rockets – Operating Rules. (2015). Retrieved from [www.caa.govt.nz/rules/Part\\_101\\_Brief.htm](http://www.caa.govt.nz/rules/Part_101_Brief.htm)
- Darvishzadeh, R., Skidmore, A., Schlerf, M., Atzberger, C., Corsi, F., & Cho, M. (2008). LAI and chlorophyll estimation for a heterogeneous grassland using hyperspectral measurements. *ISPRS Journal of Photogrammetry and Remote Sensing*, 63(4), 409–426. <http://doi.org/10.1016/j.isprsjprs.2008.01.001>
- Deery, D., Jimenez-Berni, J., Jones, H., Sirault, X., & Furbank, R. (2014). *Proximal Remote Sensing Buggies and Potential Applications for Field-Based Phenotyping. Agronomy* (Vol. 4). <http://doi.org/10.3390/agronomy4030349>
- Dell Inc. (2016). Statistica Help. Retrieved from <http://documentation.statsoft.com/>
- Duro, D. C., Franklin, S. E., & Dube, M. G. (2012). A comparison of pixel-based and object-based image analysis with selected machine learning algorithms for the classification of agricultural landscapes using SPOT-5 HRG imagery. *Remote Sensing of Environment*, 118, 259–272. <http://doi.org/10.1016/j.rse.2011.11.020>
- Erskine, R. H., Green, T. R., Ramirez, J. a., & MacDonald, L. H. (2007). Digital Elevation Accuracy and Grid Cell Size: Effects on Estimated Terrain Attributes. *Soil Science Society of America Journal*, 71(4), 1371. <http://doi.org/10.2136/sssaj2005.0142>
- ESRI ArcMap. (2017). Retrieved February 28, 2017, from <http://www.esri.com/>
- Famiani, F., Baldicchi, A., Farinelli, D., Cruz-Castillo, J. G., Marocchi, F., Mastroleo, M., ... Battistelli, A. (2012). Yield affects qualitative kiwifruit characteristics and dry matter content may be an indicator of both quality and storability. *Scientia Horticulturae*, 146, 124–130. <http://doi.org/10.1016/j.scienta.2012.08.009>
- Fraser, L. G., Seal, A. G., Montefiori, M., McGhie, T. K., Tsang, G. K., Datson, P. M., ... Allan, A. C. (2013). An R2R3 MYB transcription factor determines red petal colour in an Actinidia (kiwifruit) hybrid population. *BMC Genomics*, 14(1), 28. <http://doi.org/10.1186/1471-2164-14-28>
- Froud, K. J., Everett, K. R., Tyson, J. L., Beresford, R. M., & Cogger, N. (2015). Review of the risk factors associated with kiwifruit bacterial canker caused by *Pseudomonas syringae* pv. *actinidiae*, 327(biovar 3), 313–327.
- Gitelson, A. A. (2004). Wide Dynamic Range Vegetation Index for remote quantification of biophysical characteristics of vegetation. *Journal of Plant Physiology*, 161(2), 165–173. <http://doi.org/10.1078/0176-1617-01176>

- Gitelson, A. A., Gritz, Y., & Merzlyak, M. N. (2003). Relationships between leaf chlorophyll content and spectral reflectance and algorithms for non-destructive chlorophyll assessment in higher plant leaves. *Journal of Plant Physiology*, *160*(3), 271–282. <http://doi.org/10.1078/0176-1617-00887>
- Gitelson, A. A., & Merzlyak, M. N. (1994). Spectral Reflectance Changes Associated with Autumn Senescence of *Aesculus-hippocastanum* L. and *Acer-platanoides* L. Leaves - Spectral Features and Relation to Chlorophyll Estimation. *Journal of Plant Physiology*. [http://doi.org/10.1016/S0176-1617\(11\)81633-0](http://doi.org/10.1016/S0176-1617(11)81633-0)
- Gitelson, A. A., Peng, Y., Arkebauer, T. J., & Schepers, J. (2014). Relationships between gross primary production, green LAI, and canopy chlorophyll content in maize: Implications for remote sensing of primary production. *Remote Sensing of Environment*, *144*(August 2016), 65–72. <http://doi.org/10.1016/j.rse.2014.01.004>
- Gitelson, A., Vina, A., Arkebauer, T., Rundquist, D., Keydan, G., & Leavitt, B. (2003). Remote estimation of leaf area index and green leaf biomass in maize canopies. *Geophysical Research Letters*, *30*(5), 4–7. <http://doi.org/10.1029/2002GL016450>
- Gómez-Candón, D., De Castro, A. I., & López-Granados, F. (2014). Assessing the accuracy of mosaics from unmanned aerial vehicle (UAV) imagery for precision agriculture purposes in wheat. *Precision Agriculture*, *15*(1), 44–56. <http://doi.org/10.1007/s11119-013-9335-4>
- Gross, J. W. (2015). *A Comparison of Orthomosaic Software for Use with Ultra High Resolution Imagery of a Wetland Environment*.
- Hall, a, Lamb, D. W., Holzapfel, B., & Louis, J. (2002). Optical remote sensing applications in viticulture - a review. *Australian Journal of Grape and Wine Research*, *8*(April), 36–47. <http://doi.org/10.1111/j.1755-0238.2002.tb00209.x>
- Harvey, M. C., Rowland, J. V., & Luketina, K. M. (2016). Drone with thermal infrared camera provides high resolution georeferenced imagery of the Waikite geothermal area, New Zealand. *Journal of Volcanology and Geothermal Research*, *325*(June), 61–69. <http://doi.org/10.1016/j.jvolgeores.2016.06.014>
- Hedley, C. (2015). The role of precision agriculture for improved nutrient management on farms. *Journal of the Science of Food and Agriculture*, *95*(1), 12–19. <http://doi.org/10.1002/jsfa.6734>
- Huang, Y., Lee, M. A., Thomson, S. J., & Reddy, K. N. (2016). Ground-based hyperspectral remote sensing for weed management in crop production. *International Journal of Agricultural and Biological Engineering*, *9*(2), 98–109. <http://doi.org/10.3965/j.ijabe.20160902.2137>
- Huang, Y., Thomson, S. J., Brand, H. J., & Reddy, K. N. (2016). Development and evaluation of low-altitude remote sensing systems for crop production management, *9*(4), 1–11. <http://doi.org/10.3965/j.ijabe.20160904.2010>
- Hull, G. (2015). *University of Waikato GEOG548 Advanced GIS Modelling*.
- Hull, G. (2016). *Remote Sensing to Determine Timing of CPPU applications in Hayward Kiwifruit (Confidential)*.

- Hunt, E. R., Doraiswamy, P. C., McMurtrey, J. E., Daughtry, C. S. T., Perry, E. M., & Akhmedov, B. (2012). A visible band index for remote sensing leaf chlorophyll content at the Canopy scale. *International Journal of Applied Earth Observation and Geoinformation*, 21(1), 103–112. <http://doi.org/10.1016/j.jag.2012.07.020>
- IDB - A database for remote sensing indices. (2017). Retrieved February 28, 2017, from <http://www.indexdatabase.de/db/i.php?offset=2>
- Jackson, R., & Heute, A. (1991). Interpreting Vegetation Indices. *Preventative Veterinary Medicine*, (11), 185–200. Retrieved from <http://www.uprm.edu/biology/profs/chinea/gis/lectesc/intvegindx.pdf>
- Jager, L. Zespri Sustainability Policy (2013). Retrieved from <http://www.zespri.com/Documents/Zespri-Sustainability-Policy-suppliers.pdf>
- Jiang, Z., Huete, A. R., Didan, K., & Miura, T. (2008). Development of a two-band enhanced vegetation index without a blue band. *Remote Sensing of Environment*, 112(10), 3833–3845. <http://doi.org/10.1016/j.rse.2008.06.006>
- Kamruzzaman, M., Elmasry, G., Sun, D. W., & Allen, P. (2012). Non-destructive prediction and visualization of chemical composition in lamb meat using NIR hyperspectral imaging and multivariate regression. *Innovative Food Science and Emerging Technologies*, 16(September 2015), 218–226. <http://doi.org/10.1016/j.ifset.2012.06.003>
- Konica Minolta. (2016). *CHLOROPHYLL METER SPAD-502Plus*.
- Li-Cor. (2014). FV2200 User Guide (LAI Program Manual), 1–54.
- LI-COR References. (2016). Retrieved October 10, 2016, from [https://www.licor.com/env/products/leaf\\_area/LAI-2200C/references.html](https://www.licor.com/env/products/leaf_area/LAI-2200C/references.html)
- Lindblom, J., Lundström, C., Ljung, M., & Jonsson, A. (2016). Promoting sustainable intensification in precision agriculture: review of decision support systems development and strategies. *Precision Agriculture*, 1–23. <http://doi.org/10.1007/s11119-016-9491-4>
- Ling, Q., Huang, W., & Jarvis, P. (2011). Use of a SPAD-502 meter to measure leaf chlorophyll concentration in *Arabidopsis thaliana*. *Photosynthesis Research*, 107(2), 209–214. <http://doi.org/10.1007/s11120-010-9606-0>
- Mathews, A. J., & Jensen, J. L. R. (2013). Visualizing and quantifying vineyard canopy LAI using an unmanned aerial vehicle (UAV) collected high density structure from motion point cloud. *Remote Sensing*, 5(5), 2164–2183. <http://doi.org/10.3390/rs5052164>
- McGlone, V. A., & Kawano, S. (1998). Firmness, dry-matter and soluble-solids assessment of postharvest kiwifruit by NIR spectroscopy. *Postharvest Biology and Technology*, 13(2), 131–141. [http://doi.org/10.1016/S0925-5214\(98\)00007-6](http://doi.org/10.1016/S0925-5214(98)00007-6)
- Metternicht, G. (2003). Vegetation indices derived from high-resolution airborne videography for precision crop management. *International Journal of Remote Sensing*, 24(14), 2855–2877. <http://doi.org/10.1080/01431160210163074>
- MicaSense RedEdge Multispectral Camera User Manual. (2015), (May), 1–27.
- Moore, I. D., Gessler, P. E., Nielson, G. A., & Peterson, G. A. (1993). Soil Attribute Prediction Using Terrain Analysis. *Soil Science Society of America Journal*, 57, 443–452. <http://doi.org/10.2136/sssaj1993.03615995005700020026x>

- Mulla, D. J. (2013). Twenty five years of remote sensing in precision agriculture: Key advances and remaining knowledge gaps. *Biosystems Engineering*, 114(4), 358–371. <http://doi.org/10.1016/j.biosystemseng.2012.08.009>
- Nguy-Robertson, A. L. (2013). Remote Sensing of Green Leaf Area Index in Maize and Soybean : From Close-Range to Satellite by.
- Panda, S. S., Hoogenboom, G., & Paz, J. (2009). Distinguishing blueberry bushes from mixed vegetation land use using high resolution satellite imagery and geospatial techniques. *Computers and Electronics in Agriculture*, 67(1–2), 51–58. <http://doi.org/10.1016/j.compag.2009.02.007>
- Pix4D. (2017). Retrieved February 28, 2017, from <https://pix4d.com>
- Porra, R. J., Thompson, W. a, & Kriedemann, P. E. (1989). Determination of Accurate Extinction Coefficients and Simultaneous-Equations for Assaying Chlorophyll-a and Chlorophyll-B Extracted with 4 Different Solvents - Verification of the Concentration of Chlorophyll Standards by Atomic-Absorption Spectroscopy. *Biochimica et Biophysica Acta*, 975(3), 384–394. [http://doi.org/Doi 10.1016/S0005-2728\(89\)80347-0](http://doi.org/Doi 10.1016/S0005-2728(89)80347-0)
- Praat, J. P., Bollen, F., Gillgren, D., Taylor, J., Mowat, A., & Amos, N. (2003). Using supply chain information: Mapping pipfruit and kiwifruit quality. *Acta Horticulturae*, 604, 377–385.
- QGIS Project. (2014). QGIS User Guide, 267. <http://doi.org/10.1007/s13398-014-0173-7.2>
- Qi, J., Chehbouni, a., Huete, a. R., Kerr, Y. H., & Sorooshian, S. (1994). A modified soil adjusted vegetation index. *Remote Sensing of Environment*, 48(2), 119–126. [http://doi.org/10.1016/0034-4257\(94\)90134-1](http://doi.org/10.1016/0034-4257(94)90134-1)
- Romps, D. M., & Öktem, R. (2015). Stereo photogrammetry reveals substantial drag on cloud thermals. *Geophysical Research Letters*, 42(12), 5051–5057. <http://doi.org/10.1002/2015GL064009>
- Rouse, J., Haas, R., Schell, J., & Deering, D. (1973). Monitoring Vegetation Systems in the Great Plains using ERTS. Retrieved from [ntrs.nasa.gov](http://ntrs.nasa.gov)
- Rumpf, T., Mahlein, A., Dorschlag, D., & Plumer, L. (2009). Identification of combined vegetation indices for the early detection of plant diseases. *Remote Sensing for Agriculture, Ecosystems, and Hydrology XI*, 7472(July 2015), 747210–747217. <http://doi.org/10.1117/12.830525>
- Schaare, P. N., & Fraser, D. G. (2000). Comparison of reflectance, interactance and transmission modes of visible-near infrared spectroscopy for measuring internal properties of kiwifruit (*Actinidia chinensis*). *Postharvest Biology and Technology*, 20(2), 175–184. [http://doi.org/10.1016/S0925-5214\(00\)00130-7](http://doi.org/10.1016/S0925-5214(00)00130-7)
- SEOS Introduction to Remote Sensing. (2017). Retrieved February 28, 2017, from <http://www.seos-project.eu/modules/remotesensing/remotesensing-c03-s01-p01.html>
- Slaughter, D. C., & Crisosto, C. H. (1998). Nondestructive internal quality assessment of kiwifruit using near-infrared spectroscopy. *Seminars in Food Analysis*, 3, 131–140.
- Smith, K. A., Jackson, D. R., Misselbrook, T. H., Pain, B. F., & Johnson, R. A. (2000). PA—Precision Agriculture. *Journal of Agricultural Engineering Research*, 77(3), 277–287. <http://doi.org/10.1006/jaer.2000.0604>
- Snowball, A. M. (1995). The seasonal cycle of leaf, shoot and bud development in kiwifruit. *Journal of Horticultural Science*, 70(5), 787–797. <http://doi.org/10.1080/14620316.1995.11515353>

- St-Onge, B., Vega, C., Fournier, R. A., & Hu, Y. (2008). Mapping canopy height using a combination of digital stereo-photogrammetry and lidar. *International Journal of Remote Sensing*, 29(11), 3343–3364. <http://doi.org/10.1080/01431160701469040>
- Sui, D. Z. (2004). Tobler ' s First Law of Geography : *Annals of the Association of American Geographers*, 94(July 2003), 269–277. <http://doi.org/10.1111/j.1467-8306.2004.09402003.x>
- Tobler, W. R. (1970). A Computer Movie Simulation Urban Growth in Detroit Region. *Economic Geography*, 46, 234–240. <http://doi.org/10.1126/science.11.277.620>
- Trout, T. J., Johnson, L. F., & Gartung, J. (2008). Remote sensing of canopy cover in horticultural crops. *Hortscience*, 43(2), 333–337.
- Turner, W., Spector, S., Gardiner, N., Fladeland, M., Sterling, E., & Steininger, M. (2003). Remote sensing for biodiversity science and conservation. *Trends in Ecology and Evolution*, 18(6), 306–314. [http://doi.org/10.1016/S0169-5347\(03\)00070-3](http://doi.org/10.1016/S0169-5347(03)00070-3)
- University of Waikato. (2016). *BIOL324 Plant Function Laboratory Manual, Lab 6.5*.
- Usha, K., & Singh, B. (2013). Potential applications of remote sensing in horticulture-A review. *Scientia Horticulturae*, 153(APRIL 2013), 71–83. <http://doi.org/10.1016/j.scienta.2013.01.008>
- Welles, J. M., & Cohen, S. (1996). Canopy structure measurement by gap fraction analysis using commercial instrumentation. *Journal of Experimental Botany*, 47(302), 1335–1342. <http://doi.org/10.1093/jxb/47.9.1335>
- Yost, M. A., Kitchen, N. R., Sudduth, K. A., Sadler, E. J., Drummond, S. T., & Volkmann, M. R. (2016). Long-term impact of a precision agriculture system on grain crop production. *Precision Agriculture*, 1–20. <http://doi.org/10.1007/s11119-016-9490-5>
- Yuan, L., Pu, R., Zhang, J., Wang, J., & Yang, H. (2016). Using high spatial resolution satellite imagery for mapping powdery mildew at a regional scale. *Precision Agriculture*, 17(3), 332–348. <http://doi.org/10.1007/s11119-015-9421-x>
- Zarco-Tejada, P. J., Berjón, a., López-Lozano, R., Miller, J. R., Martín, P., Cachorro, V., ... De Frutos, a. (2005). Assessing vineyard condition with hyperspectral indices: Leaf and canopy reflectance simulation in a row-structured discontinuous canopy. *Remote Sensing of Environment*, 99(3), 271–287. <http://doi.org/10.1016/j.rse.2005.09.002>
- Zhou, R., Damerow, L., Sun, Y., & Blanke, M. M. (2012). Using colour features of cv. “Gala” apple fruits in an orchard in image processing to predict yield. *Precision Agriculture*, 13(5), 568–580. <http://doi.org/10.1007/s11119-012-9269-2>

## 8 Appendices

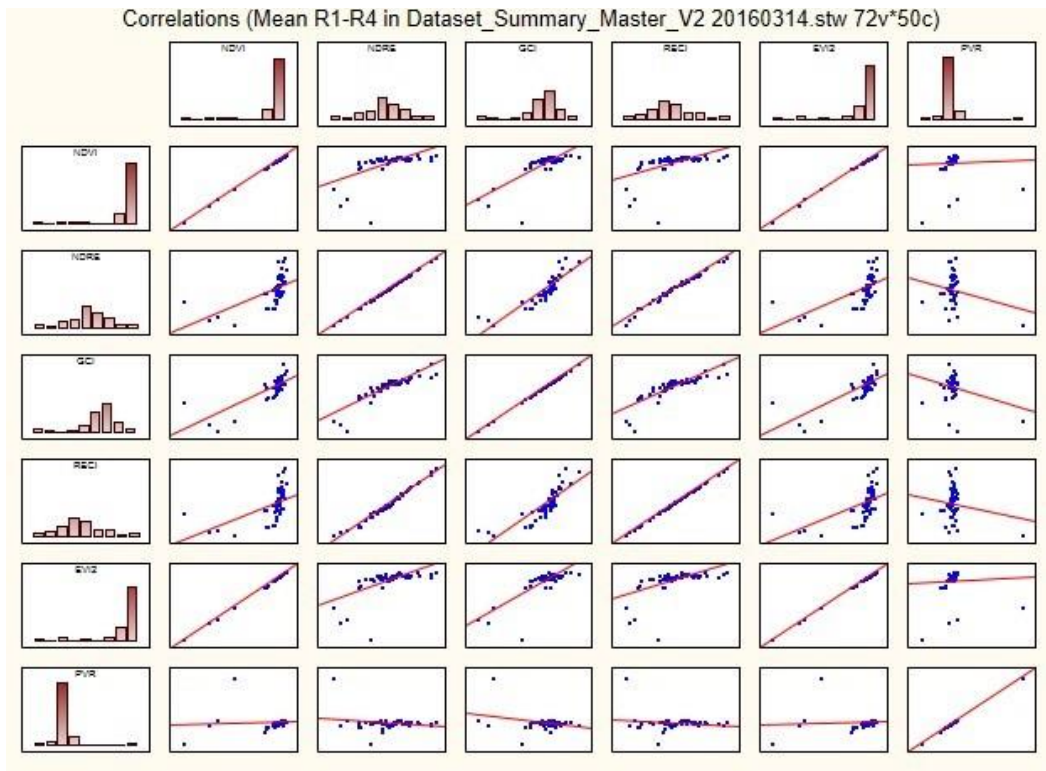
*Appendix 1 Table of raw leaf chlorophyll measurements (CHL\_SPAD) using Minolta SPAD meter (T1 – T4).*

Sample Plant	Block	Description	T1	T2	T3	T4	Mean
A1	BG1	Outlier	32.65	39.05	37.90	43.35	38.2375
A2	BG1	Outlier	34.00	37.50	38.05	42.55	38.025
A3	BG1		31.05	36.00	39.55	42.50	37.275
A4	BG1		34.70	37.35	40.85	43.20	39.025
A5	BG1		32.15	34.65	38.05	40.95	36.45
A6	BG1		32.95	35.90	38.30	44.40	37.8875
A7	BG1		32.55	37.30	38.95	40.90	37.425
A8	BG1	Outlier	31.20	39.50	41.65	41.70	38.5125
A9	BG1		33.45	35.15	37.50	42.20	37.075
A10	BG1	Outlier	35.80	39.90	43.00	44.10	40.7
A11	BG1		33.80	38.25	40.20	43.85	39.025
A12	BG1		33.30	37.90	38.10	41.55	37.7125
A13	BG1	Outlier	32.55	39.90	40.40	43.45	39.075
A14	BG1		31.95	37.45	38.65	42.15	37.55
A15	BG1		30.50	39.05	40.65	43.05	38.3125
A16	BG1	Outlier	31.80	37.50	40.90	43.15	38.3375
A17	BG1	Outlier	33.75	37.90	41.90	42.75	39.075
A18	BG1		31.75	37.15	39.55	42.25	37.675
A19	BG1	Outlier	35.55	39.75	41.55	44.80	40.4125
A20	BG1		32.20	36.70	40.40	44.20	38.375
A21	BG1	Outlier	36.65	42.10	42.80	46.00	41.8875
A22	BG1		32.45	36.55	37.95	42.50	37.3625
A23	BG1		31.55	36.45	42.00	43.50	38.375
A24	BG1	Outlier	31.20	36.45	38.80	44.05	37.625
A25	BG1		30.30	35.60	38.60	41.45	36.4875
B1	BG2		32.65	37.60	39.30	42.10	37.9125
B2	BG2		27.95	32.50	35.55	37.35	33.3375
B3	BG2		28.40	32.60	33.85	35.95	32.7
B4	BG2		28.05	32.95	34.50	36.90	33.1
B5	BG2		28.80	35.00	38.05	40.40	35.5625
B6	BG2	Outlier	0.00	28.90	32.20	36.80	24.47503
B7	BG2		29.85	35.40	37.95	41.00	36.05
B8	BG2		29.80	34.80	37.75	40.10	35.6125
B9	BG2		31.15	35.40	38.15	40.65	36.3375
B10	BG2		31.25	35.25	39.00	40.90	36.6
B11	BG2		33.45	39.35	41.55	40.85	38.8
B12	BG2		31.85	38.65	40.35	42.75	38.4
B13	BG2		33.70	39.85	41.85	44.40	39.95
B14	BG2		34.90	39.90	42.85	44.85	40.625
B15	BG2		31.90	38.85	39.85	42.90	38.375
B16	BG2		32.20	40.95	42.80	44.90	40.2125
B17	BG2		32.35	40.10	39.95	42.85	38.8125
B18	BG2		27.70	34.95	38.55	40.55	35.4375
B19	BG2		31.75	38.75	40.85	43.90	38.8125
B20	BG2		30.25	38.45	40.80	43.10	38.15
B21	BG2		31.05	38.50	39.65	43.05	38.0625
B22	BG2		28.35	35.50	39.70	42.20	36.4375
B23	BG2		29.75	36.45	38.35	38.85	35.85
B24	BG2		28.35	33.40	36.15	39.90	34.45
B25	BG2		28.30	33.35	37.90	41.15	35.175

Appendix 2 Table of Vegetation Index Correlations

Correlations (Mean R1-R4 in Dataset_Summary_Master_V2 20161021.stw)						
Marked correlations are significant at $p < .05000$						
N=39 (Casewise deletion of missing data)						
Variable	NDVI	NDRE	GCI	RECI	EVI2	PVR
NDVI	1.00000	0.61858	0.596919	0.628846	0.999604	0.826607
NDRE	0.618580	1.00000	0.921507	0.996393	0.633675	0.169063
GCI	0.596919	0.921507	1.00000	0.909773	0.612199	0.070873
RECI	0.628846	0.996393	0.909773	1.00000	0.643964	0.197852
EVI2	0.999604	0.633675	0.612199	0.643964	1.00000	0.819582
PVR	0.826607	0.169063	0.070873	0.197852	0.819582	1.00000

Appendix 3 Correlation Matrix (N.B. Includes outliers before removal)



Appendix 4 Table of Key Correlations

Variable	Correlations (Mean R1-R4 in Dataset_Summary_Master_V2.stw) Marked correlations are significant at p < .05000 N=39 (Casewise deletion of missing data)																	
	LAI_1	LAI_2	LAI_3	Mean LAI	LAI_1 x CAI	LAI_2 x CAI	LAI_3 x CAI	Mean (LAI x CAI)	Chl_SPAD	Chl_ug/cm 2	Chl_SPAD x LAI 1	Chl_SPAD x LAI 2	Chl_SPAD x LAI 3	Mean (Chl_SPAD x LAI)	Chl_SPAD x LAI_1 x CAI	Chl_SPAD x LAI_2 x CAI	Chl_SPAD x LAI_3 x CAI	Mean (Chl x LAI x CAI)
Chl_SPAD	0.669131	0.684127	0.693585	0.698259	0.658326	0.662833	0.658451	0.666589	<b>1.000000</b>	1.000000	0.734392	0.754239	0.773270	0.766852	0.706031	0.712067	0.712215	0.716043
Chl_ug/cm2	0.669131	0.684127	0.693585	0.698259	0.658326	0.662833	0.658451	0.666589	1.000000	<b>1.000000</b>	0.734392	0.754239	0.773270	0.766852	0.706031	0.712067	0.712215	0.716043
Chl_SPAD x LAI 1	<b>0.994232</b>	<b>0.947871</b>	<b>0.902314</b>	<b>0.980553</b>	<b>0.971980</b>	<b>0.934468</b>	<b>0.903714</b>	<b>0.949319</b>	0.734392	0.734392	<b>1.000000</b>	0.955430	0.909290	0.981106	0.974340	0.937276	0.908974	0.951114
Chl_SPAD x LAI 2	<b>0.943064</b>	<b>0.992977</b>	<b>0.940709</b>	<b>0.985067</b>	<b>0.934597</b>	<b>0.967057</b>	<b>0.925719</b>	<b>0.952713</b>	0.754239	0.754239	0.955430	<b>1.000000</b>	0.947246	0.988770	0.942457	0.971470	0.933486	0.958026
Chl_SPAD x LAI 3	<b>0.879810</b>	<b>0.920628</b>	<b>0.992044</b>	<b>0.945907</b>	<b>0.915225</b>	<b>0.942112</b>	<b>0.961713</b>	<b>0.947106</b>	0.773270	0.773270	0.909290	0.947246	<b>1.000000</b>	0.965419	0.934316	0.958549	0.974636	0.962472
Mean (Chl_SPAD x LAI)	0.966642	0.976218	0.958195	0.993327	0.963989	0.967326	0.945485	0.969603	0.766852	0.766852	0.981106	0.988770	0.965419	<b>1.000000</b>	0.972747	0.974352	0.953757	0.976252
Chl_SPAD x LAI_1 x CAI	0.963904	0.930613	0.931847	0.969243	0.996529	0.970908	0.962385	0.988004	0.706031	0.706031	0.974340	0.942457	0.934316	0.972747	<b>1.000000</b>	0.974209	0.964548	0.989550
Chl_SPAD x LAI_2 x CAI	0.922804	0.960443	0.957349	0.969234	0.967469	0.996252	0.981506	0.991225	0.712067	0.712067	0.937276	0.971470	0.958549	0.974352	0.974209	<b>1.000000</b>	0.984362	0.994495
Chl_SPAD x LAI_3 x CAI	0.888048	0.914328	0.973874	0.942490	0.953900	0.976162	0.996246	0.983391	0.712215	0.712215	0.908974	0.933486	0.974636	0.953757	0.964548	0.984362	<b>1.000000</b>	0.990036
Mean (Chl x LAI x CAI)	<b>0.936157</b>	<b>0.944238</b>	<b>0.960913</b>	<b>0.969911</b>	<b>0.982843</b>	<b>0.989591</b>	<b>0.987154</b>	<b>0.996369</b>	0.716043	0.716043	0.951114	0.958026	0.962472	0.976252	0.989550	0.994495	0.990036	<b>1.000000</b>

Appendix 5 Table of Key Correlations

Variable	Correlations (Mean R1-R4 in Dataset_Summary_Master_V2.stw) Marked correlations are significant at p < .05000 N=39 (Casewise deletion of missing data)						
	NDVI	NDRE	GCI	RECI	EVI2	PVR	CCCI
Mean Elevation	0.256120	0.241286	0.033818	0.285049	0.254929	0.316443	0.201733
Relative Elevation-5m	0.435894	0.121496	0.152505	0.153325	0.438715	0.479912	0.009779
Relative Elevation-10m	0.384274	0.073364	0.083943	0.109273	0.385784	0.456437	-0.030630
Relative Elevation-20m	0.318021	0.033817	0.047053	0.071291	0.318813	0.391405	-0.056569
Relative Elevation-50m	0.288630	0.075854	0.032387	0.117887	0.290579	0.381075	0.001074
Mean Slope 50m	0.193537	0.041058	0.201004	0.035736	0.192796	0.094731	-0.011077
Elevation Delta 50m	0.207119	-0.013419	-0.048304	0.027759	0.208115	0.329320	-0.077772
Canopy Mask %	0.830076	0.290837	0.300396	0.311395	0.824920	0.832411	0.085981
Canopy Area Index (CAI)	0.829959	0.293615	0.297594	0.314878	0.824945	0.836155	0.089199
LAI_1	0.831447	0.395138	0.404074	0.408582	0.830353	0.760327	0.206735
LAI_2	0.795732	0.396363	0.436610	0.409253	0.796912	0.704499	0.219627
LAI_3	0.770108	0.401122	0.394114	0.418071	0.770761	0.706500	0.232018
Mean LAI	0.825028	0.407475	0.423785	0.421962	0.825160	0.746762	0.223169
LAI_1 x CAI	0.830017	0.386418	0.395959	0.401141	0.828896	0.772077	0.196826
LAI_2 x CAI	0.807057	0.375705	0.402962	0.391224	0.806816	0.744896	0.191664
LAI_3 x CAI	0.799639	0.374723	0.373965	0.392704	0.798719	0.756403	0.192368
Mean (LAI x CAI)	0.821802	0.383287	0.396077	0.399369	0.821031	0.766038	0.195763
Ch_SPAD	0.666138	0.579162	0.530552	0.602526	0.672570	0.499160	0.471020
Ch_ug/cm2	0.666138	0.579162	0.530552	0.602526	0.672570	0.499160	0.471020
Ch_SPAD x LAI 1	0.832823	0.433878	0.436776	0.448324	0.832638	0.742636	0.251164
Ch_SPAD x LAI 2	0.798609	0.435993	0.465149	0.450174	0.800485	0.690766	0.264540
Ch_SPAD x LAI 3	0.773363	0.448759	0.435885	0.466951	0.775049	0.684416	0.286317
Mean (Ch_SPAD x LAI)	0.822352	0.447538	0.455586	0.463177	0.823383	0.724404	0.270349
Ch_SPAD x LAI_1 x CAI	0.826032	0.415782	0.421367	0.430993	0.825654	0.751435	0.232017
Ch_SPAD x LAI_2 x CAI	0.802756	0.405164	0.425960	0.421227	0.803189	0.725253	0.227024
Ch_SPAD x LAI_3 x CAI	0.796580	0.408125	0.403476	0.426644	0.796512	0.734145	0.232013
Mean (Ch x LAI x CAI)	0.816674	0.413529	0.421421	0.430124	0.816662	0.743958	0.232318

Appendix 6 Table of Key Correlations

Variable	Correlations (Mean R1-R4 in Dataset_Summary_Master_V2.stw) Marked correlations are significant at $p < .05000$ N=39 (Casewise deletion of missing data)							
	Mean Elevation	Relative Elevation-5m	Relative Elevation-10m	Relative Elevation-20m	Relative Elevation-50m	Elevation Delta 50m	Canopy Mask %	Canopy Area Index (CAI)
LAI_1	0.129736	0.545015	0.518221	0.492298	0.490071	0.432146	0.847473	0.848756
LAI_2	0.077207	0.562903	0.536561	0.521220	0.536999	0.486667	0.820384	0.817204
LAI_3	0.120106	0.624626	0.602579	0.572401	0.583812	0.536182	0.786346	0.780740
Mean LAI	0.111962	0.585873	0.559738	0.535833	0.543425	0.489294	0.844608	0.842588
LAI_1 x CAI	0.073446	0.546697	0.520689	0.486126	0.476359	0.414775	0.906864	0.905225
LAI_2 x CAI	0.046907	0.560818	0.536881	0.511284	0.513213	0.456240	0.901622	0.897519
LAI_3 x CAI	0.089759	0.592189	0.571378	0.539042	0.536640	0.479457	0.894372	0.889999
Mean (LAI x CAI)	0.069722	0.570156	0.546090	0.514906	0.511184	0.451828	0.910667	0.907377
Chl_SPAD	0.365532	0.632660	0.640118	0.624754	0.649811	0.576281	0.556813	0.562277
Chl_ug/cm2	0.365532	0.632660	0.640118	0.624754	0.649811	0.576281	0.556813	0.562277
Chl_SPAD x LAI 1	0.146439	0.577562	0.553656	0.528059	0.529705	0.468148	0.839376	0.840684
Chl_SPAD x LAI 2	0.103236	0.595498	0.573312	0.557782	0.575566	0.520718	0.813550	0.811019
Chl_SPAD x LAI 3	0.152421	0.649854	0.632455	0.604784	0.619820	0.566360	0.775799	0.771535
Mean (Chl_SPAD x LAI)	0.135833	0.614909	0.592830	0.569701	0.580596	0.522262	0.830910	0.829424
Chl_SPAD x LAI_1 x CAI	0.084411	0.568780	0.545030	0.511568	0.505918	0.442177	0.893130	0.891497
Chl_SPAD x LAI_2 x CAI	0.062140	0.581583	0.560536	0.535706	0.540728	0.481349	0.886666	0.882889
Chl_SPAD x LAI_3 x CAI	0.105751	0.611085	0.593070	0.562463	0.564410	0.504628	0.878004	0.874074
Mean (Chl x LAI x CAI)	0.083682	0.590403	0.569039	0.539081	0.539254	0.477606	0.894290	0.891240

G3 Kiwifruit Leaf Samples													
Date Collected:	29-Oct-15												
Date Analysed:	30-Oct-15												
			Spectrometer Readings			less initial calibration			less turbidity		Calculated Chlorophyll		
	Minolta Reading	Sample Size (ml)	750	663.6	646.6	750	663.6	646.6	A663.6	A646.6	Chl a	Chl b	Chl a+b
Calibration			0.000000	-0.004000	-0.005000								
Test		8.000000	0.001000	0.154000	0.058000	0.001000	0.158000	0.063000	0.157000	0.062000	14.121200	3.906800	18.028
A1	29.1	8.000000	0.002000	0.166000	0.064000	0.002000	0.170000	0.069000	0.168000	0.067000	15.097200	4.287120	19.38432
A2	37.5	8.000000	0.004000	0.321000	0.133000	0.004000	0.325000	0.138000	0.321000	0.134000	28.724400	9.163440	37.88784
A3	32.1	8.000000	0.015000	0.292000	0.122000	0.015000	0.296000	0.127000	0.281000	0.112000	25.253200	7.160080	32.41328
A4	30.7	8.000000	0.002000	0.262000	0.097000	0.002000	0.266000	0.102000	0.264000	0.100000	23.832000	5.878080	29.71008
A5	30.7	8.000000	0.003000	0.233000	0.089000	0.003000	0.237000	0.094000	0.234000	0.091000	21.075600	5.594160	26.66976
A6	28.9	8.000000	0.002000	0.240000	0.091000	0.002000	0.244000	0.096000	0.242000	0.094000	21.798400	5.767360	27.56576
A7	27.5	8.000000	0.002000	0.230000	0.086000	0.002000	0.234000	0.091000	0.232000	0.089000	20.920400	5.347760	26.26816
A8	27.7	8.000000	0.010000	0.237000	0.095000	0.010000	0.241000	0.100000	0.231000	0.090000	20.802000	5.549520	26.35152
A9	30.2	8.000000	0.004000	0.249000	0.097000	0.004000	0.253000	0.102000	0.249000	0.098000	22.402800	6.142320	28.54512
A10	26.2	8.000000	0.004000	0.229000	0.089000	0.004000	0.233000	0.094000	0.229000	0.090000	20.606000	5.628080	26.23408
A11	25.9	8.000000	0.005000	0.217000	0.089000	0.005000	0.221000	0.094000	0.216000	0.089000	19.352400	5.976240	25.32864
A12	22.5	8.000000	0.004000	0.176000	0.072000	0.004000	0.180000	0.077000	0.176000	0.073000	15.758800	4.947760	20.70656
B1	51.2	10.000000	0.002000	0.321000	0.134000	0.002000	0.325000	0.139000	0.323000	0.137000	36.074000	11.965400	48.0394
B2	44	10.000000	0.004000	0.419000	0.171000	0.004000	0.423000	0.176000	0.419000	0.172000	46.941500	14.360300	61.3018
B3	39.9	10.000000	0.004000	0.325000	0.132000	0.004000	0.329000	0.137000	0.325000	0.133000	36.421000	11.054800	47.4758
B4	37.8	10.000000	0.002000	0.302000	0.115000	0.002000	0.306000	0.120000	0.304000	0.118000	34.231000	9.039400	43.2704
B5	34.2	10.000000	0.003000	0.289000	0.117000	0.003000	0.293000	0.122000	0.290000	0.119000	32.490500	9.929900	42.4204
B6	32.2	10.000000	0.003000	0.238000	0.091000	0.003000	0.242000	0.096000	0.239000	0.093000	26.906000	7.153400	34.0594
B7	29.5	10.000000	0.003000	0.200000	0.074000	0.003000	0.204000	0.079000	0.201000	0.076000	22.684500	5.566500	28.251
B8	34.8	10.000000	0.001000	0.157000	0.060000	0.001000	0.161000	0.065000	0.160000	0.064000	17.968000	5.142400	23.1104
B9	33.9	10.000000	0.002000	0.223000	0.087000	0.002000	0.227000	0.092000	0.225000	0.090000	25.267500	7.231500	32.499
B10	42.4	10.000000	0.002000	0.327000	0.132000	0.002000	0.331000	0.137000	0.329000	0.135000	36.860000	11.264600	48.1246
B11	45	10.000000	0.002000	0.339000	0.140000	0.002000	0.343000	0.145000	0.341000	0.143000	38.126000	12.300200	50.4262
B12	46.1	10.000000	0.002000	0.399000	0.161000	0.002000	0.403000	0.166000	0.401000	0.164000	44.940500	13.619300	58.5598

Point Name	Block	Round 1		Mean Elevation	Relative Elevation-5m	Relative Elevation-10m	Relative Elevation-20m	Relative Elevation-50m	Mean Slope	Slope (Rise/Run)	Rise (Slope x Run)	Elevation Delta	Total Area	Canopy Mask Area	Canopy Mask %	Canopy Area Index (CAI)	Canopy Area Index					Mean LAI	LAI_1 x CAI	LAI_2 x CAI	LAI_3 x CAI	Mean (LAI x CAI)
		Description 1	Description 2														LAI_1	LAI_2	LAI_3							
A1	BG1	Outlier	Shelter-below	67.9180	1.0000	1.0001	0.9998	0.9985	6.7400	1.9971	3.3700	-0.0993	22.1344	13.6645	0.6173	0.6156	2.0200	1.6300	1.8200	1.8233	1.2435	1.0034	1.1204	1.1224		
A2	BG1	Outlier	Shelter-below	68.6008	0.9996	0.9985	0.9946	0.9790	9.3049	1.9580	4.6524	-1.4714	21.9043	14.0045	0.6393	0.6433	1.1200	1.3300	1.1000	1.1833	0.7205	0.8556	0.7077	0.7613		
A3	BG1			74.4185	1.0002	1.0006	1.0023	1.0145	5.9268	2.0289	2.9634	1.0602	21.6599	9.5340	0.4402	0.4383	0.9200	0.7400	0.9600	0.8733	0.4032	0.3243	0.4207	0.3828		
A4	BG1			74.4265	1.0001	1.0006	1.0020	1.0136	6.0502	2.0272	3.0251	1.0002	21.9084	13.4475	0.6138	0.6041	2.3600	1.8800	1.7900	2.0100	1.4257	1.1357	1.0813	1.2142		
A5	BG1			69.5342	1.0000	0.9996	0.9974	0.9858	8.9175	1.9716	4.4587	-1.0022	21.8482	10.9446	0.5009	0.5148	0.7300	0.5200	0.4900	0.5800	0.3758	0.2677	0.2523	0.2986		
A6	BG1			67.8796	0.9996	0.9984	0.9942	0.9783	8.6530	1.9566	4.3265	-1.5071	21.8804	14.0623	0.6427	0.6364	2.3100	1.5800	1.5400	1.8100	1.4701	1.0055	0.9801	1.1519		
A7	BG1		Psa South	67.8401	0.9997	0.9987	0.9954	0.9864	7.3607	1.9727	3.6803	-0.9373	22.6233	13.1220	0.5800	0.5868	1.3500	1.7300	1.3000	1.4600	0.7922	1.0152	0.7629	0.8568		
A8	BG1	Outlier	Ohead Shelter	67.4263	0.9992	0.9979	0.9959	0.9920	7.2402	1.9840	3.6201	-0.5426	21.0294	12.6662	0.6023	0.6045	1.1100	1.2700	0.9500	1.1100	0.6710	0.7677	0.5743	0.6710		
A9	BG1			68.0163	1.0000	0.9998	0.9986	0.9962	6.5915	1.9925	3.2958	-0.2573	20.2252	15.0317	0.7432	0.7493	2.8500	1.9800	1.9700	2.2667	2.1356	1.4837	1.4762	1.6985		
A10	BG1	Outlier	Ohead Shelter	70.3113	1.0000	1.0000	1.0004	1.0017	6.9381	2.0035	3.4690	0.1226	21.5007	14.1853	0.6598	0.6673	1.7000	1.5900	1.8900	1.7267	1.1345	1.0611	1.2613	1.1523		
A11	BG1		Psa South	70.8367	1.0001	1.0002	1.0010	1.0018	7.3621	2.0036	3.6810	0.1288	19.5540	14.7495	0.7543	0.7541	1.3500	1.4500	1.5100	1.4367	1.0180	1.0934	1.1387	1.0834		
A12	BG1		Psa North	71.7284	1.0001	1.0005	1.0015	1.0055	7.4794	2.0110	3.7397	0.3907	21.4744	12.7964	0.5959	0.6003	1.9500	2.0500	1.2600	1.7533	1.1706	1.2306	0.7564	1.0525		
A13	BG1	Outlier	Ohead Shelter	73.9314	1.0004	1.0013	1.0043	1.0158	6.0991	2.0316	3.0495	1.1483	22.3326	10.6408	0.4765	0.4817	0.8700	1.1500	1.1700	1.0633	0.4191	0.5540	0.5636	0.5122		
A14	BG1		New graft	73.1536	1.0001	1.0005	1.0020	1.0049	4.3074	2.0097	2.1537	0.3545	22.5098	7.0673	0.3140	0.3238	1.5800	0.9900	0.9500	1.1733	0.5117	0.3206	0.3076	0.3800		
A15	BG1			73.1540	1.0001	1.0005	1.0020	1.0067	5.2374	2.0134	2.6187	0.4857	21.5856	8.6588	0.4011	0.4061	0.8300	1.3300	1.2000	1.1200	0.3371	0.5402	0.4874	0.4549		
A16	BG1	Outlier	Ohead Shelter	73.6479	1.0003	1.0011	1.0036	1.0131	5.9156	2.0261	2.9578	0.9502	22.1523	8.8049	0.1718	0.1705	1.0600	0.6300	0.8000	0.8300	0.1807	0.1074	0.1364	0.1415		
A17	BG1	Outlier	Shelter-below	70.8825	1.0000	1.0002	1.0009	1.0071	6.1847	2.0142	3.0924	0.4995	20.6150	7.9860	0.3874	0.3830	1.1200	1.4700	1.3000	1.2967	0.4289	0.5629	0.4978	0.4966		
A18	BG1			70.5687	1.0001	1.0005	1.0021	1.0104	6.3115	2.0209	3.1558	0.7281	19.1859	6.6550	0.3469	0.3595	1.1000	0.9700	0.8400	0.9700	0.3955	0.3487	0.3020	0.3487		
A19	BG1	Outlier	Shelter-below	68.0069	0.9994	0.9986	0.9973	0.9977	7.7258	1.9953	3.8629	-0.1590	22.5981	10.9301	0.4837	0.4888	1.0800	2.1300	1.7500	1.6533	0.5279	1.0411	0.8553	0.8081		
A20	BG1		Psa South	66.9124	0.9998	0.9992	0.9970	0.9912	8.5202	1.9824	4.2601	-0.5943	21.5271	9.9464	0.4620	0.4652	1.2600	1.3600	1.1900	1.2700	0.5861	0.6326	0.5535	0.5907		
A21	BG1	Outlier	Shelter-below	68.6403	1.0001	1.0004	1.0022	1.0083	8.2305	2.0166	4.1152	0.5646	20.3329	16.1240	0.7930	0.7919	3.1600	2.4700	2.8900	2.8400	2.5023	1.9559	2.2885	2.2489		
A22	BG1			70.6488	1.0002	1.0007	1.0032	1.0159	6.6740	2.0319	3.3370	1.1075	21.6447	11.1038	0.5130	0.5073	2.1700	1.3400	1.2600	1.5900	1.1008	0.6797	0.6391	0.8065		
A23	BG1			71.8398	1.0002	1.0007	1.0015	1.0018	5.9103	2.0035	2.9551	0.1260	21.1482	11.2050	0.5298	0.5225	1.3900	1.3500	1.0600	1.2667	0.7263	0.7054	0.5539	0.6619		
A24	BG1	Outlier	Shelter-below	71.3860	0.9997	0.9988	0.9960	0.9899	5.1659	1.9797	2.5830	-0.7317	21.2397	11.4220	0.5378	0.5349	1.9300	1.6600	1.7300	1.7333	1.0323	0.8879	0.9254	0.9485		
A25	BG1			71.1434	0.9998	0.9993	0.9978	0.9938	5.4046	1.9877	2.7023	-0.4414	20.9567	12.2177	0.6080	0.5668	2.3100	2.0700	1.6500	2.0100	1.3093	1.1732	0.9352	1.1392		
B1	BG2			46.7166	1.0002	1.0000	0.9994	0.9918	7.7138	1.9835	3.8569	-0.3878	22.6089	14.3474	0.6346	0.6321	2.3300	2.3500	2.1900	2.2900	1.4728	1.4855	1.3843	1.4476		
B2	BG2			46.3527	0.9995	0.9982	0.9942	0.9806	8.0112	1.9612	4.0056	-0.9182	21.6838	11.6458	0.5371	0.5311	1.8500	2.2400	1.7900	1.9600	0.9825	1.1896	0.9506	1.0409		
B3	BG2			46.3421	0.9995	0.9982	0.9943	0.9780	8.2156	1.9560	4.1078	-1.0430	20.8916	8.4575	0.4048	0.4047	1.0600	1.2200	1.2500	1.1767	0.4290	0.4937	0.5059	0.4762		
B4	BG2		Little canopy	46.1907	0.9993	0.9980	0.9943	0.9752	8.4065	1.9504	4.2032	-1.1754	21.1475	12.6686	0.5991	0.5988	1.2800	0.9200	1.1800	1.1267	0.7665	0.5509	0.7066	0.6747		
B5	BG2		Little canopy	45.6851	0.9997	0.9988	0.9953	0.9794	7.7845	1.9588	3.8922	-0.9603	21.1986	6.3273	0.2985	0.2866	0.2400	0.4900	0.9700	0.5667	0.0688	0.1405	0.2780	0.1624		
B6	BG2	Outlier	No canopy	45.5195	0.9997	0.9989	0.9949	0.9756	7.9910	1.9512	3.9955	-1.1388	21.9013	5.7912	0.2644	0.2735	0.1700	0.2300	0.3000	0.2333	0.0465	0.0629	0.0821	0.0638		
B7	BG2			46.6478	0.9998	0.9986	0.9949	0.9813	8.8749	1.9626	4.4374	-0.8879	21.6219	15.3420	0.7096	0.7120	1.3700	1.5100	1.3600	1.4133	0.9754	1.0750	0.9683	1.0062		
B8	BG2			48.8368	1.0005	1.0012	1.0029	0.9986	9.5141	1.9972	4.7570	-0.0686	21.6219	12.5699	0.5814	0.5634	1.5300	1.2100	1.3900	1.3767	0.8620	0.6817	0.7831	0.7756		
B9	BG2			50.1270	1.0003	1.0011	1.0035	1.0012	9.9200	2.0025	4.9600	0.0621	21.3270	12.7321	0.5970	0.5943	0.9100	1.7000	1.6400	1.4167	0.5408	1.0104	0.9747	0.8420		
B10	BG2			49.4261	0.9995	0.9986	0.9948	0.9756	10.0042	1.9511	5.0021	-1.2373	21.4641	13.8889	0.6471	0.6494	2.1600	1.6600	1.6000	1.8067	1.4027	1.0780	1.0390	1.1732		
B11	BG2			52.5638	1.0000	0.9998	0.9994	0.9984	9.8435	1.9969	4.9218	-0.0826	21.6589	12.0691	0.5572	0.5503	1.4600	1.9200	1.6200	1.6667	0.8035	1.0567	0.8915	0.9172		
B12	BG2			53.5051	1.0002	1.0006	1.0013	1.0064	9.6272	2.0129	4.8136	0.3417	21.5553	14.2698	0.6620	0.6599	1.9400	1.6500	1.6700	1.7533	1.2802	1.0888	1.1020	1.1570		
B13	BG2			53.6285	1.0003	1.0010	1.0028	1.0134	9.3872	2.0269	4.6936	0.7111	21.7631	15.4055	0.7079	0.7070	2.7300	1.7100	1.7800	2.0733	1.9302	1.2090	1.2585	1.4659		
B14	BG2			52.9739	1.0003	1.0010	1.0030	1.0130	9.7747	2.0261	4.8873	0.6820	21.3485	14.3051	0.6701	0.6621	2.9700	2.6000	1.9600	2.5100	1.9665	1.7215	1.2977	1.6619		
B15	BG2			52.2235	1.0003	1.0011	1.0026	1.0117	10.0232	2.0234	5.0116	0.6046	21.9189	15.9345	0.7270	0.7259	1.3900	2.0100	1.7700	1.7233	1.0091	1.4591	1.2849	1.2510		
B16	BG2			51.0105	1.0003	1.0010	1.0023	1.0094	9.9315	2.0188	4.9658	0.4744	21.6915	14.2134	0.6553	0.6499	1.7200	1.5500	1.8600	1.7100	1.1178	1.0073	1.2088	1.1113		
B17	BG2			50.1713	1.0001	1.0003	1.0011	1.0058	9.7469	2.0115	4.8735	0.2879	21.8338	17.2113	0.7883	0.7838	2.8400	2.4600	2.3600	2.5533	2.2260	1.9282	1.8498	2.0014		
B18	BG2			49.5912	1.0000	0.9998	0.9995	1.0019	9.9488	2.0037	4.9744	0.0925	21.5526	13.8819	0.6441	0.6500	2.2000	1.6000	1.3700	1.7233	1.4300	1.0400	0.8905	1.1202		
B19	BG2			47.5586	1.0002	1.0003	1.0005	0.9974	9.4358	1.9949	4.7179	-0.1223	21.9192	18.4245	0.8406	0.8253	2.5100	2.3500	1.9600	2.2733	2.0716	1.9395	1.6177	1.8763		
B20	BG2			46.7354	0.9999	0.9998	0.9990	0.9916	9.0748	1.9832	4.5374	-0.3952	21.1024	14.6084	0.6923	0.6918	1.9700	1.9600	1.6300	1.8533	1.3629	1.3559	1.1277	1.2822		
B21	BG2			45.2496	0.9993	0.9980	0.9954	0.9863	8.5870																	

Point Name	Block	Round 1		Chl_SPAD	Chl_ug/c	Chl_SPAD x LAI 1	Chl_SPAD x LAI 2	Chl_SPAD x LAI 3	Mean (Chl x LAI)	Chl_SPAD x LAI_1 x CAI	Chl_SPAD x LAI_2 x CAI	Chl_SPAD x LAI_3 x CAI	Mean (Chl x LAI x CAI)	Macro x LAI x Chl	Micro x LAI x Chl	Nutrients x LAI x Chl	NDVI	NDRE	GCI	RECI	EVI2	PVR
		Description 1	Description 2																			
A1	BG1	Outlier	Shelter-below	32.6500	34.1893	65.9530	53.2195	59.4230	59.5318	40.5994	32.7609	36.5796	36.6466	-3.1476	-1.7066	-2.4271	0.8418	0.2651	3.1039	0.7250	1.8978	2.9372
A2	BG1	Outlier	Shelter-below	34.0000	36.4646	38.0800	45.2200	37.4000	40.2333	24.4980	29.0913	24.0605	25.8833	0.1066	-1.3233	-0.6084	0.8358	0.2813	3.3167	0.7887	1.8818	2.789
A3	BG1			31.0500	31.4927	28.5660	22.9770	29.8080	27.1170	12.5197	10.0702	13.0640	11.8847	-0.5570	-1.7782	-1.1676	0.8185	0.2381	2.7903	0.6293	1.8185	2.7444
A4	BG1			34.7000	37.6444	81.8920	65.2360	62.1130	69.7470	49.4702	39.4084	37.5219	42.1335	-1.9516	-4.8134	-3.3825	0.8467	0.2666	3.1798	0.7310	1.9137	2.9641
A5	BG1			32.1500	33.3466	23.4695	16.7180	15.7535	18.6470	12.0829	8.6070	8.1104	9.6001	-0.3924	0.5146	0.0611	0.8333	0.2670	3.2331	0.7347	1.8695	2.7393
A6	BG1			32.9500	34.6949	76.1145	52.0610	50.7430	59.6395	48.4410	33.1328	32.2940	37.9559	-2.0307	-0.4274	-1.2291	0.8433	0.2920	3.4844	0.8301	1.9025	2.7359
A7	BG1		Psa South	32.5500	34.0208	43.9425	56.3115	42.3150	47.5230	25.7876	33.0463	24.8325	27.8888	0.5579	0.9111	0.7345	0.8376	0.3038	3.5994	0.8828	1.8879	2.6884
A8	BG1	Outlier	Ohead Shelter	31.2000	31.7455	34.6320	39.6240	29.6400	34.6320	20.9353	23.9530	17.9176	20.9353	-2.1675	-4.4124	-3.2899	0.6220	0.2109	1.7670	0.5521	1.2878	2.1151
A9	BG1			33.4500	35.5376	95.3325	66.2310	65.8965	75.8200	71.4360	49.6292	49.3785	56.8146	-4.6395	-12.9567	-8.7981	0.8603	0.2846	3.4170	0.8004	1.9608	3.1051
A10	BG1	Outlier	Ohead Shelter	35.8000	39.4983	60.8600	56.9220	67.6620	61.8147	40.6137	37.9858	45.1529	41.2508	-4.0887	-3.2389	-3.6638	0.6916	0.2479	2.2847	0.6837	1.4622	2.7428
A11	BG1		Psa South	33.8000	36.1275	45.6300	49.0100	51.0380	48.5593	34.4094	36.9583	38.4876	36.6184	-2.4094	-3.4158	-2.9126	0.8402	0.2875	3.6086	0.8164	1.8938	2.6708
A12	BG1		Psa North	33.3000	35.2848	64.9350	68.2650	41.9580	58.3860	38.9794	40.9783	25.1867	35.0481	-7.0305	-8.1587	-7.5946	0.8307	0.2735	3.2820	0.7592	1.8606	2.6614
A13	BG1	Outlier	Ohead Shelter	32.5500	34.0208	28.3185	37.4325	38.0835	34.6115	13.6416	18.0320	18.3456	16.6731	-0.7944	-2.3879	-1.5912	0.7545	0.2102	1.9776	0.5695	1.6529	14.702
A14	BG1		New graft	31.9500	33.0095	50.4810	31.6305	30.3525	37.4880	16.3474	10.2430	9.8291	12.1398	-1.5665	-3.0562	-2.3113	0.8201	0.2750	3.1091	0.7624	1.8275	2.6035
A15	BG1			30.5000	30.5657	25.3150	40.5650	36.6000	34.1600	10.2816	16.4754	14.8650	13.8740	-2.3891	-2.6808	-2.5350	0.8312	0.2587	3.1577	0.7019	1.8615	2.7125
A16	BG1	Outlier	Ohead Shelter	31.8000	32.7567	33.7080	20.0340	25.4400	26.3940	5.7477	3.4161	4.3379	4.5006	-1.2946	-1.9177	-1.6062	0.8431	0.2679	3.1371	0.7356	1.9052	2.9661
A17	BG1	Outlier	Shelter-below	33.7500	36.0433	37.8000	49.6125	43.8750	43.7625	14.4757	18.9994	16.8022	16.7591	-2.7328	-3.0182	-2.8755	0.8304	0.2628	3.2225	0.7166	1.8581	2.6482
A18	BG1			31.7500	32.6725	34.9250	30.7975	26.6700	30.7975	12.5559	11.0720	9.5881	11.0720	0.8110	-1.6491	-0.4190	0.8218	0.2497	3.0007	0.6689	1.8286	2.6285
A19	BG1	Outlier	Shelter-below	35.5500	39.0770	38.3940	75.7215	62.2125	58.7760	18.7654	37.0095	30.4069	28.7272	-2.6971	-1.7945	-2.2458	0.8277	0.2683	3.2753	0.7377	1.8512	2.6233
A20	BG1		Psa South	32.2000	33.4309	40.5720	43.7920	38.3180	40.8940	17.8239	17.8239	19.0221	18.0221	-0.5942	-0.1020	-0.3481	0.8314	0.2783	3.2272	0.7781	1.8614	2.6685
A21	BG1	Outlier	Shelter-below	36.6500	40.9309	115.8140	90.5255	105.9185	104.0860	91.7079	71.6830	83.8721	82.4210	-5.5211	-6.6043	-6.0627	0.8496	0.2817	3.1921	0.7890	1.9238	3.0207
A22	BG1			32.4500	33.8522	70.4165	43.4830	40.8870	51.5955	35.7195	22.0572	20.7404	26.1723	-0.9452	-2.9736	-1.9594	0.8265	0.2587	2.9509	0.7022	1.8457	2.7559
A23	BG1			31.5500	32.3354	43.8545	42.5925	33.4430	39.9633	22.9155	17.4751	20.8822	22.2561	-2.6983	-4.1186	-3.4085	0.8379	0.2566	3.1975	0.6952	1.8841	2.8103
A24	BG1	Outlier	Shelter-below	31.2000	31.7455	60.2160	51.7920	53.9760	55.3280	32.2093	27.7033	28.8716	29.5947	-3.5738	-3.4790	-3.5264	0.8468	0.2408	3.0235	0.6382	1.9141	3.0797
A25	BG1			30.3000	30.2286	69.9930	62.7210	49.9950	60.9030	39.6705	35.5489	28.3361	34.5185	-0.2087	-5.3382	-2.7735	0.8451	0.2626	3.0844	0.7162	1.9082	3.004
B1	BG2			32.6500	34.1893	76.0745	76.7275	71.5035	74.7685	48.0881	48.5009	45.1987	47.2626	-1.4494	-5.6620	-3.5557	0.8505	0.2545	2.9892	0.6858	1.9255	3.1452
B2	BG2			27.9500	26.2679	51.7075	62.6080	50.0305	54.7820	27.4596	33.2484	26.5690	29.0923	-2.1014	-6.4487	-4.2750	0.8283	0.2421	2.8606	0.6419	1.8504	2.8326
B3	BG2			28.4000	27.0264	30.1040	34.6480	35.5000	33.4173	12.1829	14.0219	14.3666	13.5238	-2.8747	-3.4640	-3.1694	0.8093	0.2458	2.8713	0.6569	1.7878	2.5531
B4	BG2		Little canopy	28.0500	26.4365	35.9040	25.8060	33.0990	31.6030	21.5011	15.4539	19.8213	18.9254	-2.5081	-2.7044	-2.6062	0.8233	0.2560	2.9852	0.6931	1.8339	2.6782
B5	BG2		Little canopy	28.8000	27.7005	6.9120	14.1120	27.9360	16.3200	1.9812	4.0450	8.0075	4.6779	-0.0652	-1.0446	-0.5549	0.7988	0.2529	2.9485	0.6799	1.7586	2.4547
B6	BG2	Outlier	No canopy	0.0001	-20.8388	0.0000	0.0000	0.0000	0.0000	0.0000	0.0000	0.0000	0.0000	0.0000	0.0000	0.0000	0.6064	0.2444	2.7005	0.6545	1.2000	1.1795
B7	BG2			29.8500	29.4702	40.8945	45.0735	40.5960	42.1880	29.1149	32.0902	28.9024	30.0358	0.8589	-2.1245	-0.6328	0.8266	0.2668	3.2161	0.7334	1.8466	2.6338
B8	BG2			29.8000	29.3859	45.5940	36.0580	41.4220	41.0247	25.6870	20.3146	23.3366	23.1127	0.8817	-2.7194	-0.9188	0.8234	0.2492	3.0127	0.6672	1.8344	2.6511
B9	BG2			31.1500	31.6612	28.3465	52.9550	51.0860	44.1292	16.8470	31.4725	30.3617	26.2271	-0.9879	-1.6792	-1.3335	0.8160	0.2492	2.9228	0.6669	1.8099	2.595
B10	BG2			31.2500	31.8298	67.5000	51.8750	50.0000	56.4583	43.8337	33.6870	32.4694	36.6634	-0.4232	-0.3175	-0.3703	0.8356	0.2489	3.0315	0.6663	1.8753	2.839
B11	BG2			33.4500	35.5376	48.8370	64.2240	54.1890	55.7500	26.8769	35.3450	29.8223	30.6814	-1.1767	0.4505	-0.3631	0.8238	0.2710	3.1719	0.7473	1.8352	2.5519
B12	BG2			31.8500	32.8410	61.7890	52.5525	53.1895	55.8437	40.7739	34.6788	35.0992	36.8506	0.1545	-1.9679	-0.9067	0.8126	0.2322	2.6513	0.6079	1.7980	2.7226
B13	BG2			33.7000	35.9590	92.0010	57.6270	59.9860	69.8713	65.0470	40.7437	42.4116	49.4008	-3.5289	-3.4962	-3.5126	0.8303	0.2543	3.0210	0.6862	1.8571	2.7552
B14	BG2			34.9000	37.9815	103.6530	90.7400	68.4040	87.5990	68.6297	60.0799	45.2910	58.0002	-2.3288	-6.2935	-4.3111	0.8291	0.2560	3.0175	0.6936	1.8537	2.7494
B15	BG2			31.9000	32.9253	44.3410	64.1190	56.4630	54.9743	32.1891	46.5468	40.9890	39.9083	-0.4909	-0.1766	-0.3338	0.8298	0.2563	2.9477	0.6945	1.8570	2.8393
B16	BG2			32.2000	33.4309	55.3840	49.9100	59.8920	55.0620	35.9933	32.4358	38.9230	35.7840	0.3329	-1.5362	-0.6017	0.8197	0.2504	2.8468	0.6727	1.8225	2.7251
B17	BG2			32.3500	33.6837	91.8740	79.5810	76.3460	82.6003	72.0126	62.3771	59.8415	64.7438	0.9485	-2.2575	-0.6545	0.8380	0.2464	2.8831	0.6576	1.8827	2.9835
B18	BG2			27.7000	25.8466	60.9400	44.3200	37.9490	47.7363	24.6667	28.8079	24.6667	31.0285	-1.7223	-4.5099	-3.1161	0.8062	0.2267	2.6784	0.5904	1.7767	2.6051
B19	BG2			31.7500	32.6725	79.6925	74.6125	62.2300	72.1783	65.7729	61.5802	51.3605	59.5712	-1.6299	-6.4970	-4.0634	0.8477	0.2675	3.2130	0.7347	1.9166	2.9563
B20	BG2			30.2500	30.1444	59.5925	59.2900	49.3075	56.0633	41.2267	41.0174	34.1114	38.7852	-1.2620	-5.5146	-3.3883	0.8319	0.2622	3.0980	0.7158	1.8654	2.811
B21	BG2			31.0500	31.4927	36.6390	37.2600	37.5705	37.1565	22.0117	22.3847	22.5713	22.3226	-1.8075	-0.4348	-0.8224	0.8224	0.2567	3.0299	0.6940	1.8305	2.623
B22	BG2			28.3500	26.9421	49.8960	37.7055	33.1695	40.2570	34.2162	25.8566	22.7460	27.6063	0.3542	-3.7310	-1.6884	0.8179	0.2457	2.7651	0.6564	1.8165	2.7504
B23	BG2			29.7500	29.3017	52.3600	48.1950	42.2450	47.6000	22.2825	20.5100	17.9779	20.2568	-1.6046	-4.2520	-2.9283	0.8290	0.2623	3.0823	0.7157	1.8557	2.7628
B24	BG2			28.3500	26.9421	71.7255	68.60															

Point Name	Block	Round 2 Description 1	Description 2	Mean	Relative Elevation	Relative Elevation	Relative Elevation	Relative Elevation	Relative Elevation	Mean Slope	Elevation	Delta	Total Area	Canopy Mask	Canopy Mask %	Canopy Area Index (CAI)	Mean LAI			Mean LAI x CAI			
				Elevation	5m	10m	20m	50m	50m	50m	Area	Area	(CAI)	LAI_1	LAI_2	LAI_3	LAI	LAI_1 x CAI	LAI_2 x CAI	LAI_3 x CAI	Mean (LAI x CAI)		
A1	BG1	Outlier	Shelter-below	67.9180	1.0000	1.0001	0.9998	0.9985	0.9985	6.7400	-0.0993	22.1344	15.3329	0.6927	0.6874	3.7400	3.9500	3.6200	3.7700	2.5708	2.7151	2.4883	2.5914
A2	BG1	Outlier	Shelter-below	68.6008	0.9996	0.9985	0.9946	0.9790	0.9309	9.3049	-1.4714	21.9043	15.4576	0.7057	0.7028	2.3200	3.1900	2.5100	2.6733	1.6304	2.2419	1.7640	1.8788
A3	BG1			74.4185	1.0002	1.0006	1.0023	1.0145	0.9268	5.9268	1.0602	21.6599	13.4557	0.6212	0.6255	2.9800	2.6100	2.6300	2.7400	1.8640	1.6326	1.6451	1.7139
A4	BG1			74.4265	1.0001	1.0006	1.0020	1.0136	6.0502	6.0502	1.0002	21.9084	16.3742	0.7474	0.7402	3.3400	4.2800	3.7000	3.7733	2.4723	3.1680	2.7387	2.7930
A5	BG1			69.5342	1.0000	0.9996	0.9974	0.9858	8.9175	-1.0022	21.8482	13.8664	0.6347	0.6449	1.9200	2.0200	2.0100	1.9833	1.2382	1.3027	1.2962	1.2790	
A6	BG1			67.8796	0.9996	0.9984	0.9942	0.9783	8.6530	-1.5071	21.8804	15.8316	0.7235	0.7129	3.7500	3.5300	2.8300	3.3700	2.6735	2.5167	2.0176	2.4026	
A7	BG1		Psa South	67.8401	0.9997	0.9987	0.9954	0.9864	7.3607	-0.9373	22.6233	11.4025	0.5040	0.5121	2.6700	1.7400	1.5300	1.9800	1.3672	0.8910	0.7835	1.0139	
A8	BG1	Outlier	Ohead Shelter	67.4263	0.9992	0.9979	0.9959	0.9920	7.2402	-0.5426	21.0294	8.1248	0.3864	0.3946	3.4500	3.3000	3.0100	3.2533	1.3614	1.3022	1.1877	1.2838	
A9	BG1			68.0163	1.0000	0.9998	0.9986	0.9962	6.5915	-0.2573	20.2252	13.3897	0.6620	0.6637	6.1600	4.5600	4.5500	5.0900	4.0882	3.0263	3.0197	3.3780	
A10	BG1	Outlier	Ohead Shelter	70.3113	1.0000	1.0000	1.0004	1.0017	6.9381	0.1226	21.5007	7.4135	0.3448	0.3596	4.5500	5.0400	4.4400	4.6767	1.6362	1.8124	1.5966	1.6817	
A11	BG1		Psa South	70.8367	1.0001	1.0002	1.0010	1.0018	7.3621	0.1288	19.5540	12.5978	0.6443	0.6478	4.3000	3.0800	2.8000	3.3933	2.7857	1.9953	1.8139	2.1983	
A12	BG1		Psa North	71.7284	1.0001	1.0005	1.0015	1.0055	7.4794	0.3907	21.4744	12.2531	0.5706	0.5788	3.8300	2.7500	2.5500	3.0433	2.2167	1.5916	1.4759	1.7614	
A13	BG1	Outlier	Ohead Shelter	73.9314	1.0004	1.0013	1.0043	1.0158	6.0991	1.1483	22.3326	7.6848	0.3441	0.3531	4.0900	2.7700	2.4700	3.1100	1.4440	0.9780	0.8721	1.0980	
A14	BG1		New graft	73.1536	1.0001	1.0005	1.0020	1.0049	4.3074	0.3545	22.5098	10.1706	0.4518	0.4656	1.9100	2.8300	2.8400	2.5267	0.8893	1.3177	1.3223	1.1764	
A15	BG1			73.1540	1.0001	1.0005	1.0020	1.0067	5.2374	0.4857	21.5856	11.3512	0.5259	0.5272	4.5100	2.3700	2.4200	3.1000	2.3775	1.2494	1.2757	1.6342	
A16	BG1	Outlier	Ohead Shelter	73.6479	1.0003	1.0011	1.0036	1.0131	5.9156	0.9502	22.1523	11.0432	0.4985	0.5038	4.2700	3.4500	3.1200	3.6133	2.1512	1.7381	1.5718	1.8204	
A17	BG1	Outlier	Shelter-below	70.8825	1.0000	1.0002	1.0009	1.0071	6.1847	0.4995	20.6150	9.3420	0.4532	0.4521	3.0500	3.9600	2.9900	3.3333	1.3789	1.7903	1.3517	1.5070	
A18	BG1			70.5687	1.0001	1.0005	1.0021	1.0104	6.3115	0.7281	19.1859	9.7380	0.5076	0.5137	2.6700	2.1300	2.3000	2.3667	1.3717	1.0943	1.1816	1.2159	
A19	BG1	Outlier	Shelter-below	68.0069	0.9994	0.9986	0.9973	0.9977	7.7258	-0.1590	22.5981	13.2284	0.5854	0.5929	5.0900	4.1300	3.7400	4.3200	3.0180	2.4488	2.2175	2.5614	
A20	BG1		Psa South	66.9124	0.9998	0.9992	0.9970	0.9912	8.5202	-0.5943	21.5271	11.6225	0.5399	0.5433	1.8500	1.4600	1.8600	1.7233	1.0052	0.7933	1.0106	0.9364	
A21	BG1	Outlier	Shelter-below	68.6403	1.0001	1.0004	1.0022	1.0083	8.2305	0.5646	20.3329	17.9141	0.8810	0.8725	6.6400	6.4900	5.7600	6.2967	5.7932	5.6623	5.0254	5.4936	
A22	BG1			70.6488	1.0002	1.0007	1.0032	1.0159	6.6740	1.1075	21.6447	14.5190	0.6708	0.6566	3.2400	2.8700	2.7300	2.9467	2.1275	1.8846	1.7926	1.9349	
A23	BG1			71.8398	1.0002	1.0007	1.0015	1.0018	5.9103	0.1260	21.1482	14.3283	0.6775	0.6685	3.3400	2.8700	2.6700	2.9600	2.2327	1.9186	1.7849	1.9787	
A24	BG1	Outlier	Shelter-below	71.3860	0.9997	0.9988	0.9960	0.9899	5.1659	-0.7317	21.2397	15.2229	0.7167	0.7121	3.5600	4.4500	3.7300	3.9133	2.5351	3.1689	2.6562	2.7867	
A25	BG1			71.1434	0.9998	0.9993	0.9978	0.9938	5.4046	-0.4414	20.9567	16.5722	0.7908	0.7801	4.2600	2.9800	2.7400	3.3267	3.3234	2.3248	2.1376	2.5953	
B1	BG2			46.7166	1.0002	1.0000	0.9994	0.9918	7.7138	-0.3878	22.6089	15.9163	0.7040	0.6982	5.2400	4.8500	4.3700	4.8200	3.6587	3.3864	3.0512	3.3654	
B2	BG2			46.3527	0.9995	0.9982	0.9942	0.9806	8.0112	-0.9182	21.6838	13.0567	0.6021	0.5935	3.1800	2.9700	2.7500	2.9667	1.8875	1.7628	1.6322	1.7608	
B3	BG2			46.3421	0.9995	0.9982	0.9943	0.9780	8.2156	-1.0430	20.8916	8.1325	0.3893	0.3931	0.0001	0.0001	3.0000	1.0001	0.0000	0.0000	1.1794	0.3932	
B4	BG2		Little canopy	46.1907	0.9993	0.9980	0.9943	0.9752	8.4065	-1.1754	21.1475	10.8387	0.5125	0.5109	2.1300	1.9300	2.0000	2.0200	1.0881	0.9860	1.0217	1.0319	
B5	BG2		Little canopy	45.6851	0.9997	0.9988	0.9953	0.9794	7.7845	-0.9603	21.1986	6.1936	0.2922	0.2785	0.0001	0.0001	1.9100	0.6367	0.0000	0.0000	0.5319	0.1773	
B6	BG2	Outlier	No canopy	45.5195	0.9997	0.9989	0.9949	0.9756	7.9910	-1.1388	21.9013	0.4673	0.0340	0.0001	0.0001	0.0001	0.0001	0.0000	0.0000	0.0000	0.0000	0.0000	
B7	BG2			46.6478	0.9998	0.9986	0.9949	0.9813	8.8749	-0.8879	21.6219	13.3078	0.6155	0.6209	3.1300	3.1700	2.9300	3.0767	1.9435	1.9683	1.8193	1.9104	
B8	BG2			48.8368	1.0005	1.0012	1.0029	0.9986	9.5141	-0.0686	21.6219	14.1168	0.6529	0.6440	2.3100	2.1500	2.3200	2.2600	1.4877	1.3847	1.4942	1.4555	
B9	BG2			50.1270	1.0003	1.0011	1.0035	1.0012	9.9200	0.0621	21.3270	14.8143	0.6946	0.6927	2.8900	3.2700	3.1300	3.0967	2.0018	2.2650	2.1680	2.1449	
B10	BG2			49.4261	0.9995	0.9986	0.9948	0.9756	10.0042	-1.2373	21.4641	15.7838	0.7354	0.7347	3.5500	3.0200	2.5500	3.0400	2.6081	2.2188	1.8735	2.2335	
B11	BG2			52.5638	1.0000	0.9998	0.9994	0.9984	9.8435	-0.0826	21.6589	13.2729	0.6128	0.6032	4.1700	3.9500	3.0000	3.7067	2.5152	2.3825	1.8095	2.2357	
B12	BG2			53.5051	1.0002	1.0006	1.0013	1.0064	9.6272	0.3417	21.5553	16.0070	0.7426	0.7433	0.0001	3.1200	2.8500	1.9900	0.0001	2.3191	2.1184	1.4792	
B13	BG2			53.6285	1.0003	1.0010	1.0028	1.0134	9.3872	0.7111	21.7631	14.6120	0.6714	0.6648	4.4900	3.5300	3.4700	3.8300	2.9850	2.3468	2.3069	2.5462	
B14	BG2			52.9739	1.0003	1.0010	1.0030	1.0130	9.7747	0.6820	21.3485	13.8867	0.6505	0.6440	4.9000	5.0800	3.8900	4.6233	3.1555	3.2714	2.5051	2.9773	
B15	BG2			52.2235	1.0003	1.0011	1.0026	1.0117	10.0232	0.6046	21.9189	14.9817	0.6835	0.6785	4.8300	4.6700	4.0200	4.5067	3.2771	3.1685	2.7275	3.0577	
B16	BG2			51.0105	1.0003	1.0010	1.0023	1.0094	9.9315	0.4744	21.6915	15.8187	0.7293	0.7226	3.4400	3.5500	3.4300	3.4733	2.4857	2.5652	2.4785	2.5098	
B17	BG2			50.1713	1.0001	1.0003	1.0011	1.0058	9.7469	0.2879	21.8338	19.6199	0.8986	0.8912	4.9600	4.9300	3.9600	4.6167	4.4204	4.3936	3.5292	4.1144	
B18	BG2			49.5912	1.0000	0.9998	0.9995	1.0019	9.9488	0.0925	21.5526	13.4891	0.6259	0.6341	4.4600	4.5300	3.9500	4.3133	2.8281	2.8725	2.5047	2.7351	
B19	BG2			47.5586	1.0002	1.0003	1.0005	0.9974	9.4358	-0.1223	21.9192	16.1604	0.7373	0.7297	4.7200	4.6500	3.9500	4.4400	3.4443	3.3932	2.8824	3.2400	
B20	BG2			46.7354	0.9999	0.9998	0.9990	0.9916	9.0748	-0.3952	21.1024	12.0523	0.5711	0.5788	4.4300	3.8400	2.8600	3.7100	2.5642	2.2227	1.6555	2.1475	
B21	BG2			45.2496	0.9993	0.9980	0.9954	0.9863	8.5870	-0.6265	22.1470	12.5824	0.5681	0.5724	3.1000	3.6800	2.6400	3.1400	1.7745	2.1065	1.5112	1.7974	
B22	BG2			45.1931	0.9996	0.9986	0.9951	0.9778	8.3574	-1.0276	21.7843	14.4307	0.6624	0.6718	4.6700	2.9000	2.4700	3.3467	3.1373	1.9482	1.6593	2.2483	
B23	BG2			44.4072	0.9997	0.9989	0.9958	0.9842	7.4927	-0.7150	22.5824	10.3226	0.4571	0.4463	4.3100	3.8000	3.1300	3.7467	1.9236	1.6960	1.3970	1.6722	
B24	BG2			43.5262	0.9996	0.9985	0.9962	0.9884	7.4793	-0.5108	22.1481	12.4638	0.5628	0.5575	3.4900	3.4500	2.6000	3.1800	1.9457	1.9234	1.4495	1.7729	
B25	BG2	No plant	South End	43.2523	0.9996	0.9985	0.9966																

Point Name	Block	Round 2		Chl_SPAD	Chl_ug/c m2	Chl_SPAD x LAI 1	Chl_SPAD x LAI 2	Chl_SPAD x LAI 3	Mean (Chl_SPAD x LAI)	Chl_SPAD x LAI_1 x CAI	Chl_SPAD x LAI_2 x CAI	Chl_SPAD x LAI_3 x CAI	Mean (Chl_SPAD x LAI x CAI)	Macro x LAI x Chl	Micro x LAI x Chl	Nutrients x LAI x Chl	NDVI	NDRE	GCI	RECI	EV2	PVR
		Description 1	Description 2																			
A1	BG1	Outlier	Shelter-below	39.0500	44.9759	146.0470	154.2475	141.3610	147.2185	100.3881	106.0248	97.1671	101.1933	-7.7837	-4.2203	-6.0020	0.8684	0.2715	3.4317	0.7449	1.9890	3.2634
A2	BG1	Outlier	Shelter-below	37.5000	42.3635	87.0000	119.6250	94.1250	100.2500	61.1416	84.0697	66.1489	70.4534	0.2655	-3.2972	-1.5159	0.8635	0.2818	3.5139	0.7898	1.9715	3.0977
A3	BG1			36.0000	39.8354	107.2800	93.9600	94.6800	98.6400	67.1035	58.7719	59.2223	61.6992	-2.0262	-6.4684	-4.2473	0.8471	0.2563	3.0866	0.6924	1.9147	3.032
A4	BG1			37.3500	42.1107	124.7490	159.8580	138.1950	140.9340	92.3389	118.3265	102.2916	104.3190	-3.9436	-9.7262	-6.8349	0.8688	0.2858	3.5567	0.8032	1.9899	3.1707
A5	BG1			34.6500	37.5601	66.5280	69.9930	69.6465	68.7225	42.9025	45.1370	44.9136	44.3177	-1.4462	1.8965	0.2252	0.8589	0.2768	3.4987	0.7720	1.9562	3.0377
A6	BG1			35.9000	39.6669	134.6250	126.7270	101.5970	120.9830	95.9790	90.3482	72.4321	86.2531	-4.1195	-0.8670	-2.4932	0.8647	0.2931	3.6685	0.8332	1.9755	3.0007
A7	BG1		Psa South	37.3000	42.0264	99.5910	64.9020	57.0690	73.8540	50.9977	33.2345	29.2234	37.8185	0.8670	1.4160	1.1415	0.8593	0.3023	3.6739	0.8715	1.9585	2.9456
A8	BG1	Outlier	Ohead Shelter	39.5000	45.7343	136.2750	130.3500	118.8950	128.5067	53.7737	51.4357	46.9156	50.7084	-8.0428	-16.3727	-12.2077	0.8732	0.3007	3.9060	0.8576	2.0059	3.069
A9	BG1			35.1500	38.4028	216.5240	160.2840	159.9325	178.9135	143.6990	106.3746	106.1413	118.7383	-10.9480	-30.5741	-20.7610	0.8745	0.2910	3.5634	0.8261	2.0100	3.3267
A10	BG1	Outlier	Ohead Shelter	39.9000	46.4085	181.5450	201.0960	177.1560	186.5990	65.2831	72.3136	63.7048	67.1005	-12.3424	-9.7772	-11.0598	0.8732	0.3251	4.2715	0.9706	2.0066	2.9076
A11	BG1		Psa South	38.2500	43.6276	164.4750	117.8100	107.1000	129.7950	106.5519	76.3209	69.3826	84.0851	-6.4402	-9.1303	-7.7853	0.8737	0.2993	3.9208	0.8609	2.0078	3.0845
A12	BG1		Psa North	37.9000	43.0377	145.1570	104.2250	96.6450	115.3423	84.0125	60.3223	55.9352	66.7567	-13.8888	-16.1177	-15.0032	0.8585	0.2744	3.4624	0.7604	1.9549	3.0436
A13	BG1	Outlier	Ohead Shelter	39.9000	46.4085	163.1910	110.5230	98.5530	124.0890	57.6163	39.0213	34.7952	43.8110	-2.8481	-8.5612	-5.7047	0.8583	0.2863	3.7238	0.8070	1.9572	2.9498
A14	BG1		New graft	37.4500	42.2792	71.5295	105.9835	106.3580	94.6237	33.3048	49.3469	49.5213	44.0576	-3.9539	-7.7142	-5.8341	0.8490	0.2609	3.3674	0.7114	1.9241	2.9647
A15	BG1			39.0500	44.9759	176.1155	92.5485	94.5010	121.0550	92.8409	48.7878	49.8171	63.8153	-9.5003	-9.8933	-8.8531	0.8551	0.2635	3.3950	0.7197	1.9423	2.996
A16	BG1	Outlier	Ohead Shelter	37.5000	42.3635	160.1250	129.3750	117.0000	135.5000	80.6699	65.1783	58.9438	68.2640	-6.6462	-9.8450	-8.2456	0.8566	0.2705	3.5078	0.7454	1.9485	2.9664
A17	BG1	Outlier	Shelter-below	37.9000	43.0377	115.5950	150.0840	113.3210	126.3333	52.2591	67.8512	51.2311	57.1138	-7.8890	-8.7130	-8.3010	0.8605	0.2758	3.4684	0.7662	1.9615	3.0681
A18	BG1			37.1500	41.7736	99.1905	79.1295	85.4450	87.9217	50.9582	40.6521	43.8966	45.1690	2.3153	-4.7079	-1.1963	0.8496	0.2462	3.1213	0.6563	1.9225	3.0338
A19	BG1	Outlier	Shelter-below	39.7500	46.1557	202.3275	164.1675	148.6650	171.7200	119.9654	97.3393	88.1474	101.8174	-7.8800	-5.2428	-6.5614	0.8624	0.2804	3.6032	0.7811	1.9679	3.0221
A20	BG1		Psa South	36.7000	41.0152	67.8950	53.5820	68.2620	63.2463	36.8899	29.1131	37.0893	34.3641	-0.9189	-0.1577	-0.5383	0.8601	0.2784	3.4965	0.7817	1.9595	3.0544
A21	BG1	Outlier	Shelter-below	42.1000	50.1163	279.5440	273.2290	242.4960	265.0897	243.8936	238.3839	211.5703	231.2826	-14.0614	-16.8199	-15.4407	0.8751	0.3077	3.6395	0.8896	2.0126	3.2843
A22	BG1			36.5500	40.7624	118.4220	104.8985	99.7815	107.7007	77.7614	68.8812	65.5212	70.7121	-1.9729	-6.2070	-4.0900	0.8583	0.2591	3.2429	0.7038	1.9534	3.1661
A23	BG1			36.4500	40.5938	121.7430	104.6115	97.3215	107.8920	61.3833	69.9312	65.0579	72.1242	-1.9299	-9.2021	-11.1192	0.8652	0.2695	3.3761	0.7423	1.9784	3.253
A24	BG1	Outlier	Shelter-below	36.4500	40.5938	129.7620	162.2025	135.9585	142.6410	92.4043	115.5053	96.8168	101.5755	-9.2137	-8.9693	-9.0915	0.8657	0.2777	3.3465	0.7717	1.9788	3.2404
A25	BG1			35.6000	39.1612	151.6560	106.0880	97.5440	118.4293	118.3124	82.7631	76.0976	92.3910	-0.4059	-10.3805	-5.3932	0.8620	0.2706	3.2291	0.7493	1.9664	3.2733
B1	BG2			37.6000	42.5320	197.0240	182.3600	164.3120	181.2320	137.5669	127.3281	114.7266	126.5405	-3.5132	-13.7241	-8.6187	0.8721	0.2914	3.7903	0.8254	2.0015	3.0857
B2	BG2			32.5000	33.9365	103.3500	96.5250	89.3750	96.4167	61.3428	57.2919	53.0480	57.2276	-3.6985	-11.3497	-7.5241	0.8558	0.2751	3.5464	0.7618	1.9442	2.8819
B3	BG2			32.6000	34.1050	0.0033	0.0033	97.8000	32.6022	0.0013	0.0013	38.4492	12.8172	-2.8046	-3.3795	-3.0921	0.8315	0.2716	3.3836	0.7487	1.8640	2.608
B4	BG2		Little canopy	32.9500	34.6949	70.1835	63.5935	65.9000	66.5590	35.8539	32.4873	33.6656	34.0023	-5.2822	-5.6957	-5.4890	0.8352	0.2716	3.4678	0.7487	1.8749	2.5971
B5	BG2		Little canopy	35.0000	38.1500	0.0035	0.0035	66.8500	22.2857	0.0010	0.0010	18.6164	6.2061	-0.0890	-1.4264	-0.7577	0.8388	0.2820	3.7240	0.7890	1.8883	2.5461
B6	BG2	Outlier	No canopy	28.9000	27.8691	0.0029	0.0029	0.0029	0.0029	0.0001	0.0001	0.0001	0.0001	-0.0001	-0.0001	0.0000	0.4951	0.2364	2.4026	0.6267	0.9441	0.9915
B7	BG2			35.4000	38.8242	110.8020	112.2180	103.7220	108.9140	68.7987	69.6780	64.4027	67.6265	2.2172	-5.4846	-1.6337	0.8677	0.2900	3.8579	0.8202	1.9862	2.9691
B8	BG2			34.8000	37.8129	80.3880	74.8200	80.7360	78.6480	51.7727	48.1867	51.9968	50.6521	1.6904	-5.2133	-1.7615	0.8605	0.2724	3.6249	0.7523	1.9611	2.9488
B9	BG2			35.4000	38.8242	102.3060	115.7580	110.8020	109.6220	70.8631	80.1808	76.7480	75.9306	-2.4541	-4.1712	-3.3127	0.8635	0.2768	3.6294	0.7688	1.9710	2.9994
B10	BG2			35.2500	38.5714	125.1375	106.4550	89.8875	107.1600	91.9372	78.2114	66.0394	78.7294	-0.8032	-0.6026	-0.7029	0.8658	0.2753	3.6132	0.7628	1.9789	3.05
B11	BG2			39.3500	45.4815	164.0895	155.4325	118.0500	145.8573	98.9720	93.7504	71.2028	87.9751	-3.0786	-1.1786	-0.9500	0.8691	0.3011	4.0433	0.8654	1.9909	2.881
B12	BG2			38.6500	44.3017	0.0039	120.5880	110.1525	76.9148	0.0029	89.6330	81.8763	57.1708	0.2128	-2.7104	-1.2488	0.8650	0.2770	3.4869	0.7700	1.9764	3.1243
B13	BG2			39.8500	46.3242	178.9265	140.6705	138.2795	152.6255	118.9515	93.5186	91.9291	101.4664	-7.7085	-7.6371	-7.6728	0.8734	0.2944	3.9252	0.8378	2.0063	3.0508
B14	BG2			39.9000	46.4085	195.5100	202.6920	155.2110	184.4710	125.9031	130.5281	99.9516	118.7943	-4.9041	-13.2532	-9.0787	0.8731	0.2944	3.9086	0.8389	2.0053	3.0549
B15	BG2			38.8500	44.6388	187.6455	181.4295	156.1770	175.0840	127.3154	123.0980	105.9644	118.7926	-1.5635	-0.5626	-1.0630	0.8757	0.3037	4.0038	0.8764	2.0146	3.0663
B16	BG2			40.9500	48.1781	140.8680	145.3725	140.4585	142.2330	101.7897	105.0446	101.4938	102.7760	0.8599	-3.9683	-1.5542	0.8733	0.3106	3.9659	0.9071	2.0062	3.0355
B17	BG2			40.1000	46.7455	198.8960	197.6930	158.7960	185.1283	177.2573	176.1852	141.5199	164.9875	2.1259	-5.0596	-1.4668	0.8768	0.2970	3.8146	0.8516	2.0183	3.2056
B18	BG2			34.9500	38.0657	155.8770	158.3235	138.0525	150.7510	98.8437	100.3950	87.5409	95.5932	-5.4390	-14.2423	-9.8406	0.8624	0.2673	3.4462	0.7332	1.9676	3.1125
B19	BG2			38.7500	44.4703	182.9000	180.1875	153.0625	172.0500	133.4670	131.4876	111.6938	125.5495	-3.8852	-15.4867	-9.6860	0.8838	0.3098	4.2086	0.9014	2.0435	3.1406
B20	BG2			38.4500	43.9646	170.3335	147.6480	109.9670	142.6495	98.5945	85.4634	63.6524	82.5701	-3.2110	-14.0315	-8.6213	0.8741	0.2972	3.9203	0.8484	2.0089	3.0738
B21	BG2			38.5000	44.0489	119.3500	141.6800	101.6400	120.8900	68.3189	81.1011	58.1812	69.2004	3.0511	-5.8806	-1.4147	0.8648	0.2863	3.7731	0.8053	1.9762	2.9482
B22	BG2			35.5000	38.9927	165.7850	102.9500	87.6850	118.8067	111.3745	69.1619	58.9069	79.8144	1.0453	-11.0110	-4.9829	0.8653	0.2891	3.6301	0.8170	1.9777	3.0514
B23	BG2			36.4500	40.5938	157.0995	138.5100	114.0885	136													

Point Name	Block	Round 3 Description		Mean Elevation	Relative Elevation-5m	Relative Elevation-10m	Relative Elevation-20m	Relative Elevation-50m	Mean Slope 50m	Elevation Delta	Total Area	Canopy Mask		Canopy Area (CAI)	Canopy Area Index	Mean LAI			Mean LAI x CAI			
		1	Description 2									LAI_1	LAI_2			LAI_3	LAI_1 x CAI	LAI_2 x CAI	LAI_3 x CAI	Mean (LAI x CAI)		
A1	BG1	Outlier	Shelter-below	67.9180	1.0000	1.0001	0.9998	0.9985	6.7400	-0.0993	22.1344	16.4200	0.7419	0.7404	4.6500	4.8200	4.3900	4.6200	3.4429	3.5688	3.2504	3.4207
A2	BG1	Outlier	Shelter-below	68.6008	0.9996	0.9985	0.9946	0.9790	9.3049	-1.4714	21.9043	16.2194	0.7405	0.7546	5.1100	4.6900	3.7700	4.5233	3.8558	3.5389	2.8447	3.4132
A3	BG1			74.4185	1.0002	1.0006	1.0023	1.0145	5.9268	1.0602	21.6599	15.2317	0.7032	0.7006	4.4000	4.1400	4.1600	4.2333	3.0824	2.9003	2.9143	2.9657
A4	BG1			74.4265	1.0001	1.0006	1.0020	1.0136	6.0502	1.0002	21.9084	16.6964	0.7621	0.7646	3.8100	4.1100	3.8600	3.9267	2.9130	3.1423	2.9512	3.0021
A5	BG1			69.5342	1.0000	0.9996	0.9974	0.9858	8.9175	-1.0022	21.8482	14.9629	0.6849	0.6894	2.3300	1.7800	1.8700	1.9933	1.6064	1.2272	1.2892	1.3742
A6	BG1			67.8796	0.9996	0.9984	0.9942	0.9783	8.6530	-1.5071	21.8804	14.7143	0.6725	0.6627	3.9400	3.5200	3.2200	3.5600	2.6111	2.3327	2.1339	2.3592
A7	BG1		Psa South	67.8401	0.9997	0.9987	0.9954	0.9864	7.3607	-0.9373	22.6233	14.4053	0.6367	0.6442	2.5600	2.7000	2.7700	2.6767	1.6492	1.7394	1.7845	1.7244
A8	BG1	Outlier	Ohead Shelter	67.4263	0.9992	0.9979	0.9959	0.9920	7.2402	-0.5426	21.0294	11.0861	0.5272	0.5355	4.5000	3.4100	3.5300	3.8133	2.4098	1.8261	1.8903	2.0421
A9	BG1			68.0163	1.0000	0.9998	0.9986	0.9962	6.5915	-0.2573	20.2252	15.4870	0.7657	0.7638	3.5900	4.0300	4.0000	3.8733	2.7419	3.0780	3.0550	2.9583
A10	BG1	Outlier	Ohead Shelter	70.3113	1.0000	1.0000	1.0004	1.0017	6.9381	0.1226	21.5007	13.0010	0.6047	0.6167	5.9600	5.1800	4.5200	5.2200	3.6757	3.1946	2.7876	3.2193
A11	BG1		Psa South	70.8367	1.0001	1.0002	1.0010	1.0018	7.3621	0.1288	19.5540	15.5542	0.7954	0.8025	3.7900	4.6500	4.5800	4.3400	3.0413	3.7314	3.6752	3.4827
A12	BG1		Psa North	71.7284	1.0001	1.0005	1.0015	1.0055	7.4794	0.3907	21.4744	15.4736	0.7206	0.7196	3.2800	4.1900	3.9600	3.8100	2.3602	3.0150	2.8495	2.7415
A13	BG1	Outlier	Ohead Shelter	73.9314	1.0004	1.0013	1.0043	1.0158	6.0991	1.1483	22.3326	11.5565	0.5175	0.5197	4.0800	3.4000	3.4900	3.6567	2.1205	1.7670	1.8138	1.9004
A14	BG1		New graft	73.1536	1.0001	1.0005	1.0020	1.0049	4.3074	0.3545	22.5098	10.8174	0.4806	0.4848	3.7100	3.8200	3.1900	3.5733	1.7987	1.8520	1.5466	1.7324
A15	BG1			73.1540	1.0001	1.0005	1.0020	1.0067	5.2374	0.4857	21.5856	11.1067	0.5643	0.5737	4.0500	3.1100	3.3300	3.4967	2.3235	1.7842	1.9104	2.0060
A16	BG1	Outlier	Ohead Shelter	73.6479	1.0003	1.0011	1.0036	1.0131	5.9156	0.9502	22.1523	10.9047	0.4923	0.4914	3.2200	2.9800	2.6500	2.9500	1.5823	1.4643	1.3022	1.4496
A17	BG1	Outlier	Shelter-below	70.8825	1.0000	1.0002	1.0009	1.0071	6.1847	0.4995	20.6150	11.7312	0.5691	0.5685	3.3100	4.1700	3.6100	3.6967	1.8818	2.3707	2.0523	2.1016
A18	BG1			70.5687	1.0001	1.0005	1.0021	1.0104	6.3115	0.7281	19.1859	14.4590	0.7536	0.7459	3.4300	3.7600	3.4000	3.5300	2.5586	2.8047	2.5362	2.6332
A19	BG1	Outlier	Shelter-below	68.0069	0.9994	0.9986	0.9973	0.9977	7.7258	-0.1590	22.5981	16.0312	0.7094	0.7080	6.9300	5.7600	5.3500	6.0133	4.9062	4.0779	3.8776	4.2572
A20	BG1		Psa South	66.9124	0.9998	0.9992	0.9970	0.9912	8.5202	-0.5943	21.5271	12.6785	0.5890	0.5939	3.2600	3.0800	3.8300	3.3900	1.9362	1.8293	2.2748	2.0134
A21	BG1	Outlier	Shelter-below	68.6403	1.0001	1.0004	1.0022	1.0083	8.2305	0.5646	20.3329	17.9461	0.8826	0.8796	8.6000	8.3300	7.2300	8.0533	7.5645	7.3270	6.3595	7.0837
A22	BG1			70.6488	1.0002	1.0007	1.0032	1.0159	6.6740	1.1075	21.6447	17.3952	0.8037	0.8051	2.6700	3.2700	3.2800	3.0733	2.1496	2.6327	2.6407	2.4743
A23	BG1			71.8398	1.0002	1.0007	1.0015	1.0018	5.9103	0.1260	21.1482	15.6214	0.7387	0.7396	2.9600	2.8500	3.1300	2.9800	2.1892	2.1078	2.3149	2.2040
A24	BG1	Outlier	Shelter-below	71.3860	0.9997	0.9988	0.9960	0.9899	5.1659	-0.7317	21.2397	13.0077	0.6124	0.6078	5.2500	4.5700	4.2000	4.6733	3.1910	2.7777	2.5528	2.8405
A25	BG1			71.1434	0.9998	0.9993	0.9978	0.9938	5.4046	-0.4414	20.9567	13.6528	0.6515	0.6437	4.7800	4.3900	3.6600	4.2767	3.0771	2.8261	2.3561	2.7531
B1	BG2			46.7166	1.0002	1.0000	0.9994	0.9918	7.7138	-0.3878	22.6089	18.1666	0.8035	0.7962	5.7100	5.3200	4.7800	5.2700	4.5461	4.2356	3.8057	4.1958
B2	BG2			46.3527	0.9995	0.9982	0.9942	0.9806	8.0112	-0.9182	21.6838	13.8636	0.6394	0.6295	4.0100	4.8100	3.9300	4.2500	2.5242	3.0278	2.4738	2.6753
B3	BG2			46.3421	0.9995	0.9982	0.9943	0.9780	8.2156	-1.0430	20.8916	7.4851	0.3583	0.3642	0.0001	0.0001	1.8800	0.6267	0.0000	0.0000	0.6848	0.2283
B4	BG2		Little canopy	46.1907	0.9993	0.9980	0.9943	0.9752	8.4065	-1.1754	21.1475	9.4521	0.4470	0.4371	2.6500	2.6900	2.6000	2.6467	1.1582	1.1757	1.1364	1.1568
B5	BG2		Little canopy	45.6851	0.9997	0.9988	0.9953	0.9794	7.7845	-0.9603	21.1986	5.6698	0.2675	0.2582	0.0001	2.7600	3.3300	2.0300	0.0000	0.7127	0.8599	0.5242
B6	BG2	Outlier	No canopy	45.5195	0.9997	0.9989	0.9949	0.9756	7.9910	-1.1388	21.9013	0.1591	0.0073	0.0185	0.0001	0.0001	0.0001	0.0001	0.0000	0.0000	0.0000	0.0000
B7	BG2			46.6478	0.9998	0.9986	0.9949	0.9813	8.8749	-0.8879	21.6219	12.0773	0.5586	0.5424	2.8800	2.4800	2.6500	2.6700	1.5622	1.3453	1.4375	1.4483
B8	BG2			48.8368	1.0005	1.0012	1.0029	0.9986	9.5141	-0.0686	21.6219	14.9195	0.6900	0.6791	3.2300	2.8500	2.9900	3.0233	2.1935	1.9355	2.0306	2.0532
B9	BG2			50.1270	1.0003	1.0011	1.0035	1.0012	9.9200	0.0621	21.3270	14.5507	0.6823	0.6842	3.8800	3.1000	3.0700	3.3500	2.6545	2.1209	2.1003	2.2919
B10	BG2			49.4261	0.9995	0.9986	0.9948	0.9756	10.0042	-1.2373	21.4641	14.5507	0.6779	0.6792	2.3500	2.8800	2.9000	2.7100	1.5960	1.9560	1.9696	1.8405
B11	BG2			52.5638	1.0000	0.9998	0.9994	0.9984	9.8435	-0.0826	21.6589	14.7748	0.6822	0.6788	4.2900	3.5500	3.2900	3.7100	2.9122	2.4099	2.2334	2.5185
B12	BG2			53.5051	1.0002	1.0006	1.0013	1.0064	9.6272	0.3417	21.5553	16.7636	0.7777	0.7710	3.1000	3.8100	3.3800	3.4300	2.9374	2.6059	2.6444	
B13	BG2			53.6285	1.0003	1.0010	1.0028	1.0134	9.3872	0.7111	21.7631	16.3152	0.7497	0.7480	4.9200	4.5900	4.4800	4.6633	3.6801	3.4333	3.3510	3.4881
B14	BG2			52.9739	1.0003	1.0010	1.0030	1.0130	9.7747	0.6820	21.3485	16.8359	0.7886	0.7927	5.6900	5.3800	4.6800	5.2500	4.5106	4.2649	3.7100	4.1618
B15	BG2			52.2235	1.0003	1.0011	1.0026	1.0117	10.0232	0.6046	21.9189	16.9300	0.7724	0.7666	4.3700	3.9600	4.0500	4.1267	3.3503	3.0359	3.1049	3.1637
B16	BG2			51.0105	1.0003	1.0010	1.0023	1.0094	9.9315	0.4744	21.6915	17.1397	0.7902	0.7875	5.3900	4.9800	3.9700	4.7800	4.2432	3.9204	3.1253	3.7630
B17	BG2			50.1713	1.0001	1.0003	1.0011	1.0058	9.7469	0.2879	21.8338	19.6492	0.8999	0.8933	6.5400	6.7000	6.3100	6.5167	5.8419	5.9849	5.6365	5.8211
B18	BG2			49.5912	1.0000	0.9998	0.9995	1.0019	9.9488	0.0925	21.5526	14.4783	0.6718	0.6735	3.6300	3.6400	2.8300	3.3667	2.4447	2.4514	1.9059	2.2674
B19	BG2			47.5586	1.0002	1.0003	1.0005	0.9974	9.4358	-0.1223	21.9192	15.4836	0.7064	0.7022	6.1400	5.1800	4.9500	5.4233	4.3115	3.6374	3.4759	3.8082
B20	BG2			46.7354	0.9999	0.9998	0.9990	0.9916	9.0748	-0.3952	21.1024	13.8419	0.6559	0.6553	3.3200	3.2300	2.7700	3.1067	2.1755	2.1166	1.8151	2.0357
B21	BG2			45.2496	0.9993	0.9980	0.9954	0.9863	8.5870	-0.6265	22.1470	11.2384	0.5074	0.5084	2.0900	2.4300	2.7500	2.4233	1.0626	1.2355	1.3982	1.2321
B22	BG2			45.1931	0.9996	0.9986	0.9951	0.9778	8.3574	-1.0276	21.7843	15.6861	0.7201	0.7286	4.4100	4.1200	3.7300	4.0867	3.2133	3.0020	2.7178	2.9777
B23	BG2			44.4072	0.9997	0.9989	0.9958	0.9842	7.4927	-0.7150	22.5824	10.1175	0.4480	0.4389	3.2400	3.3900	3.2500	3.2933	1.4219	1.4877	1.4263	1.4453
B24	BG2			43.5262	0.9996	0.9985	0.9962	0.9884	7.4793	-0.5108	22.1481	11.0215	0.4976	0.4922	1.9200	2.2700	2.0900	2.0933	0.9450	1.1173	1.0287	1.0303
B25	BG2	No plant	South End	43.2523	0.9996	0.9985	0.9966	0.9916	7.3308	-0.3658	20.8498	5.4601	0.2619	0.2677	0.0001	2.3200</						

Point Name	Block	Round 3		Chl_SPAD	Chl_ug/c	Chl_SPAD x LAI 1	Chl_SPAD x LAI 2	Chl_SPAD x LAI 3	Mean (Chl_SPAD x LAI)	Chl_SPAD x LAI_1 x CAI	Chl_SPAD x LAI_2 x CAI	Chl_SPAD x LAI_3 x CAI	Mean (Chl_SPAD x LAI x CAI)	Macro x LAI x Chl	Micro x LAI x Chl	Nutrients x LAI x Chl	NDVI	NDRE	GCI	RECI	EVI2	PVR
		Description 1	Description 2																			
A1	BG1	Outlier	Shelter-below	37.9000	43.0377	176.2350	182.6780	166.3810	175.0980	130.4867	135.2571	123.1906	129.6448	22.8832	2.4556	12.6694	0.9011	0.3748	5.1041	1.2040	2.1070	3.1913
A2	BG1	Outlier	Shelter-below	38.0500	43.2905	194.4355	178.4545	143.4485	172.1128	146.7147	134.6560	108.2416	129.8707	21.0189	-2.4534	9.2828	0.8999	0.3728	5.0853	1.1958	2.1026	3.1666
A3	BG1			39.5500	45.8186	174.0200	163.7370	164.5280	167.4283	121.9101	114.7063	115.2605	117.2923	9.3091	-8.7161	0.2965	0.8951	0.3625	4.7046	1.1425	2.0848	3.2158
A4	BG1			40.8500	48.0096	155.6385	167.8935	157.6810	160.4043	118.9940	128.3636	120.5556	122.6377	14.8612	-7.6745	3.5934	0.9008	0.3857	5.0940	1.2606	2.1060	3.186
A5	BG1			38.0500	43.2905	88.6565	67.7290	71.1535	75.8463	61.1217	46.6939	49.0548	52.2901	5.4073	0.6306	3.0189	0.8962	0.3614	4.8770	1.1387	2.0892	3.1614
A6	BG1			38.3000	43.7118	150.9020	134.8160	123.3260	136.3480	100.0041	89.3438	81.7292	90.3590	4.4379	-3.9937	0.2221	0.8957	0.3707	5.1063	1.1834	2.0870	3.0165
A7	BG1		Psa South	38.9500	44.8073	99.7120	105.1650	107.8915	104.2562	64.2374	67.7504	69.5069	67.1649	8.1930	6.1272	7.1601	0.8901	0.3755	4.9122	1.2091	2.0673	2.9901
A8	BG1	Outlier	Ohead Shelter	41.6500	49.3579	187.4250	142.0265	147.0245	158.8253	100.3667	76.0556	78.7321	85.0514	10.5716	5.4332	8.0024	0.7027	0.3231	3.5235	0.9912	1.5341	2.1118
A9	BG1			37.5000	42.3635	134.6250	151.1250	150.0000	145.2500	102.8211	115.4232	114.5639	110.9361	3.7669	-25.0191	-10.6261	0.8920	0.3558	4.6823	1.1100	2.0736	3.1469
A10	BG1	Outlier	Ohead Shelter	43.0000	51.6332	256.2800	222.7400	194.3600	224.4600	158.0548	137.3698	119.8671	138.4306	-2.5717	-15.0927	-8.8322	0.7490	0.3175	2.7869	0.9520	1.6380	4.021
A11	BG1		Psa South	40.2000	46.9141	152.3580	186.9300	184.1160	174.4680	122.2605	150.0030	147.7449	140.0028	1.4080	-7.0186	-2.8053	0.8980	0.3874	5.5044	1.2722	2.0960	2.9153
A12	BG1		Psa North	38.1000	43.3747	124.9680	159.6390	150.8760	145.1610	89.9223	114.8702	108.5647	104.4524	0.4654	-21.8096	-10.6721	0.8894	0.3519	4.8375	1.0919	2.0641	2.9774
A13	BG1	Outlier	Ohead Shelter	40.4000	47.2512	164.8320	137.3600	140.9960	147.7293	85.6665	71.3888	73.2785	76.7779	7.3547	-14.5957	-3.6205	0.7729	0.3151	3.5017	0.9616	1.7116	2.6603
A14	BG1		New graft	38.6500	44.3017	143.3915	147.6430	123.2935	138.1093	69.5188	71.5800	59.7749	66.9579	2.0542	-16.3214	-7.1336	0.8891	0.3593	4.8369	1.1290	2.0636	2.9999
A15	BG1			40.6500	47.6725	164.6325	126.4215	135.3645	142.1395	94.4484	72.5271	77.6576	81.5444	-3.8355	-18.8514	-11.3434	0.8917	0.3575	4.8572	1.1187	2.0723	3.0207
A16	BG1	Outlier	Ohead Shelter	40.9000	48.0939	131.6980	121.8820	108.3850	120.6550	64.7141	59.8907	53.2585	59.2878	5.1280	-11.5794	-3.2257	0.8871	0.3489	4.7311	1.0768	2.0572	2.9933
A17	BG1	Outlier	Shelter-below	41.9000	49.7793	138.6890	174.7230	151.2590	154.8903	78.8471	99.3331	85.9934	88.0579	5.5854	-6.4276	-0.4211	0.8925	0.3663	5.0076	1.1633	2.0756	2.9867
A18	BG1			39.5500	45.8186	135.6565	148.7080	134.4700	139.6115	101.1909	110.9265	100.3059	104.1411	8.4084	-10.3051	-0.9484	0.8888	0.3444	4.5021	1.0561	2.0618	3.1277
A19	BG1	Outlier	Shelter-below	41.5500	49.1894	287.9415	239.3280	222.2925	249.8540	203.8526	169.4360	157.3754	176.8880	22.0571	7.8045	14.9308	0.8954	0.3802	5.2097	1.2334	2.0862	2.9763
A20	BG1		Psa South	40.4000	47.2512	131.7040	124.4320	154.7320	136.9560	78.2233	73.9042	91.9004	81.3426	7.7468	4.3103	6.0285	0.8936	0.3695	5.0370	1.1777	2.0793	2.9921
A21	BG1	Outlier	Shelter-below	42.8000	51.2961	368.0800	356.5240	309.4440	344.6827	323.7606	313.5961	272.1848	303.1805	27.1494	17.3595	22.2545	0.9008	0.3925	5.3694	1.2990	2.1061	3.0467
A22	BG1			37.9500	43.1219	101.3265	124.0965	124.4760	116.6330	81.5779	99.9100	100.2156	93.9012	11.5515	-5.2093	3.1711	0.8942	0.3537	4.7090	1.1001	2.0817	3.1775
A23	BG1			42.0000	49.9478	124.3200	119.7000	131.4600	125.1600	91.9455	88.5286	97.2261	92.5667	3.2221	-9.2524	-3.0151	0.8952	0.3614	4.9069	1.1367	2.0853	3.0996
A24	BG1	Outlier	Shelter-below	38.8000	44.5545	203.7000	177.3160	162.9600	181.3253	123.8124	107.7757	99.0499	110.2126	4.5403	7.7040	6.1222	0.8955	0.3562	4.7218	1.1107	2.0865	3.2085
A25	BG1			38.6000	44.2174	184.5080	169.4540	141.2760	165.0793	118.7767	109.0857	90.9461	106.2695	16.2120	-8.3115	3.9502	0.8920	0.3451	4.8078	1.0667	2.0737	3.0915
B1	BG2			39.3000	45.3972	224.4030	209.0760	187.8540	207.1110	178.6617	166.4589	149.5627	164.8944	10.3420	3.2060	6.7740	0.8957	0.3514	4.8100	1.0873	2.0869	3.1571
B2	BG2			35.5500	39.0770	142.5555	170.9955	139.7115	151.0875	89.7353	107.6376	87.9451	95.1060	-2.2234	-3.2763	-2.7499	0.8915	0.3531	4.6958	1.0948	2.0716	3.0919
B3	BG2			33.8500	36.2118	0.0034	0.0034	63.6380	21.2149	0.0012	0.0012	23.1801	7.7275	-1.9512	-1.8976	-1.9244	0.8757	0.3384	4.3257	1.0273	2.0151	2.8992
B4	BG2		Little canopy	34.5000	37.3073	91.4250	92.8050	89.7000	91.3100	39.9589	40.5621	39.2050	39.9086	-5.3244	-4.5282	-4.9263	0.8801	0.3395	4.4683	1.0312	2.0308	2.9266
B5	BG2		Little canopy	38.0500	43.2905	0.0038	105.0180	126.7065	77.2428	0.0010	27.1187	32.7193	19.9463	1.4145	-0.7043	0.3551	0.8858	0.3613	4.9693	1.1383	2.0517	2.8527
B6	BG2	Outlier	No canopy	32.2000	33.4309	0.0032	0.0032	0.0032	0.0032	0.0001	0.0001	0.0001	0.0001	0.0001	0.0005	0.0003	0.8637	0.3755	4.8803	1.2057	1.9730	2.4368
B7	BG2			37.9500	43.1219	109.2960	94.1160	100.5675	101.3265	59.2865	51.0523	54.5518	54.9635	7.9170	-4.5438	1.6866	0.8966	0.3541	4.8927	1.1003	2.0903	3.1458
B8	BG2			37.7500	42.7849	121.9325	107.5875	112.8725	114.1308	82.8064	73.0644	76.6536	77.5081	7.9338	-3.5429	2.1954	0.8937	0.3455	4.7803	1.0595	2.0796	3.1165
B9	BG2			38.1500	43.4590	148.0220	118.2650	117.1205	127.8025	101.2693	80.9111	80.1281	87.4362	7.4235	-10.3685	-1.4725	0.8936	0.3441	4.6957	1.0536	2.0792	3.1569
B10	BG2			39.0000	44.8916	91.6500	112.3200	113.1000	105.6900	62.2451	76.2834	76.8131	71.7805	4.7123	-6.1891	-0.7384	0.8944	0.3534	4.7054	1.0966	2.0824	3.1763
B11	BG2			41.5500	49.1894	178.2495	147.5025	136.6995	154.1505	121.0037	100.1313	92.7977	104.6443	1.5788	-15.1002	-6.7607	0.8932	0.3463	4.7832	1.0644	2.0778	3.1001
B12	BG2			40.3500	47.1669	125.0850	153.7335	136.3830	138.4005	96.4371	118.5244	105.1476	106.7030	7.5010	-5.7083	0.8963	0.8927	0.3400	4.5419	1.0343	2.0760	3.2163
B13	BG2			41.8500	49.6950	205.9020	192.0915	187.4880	195.1605	154.0126	143.6825	140.2392	145.9781	4.8380	-21.5419	-8.3519	0.8968	0.3593	4.8951	1.1261	2.0912	3.1507
B14	BG2			42.8500	51.3804	243.8165	230.5330	200.5380	224.9625	193.2810	182.7507	158.9727	178.3348	10.1142	-26.0967	-7.9913	0.8974	0.3632	4.8590	1.1465	2.0933	3.1947
B15	BG2			39.8500	46.3242	174.1445	157.8060	161.3925	164.4477	133.5077	120.9818	123.7314	126.0737	11.1502	-6.5212	2.3145	0.8990	0.3724	4.9662	1.1905	2.0994	3.1848
B16	BG2			42.8000	51.2961	230.6920	213.1440	169.9160	204.5840	181.6080	167.7937	133.7632	161.0550	24.1697	-1.6078	11.2809	0.8977	0.3722	5.0556	1.1917	2.0945	3.1035
B17	BG2			39.9500	46.4927	261.2730	267.6650	252.0845	260.3408	233.3852	239.0949	225.1775	232.5255	26.0098	6.9068	16.4583	0.8990	0.3702	5.0195	1.1798	2.0993	3.1547
B18	BG2			38.5500	44.1332	139.9365	140.3220	109.0965	129.7850	94.2436	94.5033	73.4737	87.4069	1.5853	-3.7289	-1.0718	0.8933	0.3399	4.5643	1.0343	2.0783	3.2329
B19	BG2			40.8500	48.0096	250.8190	211.6030	202.2075	221.5432	176.1244	148.5871	141.9896	155.5670	9.0233	6.5346	7.7790	0.9037	0.3827	5.3855	1.2445	2.1165	3.1233
B20	BG2			40.8000	47.9253	135.4560	131.7840	113.0160	126.7520	88.7620	86.3558	74.0574	83.0584	5.0455	-0.7544	2.1456	0.8986	0.3661	5.0391	1.1588	2.0978	3.1278
B21	BG2			39.6500	45.9871	82.8685	96.3495	109.0375	96.0852	42.1331	48.9873	55.4383	48.8529	8.4412	1.3131	4.8771	0.8958	0.3600	4.9230	1.1281	2.0874	3.1052
B22	BG2			39.7000	46.0714	175.0770	163.5640	148.0810	162.2407	127.5684	119.1795	107.8980	118.2153	11.5307	-12.5203	-0.4948	0.8934	0.3488	4.6807	1.0743	2.0788	3.1632
B23	BG2			38.3500	43.7961	124.2540																

Point Name	Block	Round 4		Mean Elevation	Relative Elevation-5m	Relative Elevation-10m	Relative Elevation-20m	Relative Elevation-50m	Mean Slope 50m	Elevation Delta 50m	Total Area	Canopy Mask Area	Canopy Mask %	Canopy Area Index (CAI)	Mean					Mean (LAI x CAI)		
		Description 1	Description 2												LAI_1	LAI_2	LAI_3	LAI	LAI_1 x CAI	LAI_2 x CAI	LAI_3 x CAI	Mean (LAI x CAI)
A1	BG1	Outlier	Shelter-below	67.9180	1.0000	1.0001	0.9998	0.9985	6.7400	-0.0993	22.1344	16.7392	0.7563	0.7558	7.3500	7.8100	6.4300	7.1967	5.5549	5.9026	4.8596	5.4391
A2	BG1	Outlier	Shelter-below	68.6008	0.9996	0.9985	0.9946	0.9790	9.3049	-1.4714	21.9037	15.8478	0.7235	0.7338	6.7000	6.7800	5.4800	6.6433	5.6285	4.9754	4.0214	4.8751
A3	BG1			74.4185	1.0002	1.0006	1.0023	1.0145	5.9268	1.0602	21.6577	15.7389	0.7267	0.7272	6.3700	5.6800	5.3600	5.8033	4.6323	4.1305	3.8978	4.2202
A4	BG1			74.4265	1.0001	1.0006	1.0020	1.0136	6.0502	1.0002	21.9109	16.4262	0.7497	0.7422	6.4300	6.0400	5.7900	6.0867	4.7722	4.4827	4.2972	4.5174
A5	BG1			69.5342	1.0000	0.9996	0.9974	0.9858	8.9175	-1.0022	21.8458	15.6709	0.7173	0.7142	3.1800	3.7400	4.1000	3.6733	2.2711	2.6711	2.9282	2.6235
A6	BG1			67.8796	0.9996	0.9984	0.9942	0.9783	8.6530	-1.5071	21.8965	15.3034	0.6989	0.6934	6.1100	5.6400	4.6400	5.4633	4.2364	3.9105	3.2172	3.7880
A7	BG1		Psa South	67.8401	0.9997	0.9987	0.9954	0.9864	7.3607	-0.9373	22.6126	12.9423	0.5723	0.5752	5.4700	5.0600	5.1800	5.2367	3.1464	2.9106	2.9796	3.0122
A8	BG1	Outlier	Ohed Shelter	67.4263	0.9992	0.9979	0.9959	0.9920	7.2402	-0.5426	21.0212	11.7583	0.5594	0.5516	4.2900	3.6700	4.0600	4.0067	2.3663	2.0243	2.2394	2.2100
A9	BG1			68.0163	1.0000	0.9998	0.9986	0.9962	6.5915	-0.2573	20.2255	14.5822	0.7210	0.7245	5.5200	4.9200	5.0000	5.1467	3.9992	3.5645	3.6225	3.7287
A10	BG1	Outlier	Ohed Shelter	70.3113	1.0000	1.0000	1.0004	1.0017	6.9381	0.1226	21.5131	9.7305	0.4523	0.4655	5.6000	4.1100	2.7300	4.1467	2.6068	1.9132	1.2708	1.9303
A11	BG1		Psa South	70.8367	1.0001	1.0002	1.0010	1.0018	7.3621	0.1288	19.5455	11.9760	0.6127	0.6132	8.0500	7.9500	6.9600	7.6533	4.9360	4.8747	4.2676	4.6928
A12	BG1		Psa North	71.7284	1.0001	1.0005	1.0015	1.0055	7.4794	0.3907	21.4552	13.7928	0.6429	0.6446	3.9500	5.1700	4.7600	4.6267	2.5460	3.3324	3.0681	2.9822
A13	BG1	Outlier	Ohed Shelter	73.9314	1.0004	1.0013	1.0043	1.0158	6.0991	1.1483	22.3232	13.4526	0.6026	0.6046	6.2400	5.4800	5.3900	5.7033	3.7726	3.3131	3.2587	3.4482
A14	BG1		New graft	73.1536	1.0001	1.0005	1.0020	1.0049	4.3074	0.3545	22.4969	9.6080	0.4271	0.4392	4.5800	4.1000	3.7700	4.1500	2.0113	1.8006	1.6556	1.8225
A15	BG1		Psa South	73.1540	1.0001	1.0005	1.0020	1.0067	5.2374	0.4857	21.5203	13.8133	0.6397	0.6488	3.8100	4.7500	4.7900	4.4500	2.4718	3.0817	3.1076	2.8871
A16	BG1	Outlier	Ohed Shelter	73.6479	1.0003	1.0011	1.0036	1.0131	5.9156	0.9502	22.1569	12.5680	0.5672	0.5653	4.6200	3.4500	3.7300	3.9333	2.6117	1.9503	2.1086	2.2235
A17	BG1	Outlier	Shelter-below	70.8825	1.0000	1.0002	1.0009	1.0071	6.1847	0.4995	20.6089	10.2204	0.4959	0.5011	5.9700	4.6200	4.6000	5.0633	2.9917	2.3152	2.3052	2.5374
A18	BG1			70.5687	1.0001	1.0005	1.0021	1.0104	6.3115	0.7281	19.1910	14.4937	0.7552	0.7561	6.7600	6.5200	5.2700	6.1833	5.1111	4.9296	3.9845	4.6751
A19	BG1	Outlier	Shelter-below	68.0069	0.9994	0.9986	0.9973	0.9977	7.7258	-0.1590	22.5981	14.6026	0.6462	0.6398	9.5800	8.6700	7.1600	8.4700	6.1289	5.5468	4.5807	5.4188
A20	BG1		Psa South	66.9124	0.9998	0.9992	0.9970	0.9912	8.5202	-0.5943	21.5203	12.5476	0.5831	0.5895	3.8300	3.6700	4.0400	3.8467	2.2578	2.1634	2.3815	2.2676
A21	BG1	Outlier	Shelter-below	68.6403	1.0001	1.0004	1.0022	1.0083	8.2305	0.5646	20.3195	16.5555	0.8148	0.8100	9.7200	9.8400	8.4500	9.3367	7.8728	7.9700	6.8441	7.5623
A22	BG1			70.6488	1.0002	1.0007	1.0032	1.0159	6.6740	1.1075	21.6505	16.4058	0.7578	0.7565	5.6400	6.0900	5.8000	5.8433	4.2666	4.6070	4.3877	4.4204
A23	BG1			71.8398	1.0002	1.0007	1.0015	1.0018	5.9103	0.1260	21.1442	14.7115	0.6958	0.6986	4.9200	5.0900	4.9000	4.9700	3.4373	3.5561	3.4233	3.4722
A24	BG1	Outlier	Shelter-below	71.3860	0.9997	0.9988	0.9960	0.9899	5.1659	-0.7317	21.2310	14.0242	0.6606	0.6590	6.0000	5.3700	5.0400	5.4700	3.9542	3.5390	3.3215	3.6049
A25	BG1			71.1434	0.9998	0.9993	0.9978	0.9938	5.4046	-0.4414	20.9488	14.1263	0.6743	0.6658	5.3900	5.0300	4.6700	5.0300	3.5884	3.3488	3.1091	3.3488
B1	BG2			46.7166	1.0002	1.0000	0.9994	0.9918	7.7138	-0.3878	22.6089	18.4425	0.8157	0.8041	6.2100	6.8000	6.3300	6.4467	4.9934	5.4678	5.0899	5.1837
B2	BG2			46.3527	0.9995	0.9982	0.9942	0.9806	8.0112	-0.9182	21.6838	13.6613	0.6300	0.6253	2.8500	3.7000	3.4500	3.3333	1.7822	2.3138	2.1574	2.0845
B3	BG2			46.3421	0.9995	0.9982	0.9943	0.9780	8.2156	-1.0430	20.8916	8.4322	0.4036	0.3973	0.0001	0.0001	1.8400	0.6134	0.0000	0.0000	0.7311	0.2437
B4	BG2		Little canopy	46.1907	0.9993	0.9980	0.9943	0.9752	8.4065	-1.1754	21.1475	9.4285	0.4458	0.4530	2.5700	1.7100	1.6800	1.9867	1.1642	0.7746	0.7611	0.9000
B5	BG2		Little canopy	45.6851	0.9997	0.9988	0.9953	0.9794	7.7845	-0.9603	21.1986	7.2954	0.3441	0.3317	0.5700	0.7700	1.7300	1.0233	0.1891	0.2554	0.5738	0.3394
B6	BG2	Outlier	No canopy	45.5195	0.9997	0.9989	0.9949	0.9756	7.9910	-1.1388	21.9013	1.3240	0.0605	0.0720	0.0001	0.0500	0.0300	0.0267	0.0000	0.0036	0.0022	0.0019
B7	BG2			46.6478	0.9998	0.9986	0.9949	0.9813	8.8749	-0.8879	21.6219	13.6948	0.6334	0.6363	5.5700	5.7600	4.7300	5.3533	3.5443	3.6652	3.0098	3.4064
B8	BG2			48.8368	1.0005	1.0012	1.0029	0.9986	9.5141	-0.0686	21.6219	16.0285	0.7413	0.7299	4.6400	4.7400	4.1200	4.5000	3.3866	3.4596	3.0071	3.2845
B9	BG2			50.1270	1.0003	1.0011	1.0035	1.0012	9.9200	0.0621	21.3270	15.5805	0.7306	0.7262	5.4400	5.2200	4.9000	5.1867	3.9503	3.7905	3.5582	3.7663
B10	BG2			49.4261	0.9995	0.9986	0.9948	0.9756	10.0042	-1.2373	21.4641	15.4935	0.7218	0.7206	6.1600	4.8900	4.1700	5.0733	4.4387	3.5236	3.0048	3.6557
B11	BG2			52.5638	1.0000	0.9998	0.9994	0.9984	9.8435	-0.0826	21.6589	14.6710	0.6774	0.6775	6.2400	6.4400	5.4600	6.0467	4.2276	4.3631	3.6991	4.0966
B12	BG2			53.5051	1.0002	1.0006	1.0013	1.0064	9.6272	0.3417	21.5553	16.9045	0.7842	0.7820	7.9400	6.3300	5.2600	6.5100	6.2095	4.9504	4.1136	5.0911
B13	BG2			53.6285	1.0003	1.0010	1.0028	1.0134	9.3872	0.7111	21.7631	17.0850	0.7850	0.7752	8.2300	6.3300	5.6900	6.7500	6.3803	4.9073	4.4111	5.2329
B14	BG2			52.9739	1.0003	1.0010	1.0030	1.0130	9.7747	0.6820	21.3485	15.7878	0.7395	0.7472	5.7400	6.7600	6.1600	6.2200	4.2888	5.0509	4.6026	4.6474
B15	BG2			52.2235	1.0003	1.0011	1.0026	1.0117	10.0232	0.6046	21.9189	16.1823	0.7383	0.7299	7.9000	6.4800	6.1200	6.8333	5.7663	4.7299	4.4671	4.9878
B16	BG2			51.0105	1.0003	1.0010	1.0023	1.0094	9.9315	0.4744	21.6915	15.2796	0.7044	0.6976	7.7700	7.0900	6.3600	7.0733	5.4202	4.9458	4.4366	4.9342
B17	BG2			50.1713	1.0001	1.0003	1.0011	1.0058	9.7469	0.2879	21.8338	16.8443	0.7715	0.7705	7.9700	8.5600	7.8000	8.1100	6.1410	6.5956	6.0100	6.2489
B18	BG2			49.5912	1.0000	0.9998	0.9995	1.0019	9.9488	0.0925	21.5526	14.2297	0.6602	0.6648	5.2300	4.5800	3.9300	4.5800	3.4768	3.0447	2.6126	3.0447
B19	BG2			47.5586	1.0002	1.0003	1.0005	0.9974	9.4358	-0.1223	21.9192	14.5841	0.6654	0.6680	6.8900	6.0500	5.3300	6.0900	4.6027	4.0415	3.5605	4.0682
B20	BG2			46.7354	0.9999	0.9998	0.9990	0.9916	9.0748	-0.3952	21.1024	13.8887	0.6582	0.6624	7.6700	5.8500	4.6000	6.0400	5.0806	3.8751	3.0471	4.0009
B21	BG2			45.2496	0.9993	0.9980	0.9954	0.9863	8.5870	-0.6265	22.1470	13.7416	0.6205	0.6123	2.6300	3.4100	3.2800	3.1067	1.6103	2.0879	2.0083	1.9022
B22	BG2			45.1931	0.9996	0.9986	0.9951	0.9778	8.3574	-1.0276	21.7843	14.5841	0.6695	0.6794	6.2700	4.9500	4.2100	5.1433	4.2598	3.3630	2.8602	3.4943
B23	BG2			44.4072	0.9997	0.9989	0.9958	0.9842	7.4927	-0.7150	22.5824	9.3416	0.4137	0.4032	3.1500	4.7300	3.8900	3.9233	1.2700	1.9069	1.5683	1.5817
B24	BG2			43.5262	0.9996	0.9985	0.9962	0.9884	7.4793	-0.5108	22.1481	13.0194	0.5878	0.5865	2.6900	3.4300	2.7300	2.9500	1.5776	2.0116	1.6011	1.7301
B25	BG2	No plant	South End	43.2523	0.9996	0.9985	0.9966	0.9916	7													

Point Name	Block	Round 4		Chl_SPAD	Chl_ug/c	Chl_SPAD x LAI 1	Chl_SPAD x LAI 2	Chl_SPAD x LAI 3	Mean (Chl_SPAD x LAI)	Chl_SPAD x LAI_1 x CAI	Chl_SPAD x LAI_2 x CAI	Chl_SPAD x LAI_3 x CAI	Mean (Chl x LAI x CAI)	Macro x LAI x Chl	Micro x LAI x Chl	Nutrients x LAI x Chl	NDVI	NDRE	GCI	RECI	EVI2	PVR	
		Description 1	Description 2																				
A1	BG1	Outlier	Shelter-below	43.3500	52.2231	318.6225	338.5635	278.7405	311.9755	240.8067	255.8776	210.6649	235.7831	40.7714	4.3751	22.5733	0.9244	0.4153	5.2539	1.4287	2.1950	4.145	
A2	BG1	Outlier	Shelter-below	42.5500	50.8748	326.3585	288.4890	233.1740	282.6738	239.4914	211.7017	171.1099	207.4343	34.5210	-4.0294	15.2458	0.9260	0.4174	5.3996	1.4437	2.2011	4.1621	
A3	BG1			42.5000	50.7905	270.7250	241.4000	227.8000	246.6417	196.8728	175.5474	165.6574	179.3592	13.7135	-12.8398	0.4368	0.9201	0.4008	4.8983	1.3463	2.1787	4.1572	
A4	BG1			43.2000	51.9703	277.7760	260.9280	250.1280	262.9440	206.1581	193.6540	185.6385	195.1502	24.3614	-12.5805	5.8904	0.9198	0.4068	5.0187	1.3803	2.1776	4.0497	
A5	BG1			40.9500	48.1781	130.2210	153.1530	167.8950	150.4230	93.0025	109.3803	119.9089	107.4306	10.7241	1.2506	5.9873	0.9239	0.4056	5.2056	1.3743	2.1931	4.1674	
A6	BG1			44.4000	53.9928	271.2840	250.4160	206.0160	242.5720	188.0953	173.6264	142.8416	168.1878	7.8953	-7.1051	0.3951	0.9234	0.4191	5.3151	1.4506	2.1913	4.0347	
A7	BG1		Psa South	40.9000	48.0939	223.7230	206.9540	211.8620	214.1797	128.6895	119.0437	121.8668	123.2000	16.8314	12.5874	14.7094	0.9221	0.4186	5.1747	1.4500	2.1863	4.0684	
A8	BG1	Outlier	Ohead Shelter	41.7000	49.4422	178.8930	153.0390	169.3020	167.0780	98.6747	84.4141	93.3845	92.1578	11.1209	5.7155	8.4182	0.8422	0.3410	3.2757	1.0961	1.9266	5.015	
A9	BG1			42.2000	50.2849	232.9440	207.6240	211.0000	217.1893	168.7660	150.4219	152.8678	157.3519	5.6325	-37.4106	-15.8890	0.9188	0.3918	4.9505	1.2972	2.1736	4.0484	
A10	BG1	Outlier	Ohead Shelter	44.1000	53.4871	246.9600	181.2510	120.3930	182.8680	114.9595	84.3721	56.0428	85.1248	-2.0952	-12.2960	-7.1956	0.7859	0.3023	2.5178	0.9368	1.7414	3.9323	
A11	BG1		Psa South	43.8500	53.0658	352.9925	348.6075	305.1960	335.5987	216.4427	213.7539	187.1355	205.7774	2.7084	-13.5006	-5.3961	0.9222	0.4292	6.5590	1.5120	2.1865	3.7783	
A12	BG1		Psa North	41.5500	49.1894	164.1225	214.8135	197.7780	192.2380	105.7870	138.4604	127.8000	123.9091	0.6164	-28.8827	-14.1331	0.9175	0.3963	5.0587	1.3201	2.1688	3.9042	
A13	BG1	Outlier	Ohead Shelter	43.4500	52.3916	271.1280	238.1060	234.1955	247.8098	163.9209	143.9562	141.5919	149.8230	12.3372	-24.4837	-6.0732	0.8231	0.3451	3.6891	1.1243	1.8656	3.4832	
A14	BG1		New graft	42.1500	50.2006	193.0470	172.8150	158.9055	174.9225	84.7784	75.8933	69.7848	76.8189	2.6018	-20.6718	-9.0350	0.9156	0.3984	5.0053	1.3319	2.1615	3.8458	
A15	BG1			43.0500	51.7175	164.0205	204.4875	206.2095	191.5725	106.4125	132.6665	133.7837	106.4125	124.2876	-5.1694	-25.4075	-15.2884	0.9165	0.3989	4.9360	1.3350	2.1648	3.9301
A16	BG1	Outlier	Ohead Shelter	43.1500	51.8860	199.3530	148.8675	160.9495	169.7233	112.6957	84.1559	90.9859	95.9458	7.2134	-16.2885	-4.5376	0.9151	0.3920	4.8953	1.2956	2.1597	3.9057	
A17	BG1	Outlier	Shelter-below	42.7500	51.2119	255.2175	197.5050	196.6500	216.4575	127.8957	98.9746	98.5461	108.4721	7.8056	-8.9825	-0.5884	0.9194	0.4079	5.0626	1.3900	2.1759	4.0105	
A18	BG1			42.2500	50.3692	285.6100	275.4700	222.6575	261.2458	215.9441	208.2774	168.3469	197.5228	15.7341	-19.2833	-1.7746	0.9157	0.3805	4.6922	1.2357	2.1620	4.0668	
A19	BG1	Outlier	Shelter-below	44.8000	54.6669	429.1840	388.4160	320.7680	379.4560	274.5769	248.4949	205.2161	242.7626	33.4983	11.8528	22.6755	0.9223	0.4185	5.3277	1.4471	2.1870	3.9811	
A20	BG1		Psa South	44.2000	53.6557	169.2860	162.2140	178.5680	170.0227	99.7926	95.6237	105.2642	100.2268	9.6172	5.3510	7.4841	0.9211	0.4124	5.1959	1.4138	2.1825	4.0075	
A21	BG1	Outlier	Shelter-below	46.0000	56.6894	447.1200	452.6400	388.7000	429.4867	362.1477	366.6187	314.8301	347.8655	33.8291	21.6306	27.7299	0.9254	0.4321	5.5962	1.5299	2.1987	3.975	
A22	BG1			42.5000	50.7905	239.7000	258.8250	246.5000	248.3417	181.3313	195.7992	186.4754	187.8686	24.5961	-11.0920	6.7521	0.9208	0.4013	5.0672	1.3498	2.1812	4.075	
A23	BG1			43.5000	52.4759	214.0200	221.4150	213.1500	216.1950	149.5233	154.6898	148.9155	151.0429	5.5657	-15.9821	-5.2082	0.9144	0.3999	5.0160	1.3410	2.1570	3.7871	
A24	BG1	Outlier	Shelter-below	44.0500	53.4029	264.3000	236.5485	222.0120	240.9535	174.1816	155.8925	146.3125	158.7955	6.0334	10.2374	8.1354	0.9183	0.4021	5.0852	1.3511	2.1718	3.9219	
A25	BG1			41.4500	49.0208	223.4155	208.4935	193.5715	208.4935	148.7409	138.8065	128.8720	138.8065	20.4756	-10.9474	4.9891	0.9169	0.3950	5.0785	1.3202	2.1667	3.9004	
B1	BG2			42.1000	50.1163	261.4410	286.2800	266.4930	271.4047	210.2208	230.1935	214.2831	218.2325	13.5525	4.2012	8.8769	0.9233	0.3911	5.1089	1.2898	2.1909	4.1652	
B2	BG2			37.3500	42.1107	106.4475	138.1950	128.8575	124.5000	66.5658	86.4187	80.5796	77.8547	-1.8322	-2.6998	-2.2660	0.9174	0.3827	4.8897	1.2463	2.1685	4.0201	
B3	BG2			35.9500	39.7511	0.0036	0.0036	66.1480	22.0517	0.0014	0.0014	26.2830	8.7620	-2.0281	-1.9724	-2.0003	0.9058	0.3644	4.4888	1.1505	2.1249	3.7691	
B4	BG2		Little canopy	36.9000	41.3523	94.8330	63.0990	61.9920	73.3080	42.9603	28.5845	28.8030	33.2092	-4.2747	-3.6355	-3.9551	0.9029	0.3577	4.4402	1.1177	2.1139	3.6656	
B5	BG2		Little canopy	40.4000	47.2512	23.0280	31.1080	69.8920	41.3427	7.6385	10.3186	23.1835	13.7135	0.7571	-0.3769	0.1901	0.9018	0.3820	4.7396	1.2468	2.1114	3.5683	
B6	BG2	Outlier	No canopy	36.8000	41.1837	0.0037	1.8400	1.1040	0.9826	0.0003	0.1326	0.0795	0.0708	0.0269	0.1471	0.0870	0.9027	0.3933	4.7693	1.3034	2.1145	3.5785	
B7	BG2			41.0000	48.2624	228.3700	236.1600	193.9300	219.4867	145.3155	150.2724	123.4008	139.6629	17.1493	-9.8424	3.6534	0.9204	0.3938	5.0336	1.3062	2.1796	4.0672	
B8	BG2			40.1000	46.7455	186.0640	190.0740	165.2120	180.4500	135.8043	138.7311	120.5848	131.7067	12.5440	-5.6017	3.4712	0.9169	0.3846	4.9495	1.2564	2.1666	3.9449	
B9	BG2			40.6500	47.6725	221.1360	212.1930	199.1850	210.8380	160.5791	154.0851	144.6393	153.1012	12.2467	-17.1051	-2.4292	0.9164	0.3830	4.8283	1.2484	2.1647	3.999	
B10	BG2			40.9000	48.0939	251.9440	200.0010	170.5530	207.4993	181.5440	144.1153	122.8959	149.5184	9.2516	-12.1509	-1.4497	0.9205	0.3878	5.0195	1.2738	2.1802	4.0922	
B11	BG2			40.8500	48.0096	254.9040	263.0740	223.0410	247.0063	172.6971	178.2322	151.1099	167.3464	2.5299	-24.1962	-10.8331	0.9182	0.3821	4.8639	1.2433	2.1714	4.0695	
B12	BG2			42.7500	51.2119	339.4350	270.6075	224.8650	278.3025	265.4548	211.6283	175.8555	217.6462	15.0834	-11.4786	1.8024	0.9222	0.3899	5.0062	1.2853	2.1865	4.19	
B13	BG2			44.4000	53.9928	365.4120	281.0520	252.6360	299.7000	283.2841	217.8844	195.8550	232.3410	7.4296	33.0810	-12.8257	0.9193	0.3995	5.0823	1.3374	2.1755	3.9806	
B14	BG2			44.8500	54.7512	257.4390	303.1860	276.2760	278.9670	192.3528	226.5340	206.4274	208.4381	12.5422	-32.3615	-9.9097	0.9200	0.4007	5.1843	1.3452	2.1784	3.9604	
B15	BG2			42.9000	51.4647	338.9100	277.9920	262.5480	293.1500	247.3764	202.9113	191.6384	213.9754	19.8767	-11.6248	4.1259	0.9211	0.4053	5.1725	1.3693	2.1822	4.001	
B16	BG2			44.9000	54.8355	348.8730	318.3410	285.5640	317.5927	243.3655	222.0671	199.2027	221.5451	37.5200	-2.4960	-7.5123	0.9240	0.4149	5.4031	1.4260	2.1934	4.0254	
B17	BG2			42.8500	51.3804	341.5145	366.7960	334.2300	347.5135	263.1418	282.6215	257.5290	267.7641	34.7189	9.2195	21.9692	0.9241	0.4056	5.2070	1.3716	2.1938	4.1479	
B18	BG2			40.5500	47.5040	212.0765	185.7190	159.3615	185.7190	140.9858	123.4637	105.9415	123.4637	2.2685	-5.3359	-1.5337	0.9183	0.3860	4.8387	1.2633	2.1717	4.085	
B19	BG2			43.9000	53.1501	302.4710	265.5950	233.9870	267.3510	202.0564	177.4225	156.3077	178.5955	10.8891	7.8858	9.3874	0.9207	0.4082	5.2945	1.3881	2.1809	3.9226	
B20	BG2			43.1000	51.8017	330.5770	252.1350	198.2600	260.3240	218.9750	167.0148	131.3279	172.8991	10.3625	-1.5493	4.4066	0.9200	0.4044	5.1733	1.3646	2.1784	3.9537	
B21	BG2			43.0500	51.7175	113.2215	146.8005	141.2040	133.7420	69.3254	89.8858	86.4591	81.8901	11.7494	1.8277	6.7885	0.9158	0.4006	4.9632	1.3422	2.1623	3.8642	
B22	BG2			42.2000	50.2849	264.5940	208.8900	177.6620	217.0487	179.7615	141.9170	120.7011	147.4599										